

DTIC FILE COPY

4



RADC-TR-87-160
Final Technical Report
October 1987

AD-A196 286

***ON ADAPTIVE CELL-AVERAGING CFAR
RADAR SIGNAL DETECTION***

Syracuse University

Moured Barkat and Pramod K. Varshney

APPROVED FOR PUBLIC RELEASE; DISTRIBUTION UNLIMITED

DTIC
ELECTE
JUN 07 1988
S D
ah

ROME AIR DEVELOPMENT CENTER
Air Force Systems Command
Griffiss Air Force Base, NY 13441-5700

38 6 7 006

This report has been reviewed by the RADC Public Affairs Office (PA) and is releasable to the National Technical Information Service (NTIS). At NTIS it will be releasable to the general public, including foreign nations.

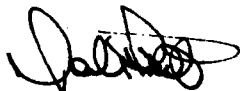
RADC-TR-87-160 has been reviewed and is approved for publication.

APPROVED:



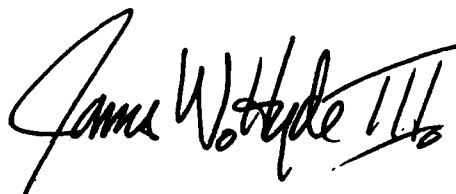
VINCENT C. VANNICOLA
Project Engineer

APPROVED:



DAVID J. PRATT, Col, USAF
Director of Surveillance

FOR THE COMMANDER:



JAMES W. HYDE, III.
Directorate of Plans & Programs

If your address has changed or if you wish to be removed from the RADC mailing list, or if the addressee is no longer employed by your organization, please notify RADC (OCTS) Griffiss AFB NY 13441-5700. This will assist us in maintaining a current mailing list.

Do not return copies of this report unless contractual obligations or notice on a specific document requires that it be returned.

UNCLASSIFIED

SECURITY CLASSIFICATION OF THIS PAGE

| REPORT DOCUMENTATION PAGE | | | | Form Approved OMB No. 0704-0188 | |
|--|-------|--|---|------------------------------------|-----------------------|
| 1a. REPORT SECURITY CLASSIFICATION UNCLASSIFIED | | 1b. RESTRICTIVE MARKINGS N/A | | | |
| 2a. SECURITY CLASSIFICATION AUTHORITY N/A | | 3. DISTRIBUTION/AVAILABILITY OF REPORT Approved for public release; distribution unlimited. | | | |
| 2b. DECLASSIFICATION/DOWNGRADING SCHEDULE N/A | | | | | |
| 4. PERFORMING ORGANIZATION REPORT NUMBER(S) N/A | | 5. MONITORING ORGANIZATION REPORT NUMBER(S) RADC-TR-87-160 | | | |
| 6a. NAME OF PERFORMING ORGANIZATION Syracuse University | | 6b. OFFICE SYMBOL (if applicable) | 7a. NAME OF MONITORING ORGANIZATION Rome Air Development Center (OCTS) | | |
| 6c. ADDRESS (City, State, and ZIP Code) Department of Electrical and Computer Engr Link Hall Syracuse NY 13244-1240 | | | 7b. ADDRESS (City, State, and ZIP Code) Griffiss AFB NY 13441-5700 | | |
| 8a. NAME OF FUNDING/SPONSORING ORGANIZATION Rome Air Development Center | | 8b. OFFICE SYMBOL (if applicable) OCTS | 9. PROCUREMENT INSTRUMENT IDENTIFICATION NUMBER F30602-81-C-0169 | | |
| 8c. ADDRESS (City, State, and ZIP Code) Griffiss AFB NY 13441-5700 | | 10. SOURCE OF FUNDING NUMBERS | PROGRAM ELEMENT NO. 61102F | PROJECT NO. 2305 | TASK NO. J8 |
| | | | | WORK UNIT ACCESSION NO. PD | |
| 11. TITLE (Include Security Classification) ON ADAPTIVE CELL-AVERAGING CFAR RADAR SIGNAL DETECTION | | | | | |
| 12. PERSONAL AUTHOR(S) Mourad Barkat, Pramod K. Varshney | | | | | |
| 13a. TYPE OF REPORT Final | | 13b. TIME COVERED FROM Jun 84 TO Dec 86 | 14. DATE OF REPORT (Year, Month, Day) October 1987 | | 15. PAGE COUNT 172 |
| 16. SUPPLEMENTARY NOTATION N/A | | | | | |
| 17. COSATI CODES | | | 18. SUBJECT TERMS (Continue on reverse if necessary and identify by block number) | | |
| FIELD | GROUP | SUB-GROUP | | | |
| 09 | 03 | | Fusion Detection | | |
| 17 | 04 | | Surveillance Estimation | | |
| | | | Remote Receivers | | |
| 19. ABSTRACT (Continue on reverse if necessary and identify by block number) | | | | | |
| <p>In radar signal detection, the problem is to automatically detect a target in a nonstationary noise and clutter background while maintaining a constant probability of false-alarm. Classical detection using a matched filter receiver and a fixed threshold is not applicable due to the nonstationary nature of the background noise. Therefore, adaptive threshold techniques are needed to maintain a constant false-alarm rate (CFAR). One approach to adaptive detection in nonstationary noise and clutter background is to compare the processed target signal to an adaptive threshold. In the cell-averaging CFAR processing, an estimate of the background noise from the leading and the lagging reference windows is used to set the adaptive threshold. A threshold multiplier (or scaling factor) is used to scale the threshold to achieve the desired probability of false-alarm.</p> <p>In the first part of this report, we have proposed two modified cell-averaging detectors for multiple target situations. The first one is a weighted cell-averaging CFAR detector.</p> | | | | | |
| 20. DISTRIBUTION/AVAILABILITY OF ABSTRACT <input type="checkbox"/> UNCLASSIFIED/UNLIMITED <input checked="" type="checkbox"/> SAME AS RPT. <input type="checkbox"/> DTIC USERS | | | 21. ABSTRACT SECURITY CLASSIFICATION UNCLASSIFIED | | |
| 22a. NAME OF RESPONSIBLE INDIVIDUAL Vincent C. Vannicola | | 22b. TELEPHONE (Include Area Code) (315) 330-4437 | | 22c. OFFICE SYMBOL RADC (OCTS) | |

DD Form 1473, JUN 86

ATP FORME, 86145/29-4-88-138 1/211

Previous editions are obsolete.

SECURITY CLASSIFICATION OF THIS PAGE

UNCLASSIFIED

UNCLASSIFIED

WCA-CFAR, where weighted leading and lagging reference windows are used to obtain the adaptive threshold. The second is a cell-censored, cell averaging CFAR processor where a predetermined fixed threshold is used to eliminate those cells that may contain interference.

In the second part of the report, the theory of distributed CFAR detection with data fusion is developed. First, a system consisting of n CA-CFAR detectors with data fusion is considered. The overall system is optimized so that the overall probability of detection is maximum while the overall probability of false-alarm is fixed at the desired value. Next, CFAR detection with multiple background estimators and a data fusion center is studied. Finally, adaptive CFAR detection with multiple detectors for different network topologies is considered. Two topologies, namely, a parallel and a tandem topology are investigated. The overall systems are optimized so that the probability of detection is maximum while CFAR is achieved.

| | |
|----------------------|-------------------------------------|
| Accession For | |
| NTIS GRA&I | <input checked="" type="checkbox"/> |
| DTIC TAB | <input type="checkbox"/> |
| Unannounced | <input type="checkbox"/> |
| Justification | |
| By | |
| Distribution/ | |
| Availability Codes | |
| Dist | Avail and/or Special |
| A-1 | |

UNCLASSIFIED

TABLE OF CONTENTS

| | Page |
|--|------|
| LIST OF ILLUSTRATIONS----- | iv |
| LIST OF TABLES----- | vii |
| CHAPTER I. INTRODUCTION----- | 1 |
| 1.1 Constant False-Alarm Rate (CFAR) Processors----- | 1 |
| 1.1-1 Background and Literature Review----- | 1 |
| 1.1-2 System Description, Notation, and Terminology- | 8 |
| 1.2 Detection with Distributed Sensors and Data Fusion----- | 12 |
| 1.3. Dissertation Organization----- | 15 |
| CHAPTER II. A WEIGHTED ADAPTIVE CELL-AVERAGING CFAR DETECTOR FOR MULTIPLE TARGET SITUATIONS----- | 18 |
| 2.1 Introduction----- | 18 |
| 2.2 Preliminaries----- | 19 |
| 2.3 Cell-Averaging CFAR Processors--- | 20 |
| 2.3-1 CA-CFAR Detector----- | 20 |
| 2.3-2 GO-CFAR Detector----- | 23 |
| 2.3-3 SO-CFAR Detector----- | 25 |
| 2.3-4 Threshold Multipliers----- | 27 |
| 2.4 Weighted Cell-Averaging CFAR Detector----- | 29 |
| 2.5 Summary and Conclusions----- | 36 |
| CHAPTER III. A CELL-CENSORED CFAR DETECTOR FOR MULTIPLE TARGET SITUATIONS----- | 44 |
| 3.1 Introduction----- | 44 |

| | Page |
|--|------|
| 3.2 Cell-Censored CFAR Detection----- | 44 |
| 3.3 Summary and Conclusions----- | 54 |
| CHAPTER IV. CA-CFAR DETECTION WITH DISTRIBUTED RADARS AND DATA FUSION----- | 58 |
| 4.1 Introduction----- | 58 |
| 4.2 Distributed CFAR Detection with Data Fusion----- | 59 |
| 4.2-1 "AND" Fusion Rule----- | 64 |
| 4.2-2 "OR" Fusion Rule----- | 67 |
| 4.2-3 Example----- | 72 |
| 4.2-4 A Comment on the Perform- ance of the "AND" and "OR" Fusion Rules----- | 78 |
| 4.3 Optimization of the Overall System----- | 81 |
| 4.4 Summary and Discussion----- | 90 |
| CHAPTER V. ADAPTIVE CFAR DETECTION WITH MULTIPLE BACKGROUND ESTIMATORS----- | 92 |
| 5.1 Introduction----- | 92 |
| 5.2 Adaptive CFAR Detection with Multiple Background Estimators--- | 94 |
| 5.2-1 CA-CFAR Detection----- | 96 |
| 5.2-2 GO-CFAR Detection----- | 99 |
| 5.2-3 SO-CFAR Detection----- | 102 |
| 5.3 Example----- | 103 |
| 5.4 An Extension----- | 112 |
| 5.5 Summary and Discussion----- | 117 |
| CHAPTER VI. ADAPTIVE CFAR DETECTION WITH DIFFERENT NETWORK TOPOLOGIES----- | 119 |
| 6.1 Introduction----- | 119 |
| 6.2 System Optimization and Performance Analysis----- | 120 |
| 6.2-1 Adaptive CFAR Detection with Parallel Network Topology----- | 120 |

| | Page |
|---|------|
| 6.2-2 Adaptive CFAR Detection with Tandem Network Topology----- | 127 |
| 6.3 Example----- | 131 |
| 6.4 A Comparison----- | 136 |
| 6.5 Summary and Conclusions----- | 138 |
| CHAPTER VII. SUMMARY AND SUGGESTIONS FOR FUTURE RESEARCH WORK----- | 140 |
| 7.1 Summary----- | 140 |
| 7.2 Suggestions for Future Research Work----- | 143 |
| APPENDIX A----- | 144 |
| REFERENCES----- | 152 |

LIST OF ILLUSTRATIONS

| <u>Figure No.</u> | <u>Title</u> | <u>Page</u> |
|-------------------|---|-------------|
| 1-1 | Effect of the Noise Power Increase on the Probability of False-Alarm for a Fixed Threshold. Design $P_F = 10^{-8}$ ----- | 2 |
| 1-2 | Cell-Averaging CFAR Detector----- | 4 |
| 1-3 | Variation of Noise Power as a Function of Range----- | 5 |
| 1-4 | Distributed Sensor System with Central Computation----- | 13 |
| 1-5 | Distributed Sensor System with Data Fusion----- | 14 |
| 2-1 | Weighted Cell-Averaging CFAR Detector----- | 30 |
| 2-2 | Detection Probability for CA, GO, SO and WCA-CFAR Detectors for $N=4$, $P_F=10^{-4}$ and $I=S \div 10$ ----- | 37 |
| 2-3 | Detection Probability for CA, SO, GO and WCA-CFAR Detectors for $N=4$, $P_F=10^{-4}$ and $I=S$ ----- | 38 |
| 2-4 | Detection Probability CA, GO, SO and WCA-CFAR Detectors for $N=4$, $P_F=10^{-4}$ and $I=S \times 10$ ----- | 39 |
| 2-5 | Detection Probability for WCA-CFAR Detector when $N=4$, $P_F=10^{-4}$, $I=S \div 10$, $I=S$, and $I=S \times 10$ ----- | 40 |
| 2-6 | Detection Probability for WCA-CFAR Detector when $P_F=10^{-4}$, $I=S \div 10$, $N=4$ and $N=8$ ----- | 41 |

| <u>Figure No.</u> | <u>Title</u> | <u>Page</u> |
|-------------------|--|-------------|
| 2-7 | Detection Probability for WCA-CFAR Detector when $P_F=10^{-4}$, $I=S$, $N=4$ and $N=8$ ----- | 42 |
| 2-8 | Detection Probability for WCA-CFAR Detector when $P_F=10^{-4}$, $I=S \times 10$, $N=4$ and $N=8$ ----- | 43 |
| 3-1 | Cell-Censored CFAR Detector----- | 45 |
| 3-2 | Performance of the Cell-Censored CFAR Detector $P_F=10^{-5}$, $P_0=0.5$ and $I=S \div 10$ ----- | 53 |
| 3-3 | A Performance Comparison of the Cell- Censored (CC) CFAR Detector and the CA-CFAR Detector. $P_F=10^{-5}$, $P_{F_1}^c = 10^{-6}$, $P_0=0.5$ and $I=S \div 10$ ----- | 55 |
| 3-4 | A Performance Comparison of the Cell-Censored (CC) CFAR Detector and the CA-CFAR Detector. $P_F=10^{-6}$, $P_{F_1}^c = 10^{-3}$, $P_0=0.5$ and $I=S \div 10$ ----- | 56 |
| 3-5 | A Performance Comparison of the Cell-Censored (CC) CFAR Detector and the CA-CFAR Detector. $P_F=10^{-5}$, $P_{F_1}^c = 10^{-1}$, $P_0=0.5$ and $I=S \div 10$ ----- | 57 |
| 4-1 | Distributed CA-CFAR Detection with Data Fusion----- | 60 |
| 4-2 | Distributed CA-CFAR Detection and Data Fusion with Two Detectors----- | 69 |
| 4-3 | Performance Comparison of the Two Sensor System (DS) Using the "AND" Fusion Rule with a Single Sensor System (SS) $P_F=10^{-4}$, $N_1=6$, and $N_2=4$ ----- | 75 |
| 4-4 | Performance Comparison of the Two Sensor System (DS) Using the "OR" Fusion Rule with a Single Sensor System (SS). $P_F=10^{-4}$, $N_1=6$ and $N_2=4$ ----- | 78 |
| 4-5 | Performance of the Two System System for the "AND" and the "OR" fusion Rule. $P_F=10^{-4}$, $N_1=6$ and $N_2=4$ ----- | 79 |

| <u>Figure No.</u> | <u>Title</u> | <u>Page</u> |
|-------------------|--|-------------|
| 4-6 | P_D Versus P_F for the Overall Optimum System. $S=5$ dB----- | 90 |
| 4-7 | P_D Versus P_F for the Overall Optimum System $S=10$ dB----- | 91 |
| 5-1 | CFAR Processor with Multiple Background Estimators----- | 93 |
| 5-2 | Cell-Averaging CFAR Processor with Multiple Background Estimators----- | 95 |
| 5-3 | A Two-Sensor CFAR Processor with One Background Estimator----- | 104 |
| 5-4 | Performance of the CA-CFAR Detectors for $P_F=10^{-4}$ and $N=4$ ----- | 107 |
| 5-5 | Performance of the GO-CFAR Detectors for $P_F=10^{-4}$ and $N=4$ ----- | 109 |
| 5-6 | Performance of the CA, GO and SO CFAR Detectors with a Background Estimator for $P_F=10^{-4}$ and $N=4$ ----- | 111 |
| 5-7 | Hybrid CFAR Processor with Data Fusion----- | 113 |
| 5-8 | Hybrid System with Two Background Estimators and a Data Fusion Center-- | 115 |
| 5-9 | Performance of the Hybrid System with Two Background Estimators (HS) and the Two-Sensor System of Figure 4.2 (DS), $P_F=10^{-4}$, $N_1=6$ and $N_2=4$ ----- | 118 |
| 6-1 | Parallel Network Topology for Adaptive CFAR Detection----- | 121 |
| 6-2 | Tandem Network Topology for Adaptive CFAR Detection----- | 122 |
| 6-3 | A Two Sensor Network Topology for Adaptive CFAR Detection----- | 132 |
| 6-4 | Different Network Topologies for Two-Sensor CFAR Detection Systems---- | 137 |

LIST OF TABLES

| <u>Table No.</u> | <u>Title</u> | <u>Page</u> |
|------------------|--|-------------|
| 4-1 | "AND" Fusion Rule----- | 65 |
| 4-2 | "OR" Fusion Rule----- | 68 |
| 6-1 | Performance of Adaptive CFAR Detection with Two-Sensor System and a Single Sensor System. $P_F = 10^{-5}$, $N=6$, $N_1=4$ ----- | 136 |
| 6-2 | CA-CFAR Performance of the Two- Sensor Systems of Figure 6-4----- | 138 |

CHAPTER I
INTRODUCTION

1.1 Constant False Alarm - Rate (CFAR) Processors

1.1-1 Background and Literature Review

In practical radar signal detection systems, the problem is to automatically detect a target in a nonstationary noise and clutter background while maintaining a constant probability of false-alarm. "Clutter" is the term applied to any unwanted radar signal from scatterers that are not of interest to the radar user. Examples of unwanted echoes, or clutter, in radar signal detection are reflections from terrain, sea, rain, birds, insects, chaff, etc. Classical detection using a matched filter receiver and a fixed threshold is not applicable due to the nonstationary nature of the background noise. In fact, a small increase in the total noise power results in a corresponding increase of several orders of magnitude in the probability of false alarm. As shown in Figure 1-1, for a design probability of false-alarm of 10^{-8} , an increase of only 3 dB in signal-to-noise ratio causes the actual false-alarm probability to increase by almost 10^4 . This undesirable increase in the number of false alarms causes the data processing equipment, either a human operator or a digital computer, to saturate.

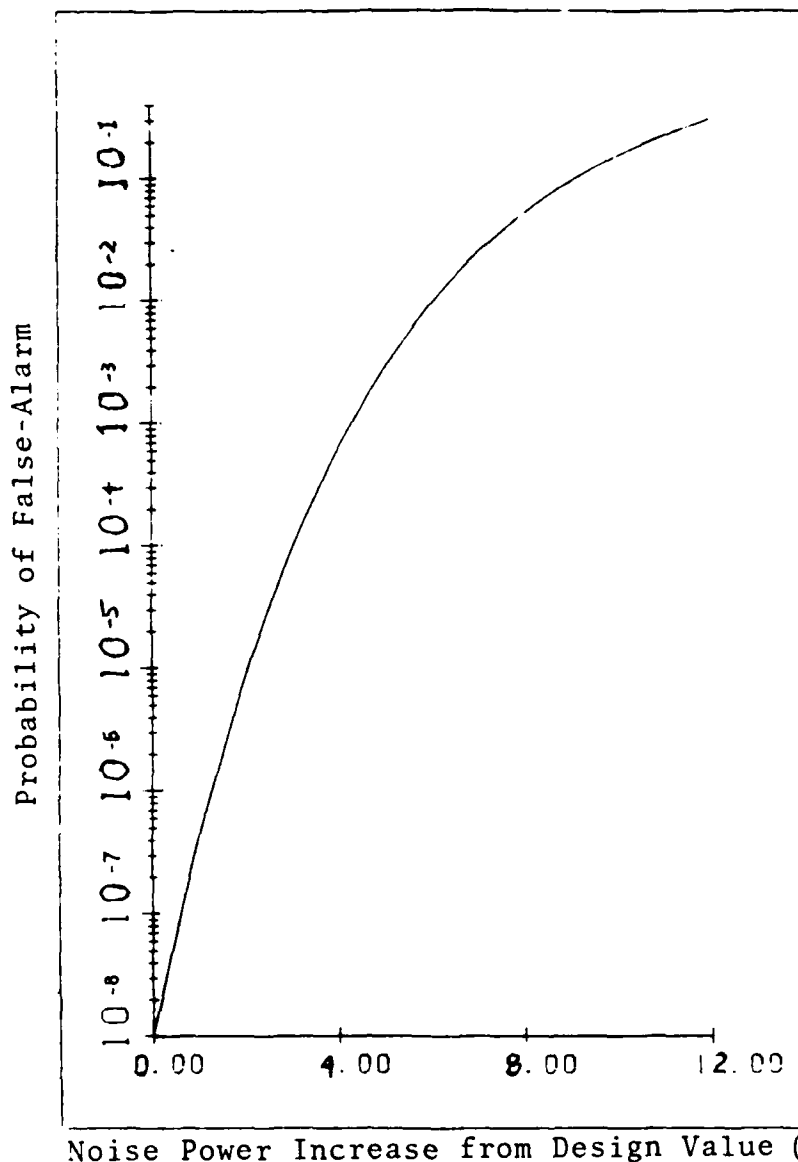


Fig. 1-1. Effect of the Noise Power Increase on the Probability of False-Alarm for a Fixed Threshold. Design $P_F = 10^{-8}$.

Therefore, adaptive threshold techniques are needed to maintain a constant false-alarm rate (CFAR).

One approach to adaptive detection in nonstationary noise and clutter background is to compare the processed target signal from the test cell to an adaptive threshold obtained from the mean level of clutter plus noise over adjacent range and/or Doppler Cells [1-3]. The conventional cell-averaging constant false-alarm rate detector is shown in Figure 1-2. In the cell-averaging constant false-alarm rate detector, CA-CFAR, the adaptive threshold is obtained from the arithmetic mean of the reference cells [4]. Finn [2] showed that in a homogeneous Gaussian noise background, where the noise samples obtained from the range cells are identically distributed, the CA-CFAR detector performs well and its performance approaches that of the Neyman-Pearson detector as the number of range cells is increased to infinity. In nonhomogeneous background, which may be caused by clutter edges and chaff, the adaptive threshold setting is seriously affected resulting in a degradation of the performance. In the situation where the transition from a clear to a clutter environment is not relatively smooth, it is assumed that the total noise power density as a function of range can be represented by the step function as shown in Figure 1-3. Two cases may be encountered in this severe clutter environment [1,2]. In the first case, the cell under test is in the clear region but a group of the reference cells are immersed in the clutter. This results in a higher adaptive

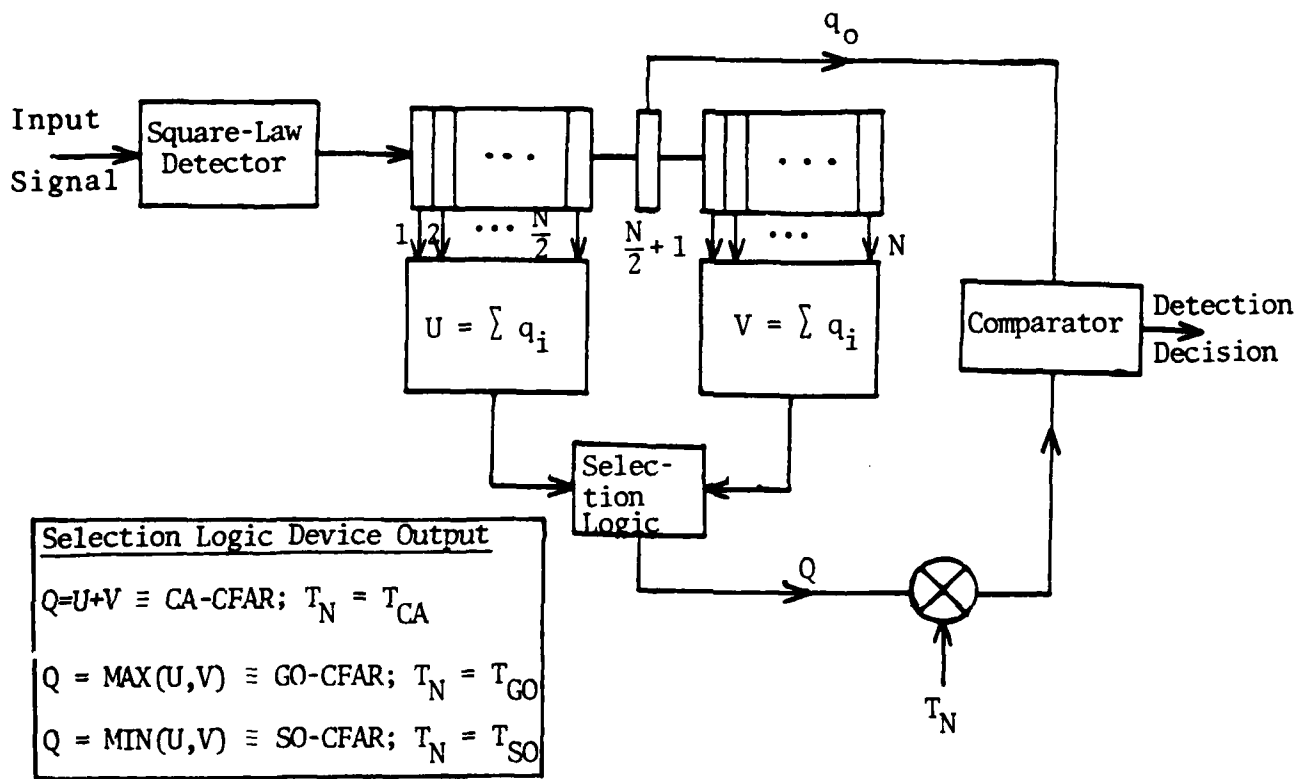


Fig. 1-2. Cell-Averaging CFAR Detector.

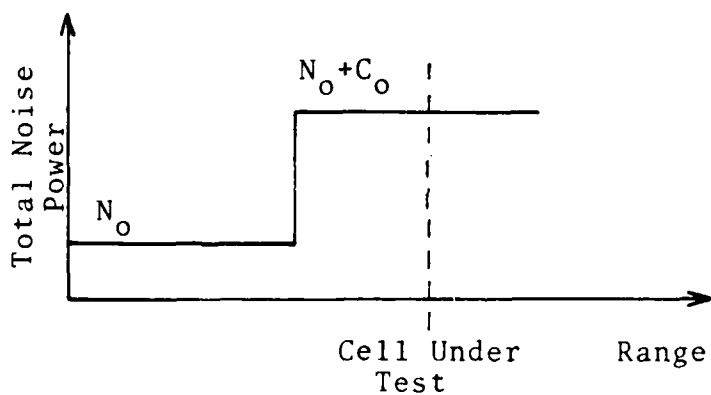
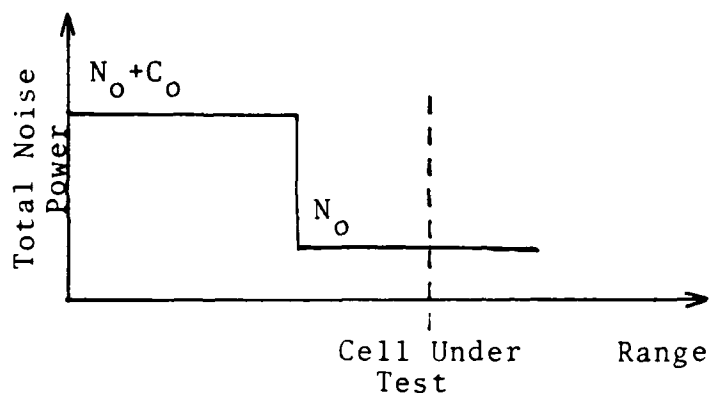


Fig. 1-3. Variation of Noise Power as a Function of Range.

N_o = Noise Power

C_o = Clutter power

threshold and the probabilities of detection and false-alarm are reduced. This is also known as the masking effect. In the second case, if the cell under test is immersed in the clutter but some of the reference cells are in the clear region, the threshold is relatively low and the probability of false-alarm is increased [1,2,5,6]. Jamming and the clutter edges mentioned above significantly affect the power level as a function of range which results in an intolerable increase in the probability of false-alarm. This situation is frequently encountered in search radar design. To control this intolerable increase in the probability of false-alarm, Hansen and Sawyers [5,6] proposed the greatest-of-selection logic in cell-averaging constant false-alarm rate detector, GO-CFAR. A comparison between the two CFAR detectors, CA-CFAR and GO-CFAR, using square law detection of Swerling I targets was treated by Moore and Lawrence [7]. The clutter map CFAR approach can also be used for nonhomogeneous background. In this technique proposed by O'Donnell, Muehe, and Labitt [8], the detector output of each resolution cell is averaged over several scans. An analysis of the clutter map CFAR technique has been performed by Nitzberg [9], to obtain the probability of detection.

Trunk [10], while studying the target range resolution of some adaptive threshold detectors, showed that targets cannot be resolved by a CA-CFAR detector if another target lies within the reference cells of the other. He proposed the smallest-of-selection logic in cell-averaging constant false-alarm

rate detector, SO-CFAR. The SO-CFAR detector is less sensitive to the detection loss than the CA-CFAR unless the number of resolution cells is relatively large. In other words, for a small number of reference cells, the detection loss of the SO-CFAR is relatively large as compared to the ideal detector. Closely separated targets may be encountered in dense civilian or military target environments. In such situations, capture effect may occur where the probability of detection rises slowly and reaches one asymptotically. Finn and Johnson [1], and Rickard and Dillard [11] studied this problem of two closely separated targets and showed the existence of the capture effect for all single-pulse Swerling target models (cases 1,2, and 4). The SO-CFAR detector proposed in [10] eliminates the capture effect that exists in the CA-CFAR and GO-CFAR detectors.

Additional work on CFAR processors in situations where one or more targets lie in the set of reference cells, i.e., in multiple target situations, is reported in the literature [12-16]. In this situation, the interfering targets raise the threshold, thereby drastically reducing the probability of detection. The noise samples of the reference cells are not identically distributed in this case. Therefore, a mathematical representation of the system model is more complicated which makes the performance analysis of the systems more involved. McLane et al. [12] proposed a threshold control technique for the CA-CFAR detector based on a priori information about location that could be supplied

by the radar's tracking system. Al Hussaini and Ibrahim [13] presented a generalization and extension of the technique in [12] for the CA-CFAR, GO-CFAR, and SO-CFAR detectors. When the interfering target is in one of the reference cells, Weiss [14] showed that the detection for a GO-CFAR detector is extremely poor. To alleviate this problem, he suggested the use of the SO-CFAR technique. Rohling [15] introduced an order statistic based estimation technique to obtain CFAR in multiple target situations. Finally, Ritcey [16] presented the performance analysis of the censored mean-level detector (CMLD), which is an alternative to the mean-level detector (MLD) considered previously [1-15]. He obtained the expressions for the probability of detection of the CMLD in a multiple-target environment when a fixed number of Swerling II targets are present. The CMLD achieves robust detection performance in a multiple-target environment by censoring several of the largest samples of the maximum likelihood estimate of the background noise level.

1.1-2. System Description, Notation, and Terminology

In this subsection, we describe the operation of the cell-averaging CFAR detector, we define some notation, and present some mathematical background that will be used throughout the report.

The conventional cell-averaging CFAR processor is shown in Figure 1-2. As shown, the output from the square

law detector is fed into a tapped delay line forming the reference cells. The delay, τ , between the taps is approximately equal to the transmitted pulsewidth. To avoid any signal energy spill from the test cell into the directly adjacent range cells, which may affect the clutter power estimation, the adjacent cells, called guard cells (usually one or two on each side of the cell under test), are completely ignored. The statistics of the reference windows U and V are obtained from the sum of the $\frac{N}{2}$ leading cells and the $\frac{N}{2}$ lagging reference cells respectively. Thus, a total of N noise samples are used to estimate the background environment. The noise samples are assumed to be statistically independent. The reference windows U and V are combined according to some selection logic to obtain the estimate of the clutter power level Q. To maintain the probability of false-alarm, P_F , at the desired value, the adaptive threshold is multiplied by a scaling factor called the threshold multiplier T_N . It should be noted that for the same value of P_F , the threshold multiplier is not the same for different selection logics. The product $T_N Q$ is the resulting adaptive threshold. The output, q_0 , from the center tap is then compared with the threshold in order to make a decision.

We assume that the target at the test cell (center tap), called the primary target, is a slowly fluctuating target model of Swerling type I. The signal-to-noise ratio, SNR, of the primary target is denoted by S. We further assume that the total background noise is white Gaussian.

Since both the noise and Rayleigh targets have Gaussian quadrature components, the output of the square-law detector has an exponential probability density function [17]. If the noise variance is σ^2 , then the conditional probability density function of the output of the detection cell, q_o , is given by

$$P_{Q_o|H_i}(q_o|H_i) = \begin{cases} \frac{1}{2\sigma^2(1+S)} e^{-q_o/2\sigma^2(1+S)} & , \text{ for hypothesis } H_1 \\ \frac{1}{2\sigma^2} e^{-q_o/2\sigma^2} & , \text{ for hypothesis } H_0 \end{cases} \quad (1-1)$$

The hypothesis H_0 represents the case of noise alone, while hypothesis H_1 represents the noise plus target signal case. The probability of detection, P_D^N , where N may represent CA, GO, or SO, is given by

$$P_D^N = \int_0^{\infty} \Pr(Q_o > T_N q | Q, H_1) P_Q^N(q) dq \quad (1-2)$$

$P_Q^N(q)$ denotes the probability density function of the adaptive threshold and

$$\Pr(Q_o > T_N q | Q, H_1) = \int_{T_N q}^{\infty} P_{Q_o|H_1}(q_o|H_1) dq_o = \exp\left[-\frac{T_N q}{2\sigma^2(1+S)}\right] \quad (1-3)$$

We easily see that P_F is directly obtained from P_D by just setting the target SNR, S , to zero, i.e.

$$\begin{aligned} P_F^N &= \int_0^{\infty} \Pr(Q_o > T_N q | Q, H_0) P_Q^N(q) dq \\ &= \int_0^{\infty} e^{-T_N q/2\sigma^2} \cdot P_Q^N(q) dq \end{aligned} \quad (1-4)$$

For simplicity, we normalize the noise power and the output from the test cell and divide by $2\sigma^2$. Then, equations (1-1) and (1-3) become

$$P_{Q_o|H_i}(q_o|H_i) = \begin{cases} \frac{1}{1+S} e^{-q_o/(1+S)} & , \text{ for hypothesis } H_1 \\ e^{-q_o} & , \text{ for hypothesis } H_0 \end{cases} \quad (1-5)$$

and

$$\Pr(Q_o > T_N q | Q, H_1) = e^{-\frac{T_N q}{1+S}} \quad (1-6)$$

When there is no interference in the reference cells, then all the noise samples are identically distributed. Since these noise samples are statistically independent, the reference windows U and V have a chi-square, χ^2 , distribution of $2(\frac{N}{2})$ degrees of freedom (see Appendix A for details), i.e.,

$$P_U(u) = \frac{1}{\Gamma(\frac{N}{2})} u^{\frac{N}{2}-1} e^{-u}, \quad u \geq 0 \quad (1-7)$$

and

$$P_V(v) = \frac{1}{\Gamma(\frac{N}{2})} v^{\frac{N}{2}-1} e^{-v}, \quad v \geq 0 \quad (1-8)$$

The corresponding cumulative distributions are

$$F_U(u) = 1 - e^{-u} \sum_{j=0}^{(N/2)-1} \frac{1}{j!} u^j, \quad u \geq 0 \quad (1-9)$$

and

$$F_V(v) = 1 - e^{-v} \sum_{j=0}^{(N/2)-1} \frac{1}{j!} v^j, \quad v \geq 0 \quad (1-10)$$

The above results will be used throughout this dissertation.

Next, we discuss distributed detection and data fusion.

1.2. Detection with Distributed Sensors and Data Fusion

The use of multiple sensors with data fusion is widely increasing in surveillance systems. One of the main goals of using multiple sensors is to improve system performance such as reliability and speed. For surveillance systems requiring a large area of coverage and/or a large number of targets under consideration, multiple sensors are used. In such systems, complete observations can be transmitted by the sensors to a central processor for data processing as shown in Figure 1-4. This requires a large communication bandwidth which may not be available. Thus, due to the constraints on the bandwidths of the communication channels, distributed signal processing with a data fusion center is preferred in many situations. In such distributed detection systems, some processing of the signal is done at each sensor which then sends partial results to the data fusion center, as shown in Figure 1-5. These partial results are combined according to a suitable data fusion rule to yield the desired global result. In our case, the partial results are the decisions from the individual detectors, D_i , $i=1,2,\dots,n$, where $D_i \in \{0,1\}$. The D_i 's are combined to yield a final decision, D_o , which may again be a zero or a one.

Some work on distributed detection has been reported in the literature [18-31]. Tenney and Sandell [18], extended the classical Bayesian theory to the case of distributed sensors for the binary hypothesis testing problem. Sadjadi [19] generalized the results of [18] to the case of multiple

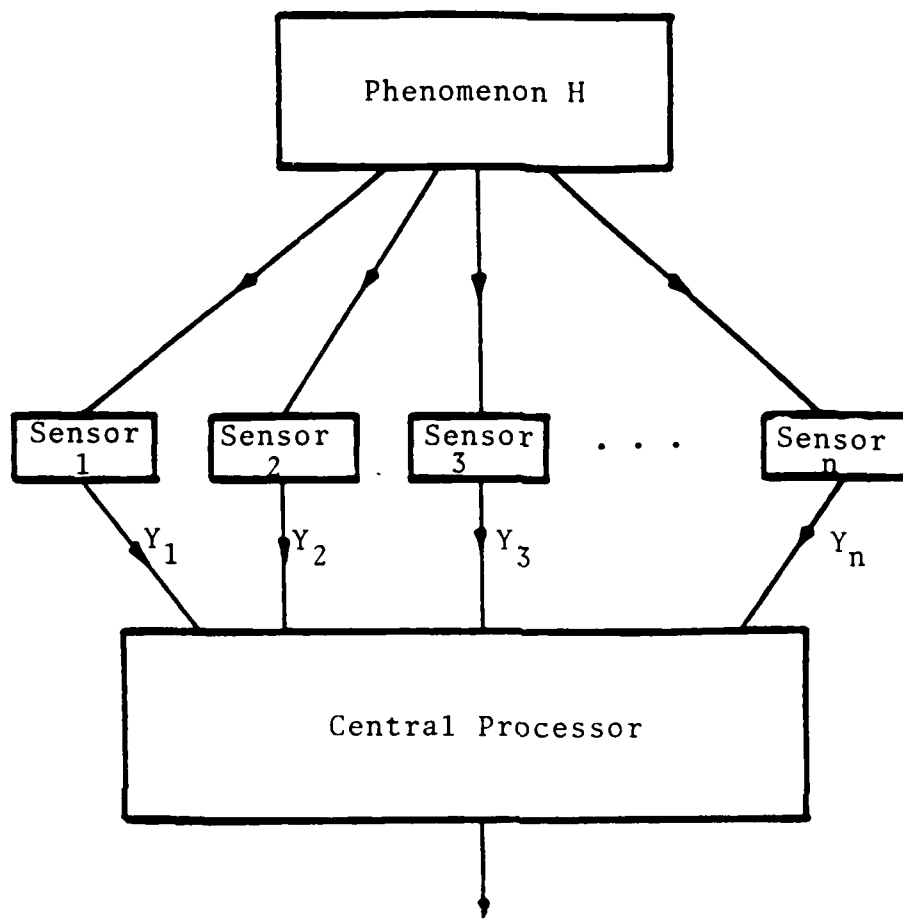


Fig. 1 -4. Distributed Sensor System with Central Computation.

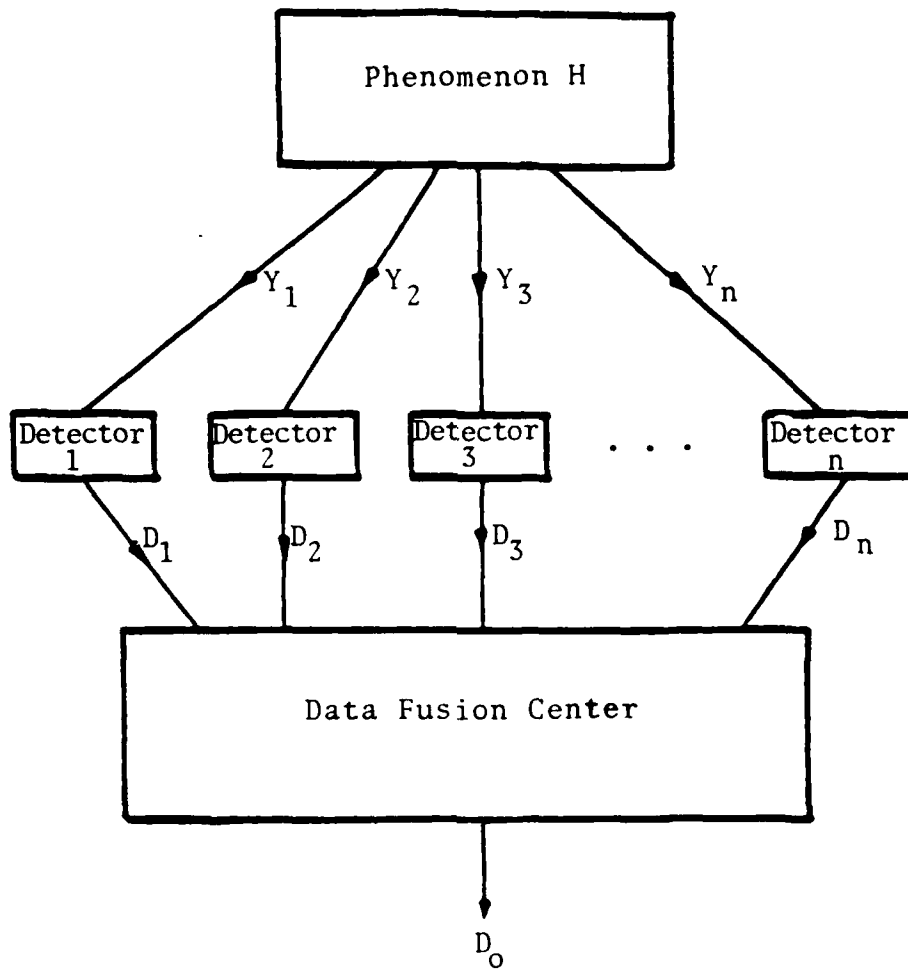


Fig. 1-5. Distributed Sensor System with Data Fusion.

hypotheses. Ekchian and Tenney [20] considered various distributed sensor network topologies and solved some associated Bayesian hypothesis testing problems. Teneketzis [21, 22] has solved the decentralized quickest detection problem and the decentralized Wald problem. Srinivasan [23] has presented some results on distributed radar detection. Kushner and Pacut [24] conducted a simulation study on the effects of specific prior probabilities and parametric dependencies on the decision rule. Chao and Lee [25] presented a distributed detection scheme based on soft local decisions. Conte, D'Addio, Farina and Longo [26] studied the design and performance evaluation of optimum and suboptimum multistatic radar receivers. Chair and Varshney [27] derived the optimum fusion rule at the data fusion center for a Bayesian detection problem with distributed sensors. Hoballah and Varshney [28] solved the problem of Neyman-Pearson detection with distributed radars. In [29], they devised an information theoretic formulation to the distributed detection problem. More work on distributed detection and data fusion has been done by Varshney and his coworkers [30,31].

1.3. Report Organization

In this report, two major topics are considered. The first part deals with CFAR detection in multiple target situations. In Chapter two, we present a weighted cell-averaging CFAR detector for multiple target situations. The leading reference window and the lagging reference window are

weighted and added to yield the adaptive threshold. The relative weights assigned to the reference windows depend upon the level of interference. These weights are selected such that the desired probability of false-alarm is maintained while the probability of detection is maximized. The performance of the weighted cell-averaging CFAR detector is analyzed and compared to the performance of the conventional cell-averaging, the greatest-of-selection cell-averaging and the smallest-of-selection cell-averaging CFAR detectors.

In Chapter three, we present a cell-censored CFAR detector. Each range cell is first compared to a predetermined fixed threshold, where a decision about the presence or absence of an interfering target is made. The cells, where the presence of an interfering target is decided, are not used while forming the adaptive threshold. This censoring scheme eliminates the cells with interfering targets which may otherwise raise the threshold and therefore, lower the probability of detection. The performance of the cell-censored CFAR detector is also studied.

The second part of this report deals with cell-averaging CFAR detection using multiple sensors and data fusion. In Chapter four, we study a system consisting of n CA-CFAR detectors and a data fusion center. Given the fusion rule, first we obtain the optimum threshold multipliers at the individual CFAR detectors by maximizing the overall probability of detection at the data fusion center, while the overall probability of false-alarm is maintained at the desired value.

Next, we consider the optimization of the overall system, i.e., we derive both the optimum fusion rule as well as the optimum threshold multipliers at individual CA-CFAR detectors.

In Chapter five, we consider a system where multiple background estimators are used for the estimation of the background noise. These estimates are transmitted to the CFAR detector. This CFAR detector computes its own estimate of the background noise and combines it with the received estimates to yield the adaptive threshold. The performance of this system is studied and an extension is also proposed.

In Chapter six, we consider adaptive CFAR detection for two distributed sensor network topologies. Specifically, we consider the parallel and the tandem network topologies. In this chapter, the compressed data transmitted amongst the detectors is assumed to be in the form of decisions instead of estimates. The overall systems are optimized to yield the maximum probability of detection for a fixed probability of false-alarm. The performance of the systems is also analyzed.

Finally, in Chapter seven, we present a summary along with a discussion. Some suggestions for future research work are also presented.

CHAPTER II
A WEIGHTED ADAPTIVE CELL-AVERAGING CFAR
DETECTOR FOR MULTIPLE TARGET SITUATIONS

2.1 Introduction

In radar signal detection, the problem is to automatically detect a target in a nonstationary noise and clutter background while maintaining a constant probability of false-alarm. Classical detection using a matched filter receiver and a fixed threshold is not applicable due to the nonstationary nature of the background noise. A small increase in the total noise power results in a corresponding increase of several orders of magnitude in the probability of false-alarm. Therefore, adaptive threshold techniques are needed to maintain CFAR.

In this chapter, we propose and analyze a modified cell-averaging detector for multiple target situations. The leading and the lagging windows are weighted in accordance with the level of interference. Optimum weights, which maintain a constant probability of false-alarm and maximize the probability of detection, are obtained. For the Swerling fluctuating target model I, we obtain the expression for the probability of detection for our weighted cell-averaging CFAR detector. In Section 2.2, we present some background material and assumptions. In Section 2.3,

we derive the expression for the probability of detection for the CA-CFAR, GO-CFAR, and SO-CFAR detectors. In Section 2.4, we evaluate the performance of the weighted cell-averaging CFAR detector, WCA-CFAR. Numerical results showing the performance of the WCA-CFAR detector are also presented. In Section 2.5, we provide a summary along with a discussion of the results.

2.2 Preliminaries

The conventional cell-averaging CFAR processor, shown in Figure 1-2, has been described in Section 1.1-2. There, its performance in the presence of interference was not discussed. In this chapter, we consider cell-averaging CFAR processors, in the presence of interference, i.e., in multiple target situations. We assume that the target at the test cell (center tap), called the primary target is a slowly fluctuating target model of Swerling type I. The signal-to-noise ratio, SNR, of the primary target is denoted by S . Without loss of generality, we assume only one interfering target, the secondary target, in one of the taps of the window U . We assume that this interfering target is also fluctuating in accordance with Swerling target model I with an SNR I . We further assume that the total background noise is white Gaussian. Since the noise samples of the reference window V are identically distributed, the probability density function and the cumulative distribution function are as defined in (1-8) and (1-10). Due to interference, the noise samples of U are

not identically distributed and the probability density function and the cumulative distribution function of U are given as follows (see Appendix A for details).

$$P_U(u) = \frac{1}{\Gamma} \cdot \left[\frac{1+\Gamma}{\Gamma}\right]^{\frac{N}{2}-2} \cdot \left\{ e^{-\frac{u}{1+\Gamma}} - e^{-u} \sum_{j=0}^{(N/2)-2} \frac{1}{j!} \left[\frac{\Gamma}{1+\Gamma}\right]^j u^j \right\},$$

$$u \geq 0 \quad (2-1)$$

$$F_U(u) = 1 - \left[\frac{1+\Gamma}{\Gamma}\right]^{\frac{N}{2}-1} e^{-\frac{u}{1+\Gamma}} + \frac{1}{\Gamma} e^{-u} \sum_{j=0}^{(N/2)-2} \left[\frac{1+\Gamma}{\Gamma}\right]^j \sum_{k=0}^{(N/2)-2-j} \frac{u^k}{k!},$$

$$u \geq 0 \quad (2-2)$$

2.3 Cell-Averaging CFAR Processors

In this section, we derive the expressions of the probability of detection for the CA-CFAR, GO-CFAR, and SO-CFAR detectors. These expressions will be used to compare the performance of these cell-averaging detectors with that of the proposed cell-averaging detector.

2.3-1 CA-CFAR Detector

In the cell-averaging CFAR detector, the adaptive threshold, Q, is obtained from the sum of the reference cells U and V, that is,

$$Q = U + V \quad (2-3)$$

Since the random variables U and V are statistically independent, the cumulative distribution function of the adaptive

threshold, $F_Q^{CA}(q)$, is just

$$\begin{aligned}
 F_Q^{CA}(q) &= \Pr \{Q \leq q\} = \Pr \{U + V \leq q\} \\
 &= \int_{-\infty}^{\infty} P_V(v) \int_{u=-\infty}^{q-v} P_U(u) \, du \, dv \quad (2-4)
 \end{aligned}$$

Using Leibniz's rule, we differentiate equation (2-4) to obtain the probability density function of the adaptive threshold which is just the convolution of the random variables U and V . That is,

$$P_Q^{CA}(q) = P_U(u) * P_V(v) = \int_{-\infty}^{\infty} P_U(u) P_V(q-u) \, du \quad (2-5)$$

where $*$ denotes convolution and Leibniz's rule is defined as follows. If

$$G(u) = \int_{a(u)}^{b(u)} H(x, u) \, dx \quad (2-6.a)$$

then,

$$\frac{dG(u)}{du} = H[b(u), u] \frac{db(u)}{du} - H[a(u), u] \frac{da(u)}{du} + \int_{a(u)}^{b(u)} \frac{\partial H(x, u)}{\partial u} \, dx \quad (2-6.b)$$

Using the fact that $U, V \geq 0$ and $U+V = Q$, equation (2-5) becomes

$$P_Q^{CA}(q) = \int_0^q P_U(u) P_V(q-u) \, du \quad (2-7)$$

Substituting equations (2-1) and (1-8) into equation (2-7),

we have

$$P_Q^{CA}(q) = \frac{1}{\Gamma(\frac{N}{2})} \cdot \frac{1}{I} \cdot \left[\frac{1+I}{I}\right]^{\frac{N}{2}-2} \cdot \left\{ \int_0^q e^{-\frac{u}{1+I}} \cdot e^{-(q-u)} \cdot (q-u)^{\frac{N}{2}-1} du \right. \\ \left. - \sum_{j=0}^{(N/2)-2} \frac{1}{j!} \left[\frac{1}{1+I}\right]^j \int_0^q e^{-u} \cdot e^{-(q-u)} \cdot (q-u)^{\frac{N}{2}-1} u^j du \right\}, q \geq 0 \quad (2-8)$$

If we integrate the right hand side of equation (2-8), we obtain a hypergeometric function for $P_Q^{CA}(q)$. In order to solve for the probability of detection, P_D^{CA} , using equation (1-2), we need to integrate this hypergeometric function from zero to infinity which may not lead to a closed-form solution. To avoid this difficulty, we use an alternate approach and make the following change of variables.

$$\int_0^\infty f(t) \int_0^t f_1(\tau) f_2(t-\tau) d\tau dt = \int_0^\infty f_1(\tau) \int_\tau^\infty f(t) f_2(t-\tau) dt d\tau \quad (2-9)$$

Using the change of variables and substituting equations (2-8) and (1-6) into equation (1-2), P_D^{CA} can then be rewritten as,

$$P_D^{CA} = \frac{1}{\Gamma(\frac{N}{2})} \cdot \frac{1}{I} \left[\frac{1+I}{I}\right]^{\frac{N}{2}-1} \left\{ \int_0^\infty e^{-q\left[\frac{1+S+T_{CA}}{1+S}\right]} \int_0^q e^{-u\left(-\frac{I}{1+I}\right)} (q-u)^{\frac{N}{2}-1} dudq \right. \\ \left. - \sum_{j=0}^{(N/2)-2} \frac{1}{j!} \left[\frac{1}{1+I}\right]^j \int_0^\infty e^{-q\left[\frac{1+S+T_{CA}}{1+S}\right]} \int_0^q (q-u)^{\frac{N}{2}-1} u^j dudq \right\} \quad (2-10)$$

Solving the double integrals, the probability of detection becomes,

$$P_D^{CA} = \frac{C}{(1+S+T_{CA})^{N/2}} \cdot \left[\frac{C'}{1+S+(1+I)T_{CA}} - \frac{1}{I} \sum_{j=0}^{(N/2)-2} \frac{C_j}{(1+S+T_{CA})^{j+1}} \right] \quad (2-11)$$

where,

$$C = \left[\frac{1+I}{I} \right]^{\frac{N}{2}-2} (1+S)^{\frac{N}{2}}$$

$$C' = \left[\frac{1+I}{I} \right] (1+S)$$

and

$$C_j = \left[\frac{I}{1+I} \right]^j (1+S)^{j+1}$$

2.3-2 GO-CFAR Detector

In this case, the adaptive threshold, Q , is the maximum of the reference windows U and V , i.e.,

$$Q = \text{MAX}(U, V) \quad (2-12)$$

The distribution function of the random variable Q is

$$F_Q^{GO}(q) = \text{Pr} \{Q \leq q\} = \text{Pr} \{U \leq q, V \leq q\} \quad (2-13)$$

Since the random variables U and V are statistically independent, we can write

$$\begin{aligned} F_Q^{GO}(q) &= \text{Pr} \{U \leq q\} \cdot \text{Pr} \{V \leq q\} \\ &= F_U(q) F_V(q) \end{aligned} \quad (2-14)$$

The probability density function is, therefore, the derivative

of $F_Q^{GO}(q)$ with respect to q , i.e.,

$$P_Q^{GO}(q) = P_U(q) F_V(q) + F_U(q) P_V(q) \quad (2-15)$$

Substituting equations (1-8), (1-10), (2-1) and (2-2) into equation (2-15), we obtain the probability density function of the adaptive threshold, which is given by

$$P_Q^{GO}(q) = \frac{1}{\Gamma} \left[\frac{1+I}{I} \right]^{\frac{N}{2}-2} \cdot \left\{ 1 - e^{-q} \sum_{j=0}^{(N/2)-1} \frac{1}{j!} q^j \right\} \cdot \left\{ e^{-\frac{q}{1+I}} - e^{-q} \sum_{j=0}^{(N/2)-2} \frac{1}{j!} \left[\frac{I}{1+I} \right]^j q^j \right\} + \frac{1}{\Gamma(\frac{N}{2})} q^{\frac{N}{2}-1} e^{-q} \cdot \left\{ 1 - \left[\frac{1+I}{I} \right]^{\frac{N}{2}-1} e^{-\frac{q}{1+I}} + \frac{1}{I} e^{-q} \sum_{j=0}^{(N/2)-2} \left[\frac{1+I}{I} \right]^j \sum_{k=0}^{(N/2)-2-j} \frac{q^k}{k!} \right\}$$

$$q \geq 0 \quad (2-16)$$

Now, substituting equations (1-3) and (2-16) into equation (1-2) and rearranging terms, the probability of detection for the GO-CFAR detector is obtained from

$$P_D^{GO} = \int_0^{\infty} e^{-\frac{T_{GO} q}{1+S}} P_Q^{GO}(q) dq \quad (2-17)$$

This results in

$$\begin{aligned}
P_D^{GO} &= \frac{1}{I} \left[\frac{1+I}{I} \right]^{\frac{N}{2}-2} \left\{ \frac{(1+S)(1+I)}{(1+S) + (1+I) T_{GO}} - \right. \\
&\sum_{j=0}^{(N/2)-1} \left[\frac{1+S}{2+I+T_{GO}} \right]^{j+1} - \sum_{j=0}^{(N/2)-2} \left[\frac{I}{1+I} \right]^j \cdot \left[\frac{1+S}{1+S+T_{GO}} \right]^{j+1} + \\
&\sum_{j=0}^{(N/2)-2} \sum_{k=0}^{(N/2)-1} \frac{(j+k)!}{j! k!} \left[\frac{I}{1+I} \right]^j \cdot \left[\frac{1+S}{2(1+S)+T_{GO}} \right]^{j+k+1} \} \\
&+ \left[\frac{1+S}{1+S+T_{GO}} \right]^{\frac{N}{2}} - \left[\frac{1+I}{I} \right]^{\frac{N}{2}-1} \cdot \left[\frac{(1+S)(1+I)}{(2+I)(1+S)+(1+I)T_{GO}} \right]^{\frac{N}{2}} \\
&+ \frac{1}{I} \cdot \frac{1}{\Gamma(\frac{N}{2})} \sum_{j=0}^{(N/2)-2} \sum_{k=0}^{(N/2)-2-j} \frac{\Gamma(\frac{N}{2}+k)}{k!} \cdot \left[\frac{1+I}{I} \right]^j \cdot \\
&\left[\frac{1+S}{2(1+S)+T_{GO}} \right]^{\frac{N}{2}+k} \tag{2-18}
\end{aligned}$$

2.3-3 SO-CFAR Detector

In this case, the adaptive threshold, Q , is the minimum of the reference windows U and V , i.e.,

$$Q = \text{MIN}(U, V) \tag{2-19}$$

The distribution function of Q is

$$\begin{aligned}
F_Q^{SO}(q) &= \text{Pr} \{ \text{Min}(U, V) \leq q \} \\
&= \text{Pr} \{ U \leq q \text{ or } V \leq q \} \tag{2-20}
\end{aligned}$$

Using the complementary function, we can write

$$\begin{aligned}
1 - F_Q^{SO}(q) &= \Pr \{ \min(U, V) > q \} \\
&= \Pr \{ U > q \text{ and } V > q \} \\
&= \Pr \{ U > q \} \cdot \Pr \{ V > q \} \\
&= [1 - F_U(q)][1 - F_V(q)] \quad (2-21)
\end{aligned}$$

Therefore, the cumulative distribution of the adaptive threshold is

$$F_Q^{SO}(q) = F_U(q) + F_V(q) - F_U(q)F_V(q) \quad (2-22)$$

Taking the derivative of equation (2-22) with respect to q , we obtain the first order probability density function of the adaptive threshold Q , i.e.,

$$\begin{aligned}
P_Q^{SO}(q) &= P_U(q) + P_V(q) - P_U(q)F_V(q) - F_U(q)P_V(q) \\
&= P_U(q) [1 - F_V(q)] + P_V(q) [1 - F_U(q)] \quad (2-23)
\end{aligned}$$

Substituting equations (1-8), (1-10), (2-1), and (2-2) into equation (2-23), the density of the adaptive threshold becomes

$$\begin{aligned}
P_Q^{SO}(q) &= \frac{1}{I} \left[\frac{1+I}{I} \right]^{\frac{N}{2}-2} \cdot \left\{ e^{-\frac{q}{1+I}} - e^{-q} \sum_{j=0}^{(N/2)-2} \frac{1}{j!} \left[\frac{I}{1+I} \right]^j q^j \right\} \cdot \\
&\quad \left\{ e^{-q} \sum_{j=0}^{(N/2)-1} \frac{1}{j!} q^j \right\} + \frac{1}{\Gamma(\frac{N}{2})} q^{\frac{N}{2}-1} e^{-q} \left\{ \left[\frac{1+I}{I} \right]^{\frac{N}{2}-1} e^{-\frac{q}{1+I}} \right. \\
&\quad \left. - \frac{1}{I} e^{-q} \sum_{j=0}^{(N/2)-2} \left[\frac{1+I}{I} \right]^{(N/2)-2-j} \sum_{k=0}^j \frac{q^k}{k!} \right\}, \quad q \geq 0 \quad (2-24)
\end{aligned}$$

Now, substituting equations (2-24) and (1-6) into equation (1-2), the probability of detection for the SO-CFAR detector is obtained from

$$P_D^{SO} = \int_0^{\infty} e^{-\frac{T_{SO}q}{1+S}} P_Q^{SO}(q) dq \quad (2-25)$$

This results in

$$P_D^{SO} = \frac{1}{I} \left[\frac{1+I}{I} \right]^{\frac{N}{2}-2} \cdot \left\{ \sum_{j=0}^{(N/2)-1} \left[\frac{(1+S)(1+I)}{(2+I)(1+S)+(1+I)T_{SO}} \right]^{j+1} - \right. \\ \left. \sum_{j=0}^{(N/2)-2} \sum_{k=0}^{(N/2)-1} \frac{(j+k)!}{j!k!} \left[\frac{I}{1+I} \right]^j \cdot \left[\frac{1+S}{2(1+S)+T_{SO}} \right]^{j+k+1} \right\} + \\ \left[\frac{1+I}{I} \right]^{\frac{N}{2}-1} \cdot \left[\frac{(1+S)(1+I)}{(2+I)(1+S)+(1+I)T_{SO}} \right]^{\frac{N}{2}} - \\ \frac{1}{I} \cdot \frac{1}{\Gamma(\frac{N}{2})} \sum_{j=0}^{(N/2)-2} \sum_{k=0}^{(N/2)-2-j} \frac{\Gamma(\frac{N}{2}+k)}{k!} \left[\frac{1+I}{I} \right]^j \cdot \left[\frac{1+S}{2(1+S)+T_{SO}} \right]^{\frac{N}{2}+k} \quad (2-26)$$

2.3-4 Threshold Multipliers

The threshold multipliers for the three schemes, T_{CA} , T_{GO} , and T_{SO} , are all different since they depend on the selection logic. To solve for these threshold multipliers, we obtain the expression for the probability of false-alarm of each detector. Then, we set the probability of false-alarm to the desired value ν , and obtain T_{CA} , T_{GO} and T_{SO} , from equations (2-27), (2-28) and (2-29), respectively, by

an iterative procedure. The probabilities of false-alarm of the three cell-averaging detectors are as follows.

$$P_F^{CA} = \frac{D^{\frac{N}{2}-2}}{(1+T_{CA})^{N/2}} \cdot \left[\frac{D}{1+(1+I)T_{CA}} - \frac{1}{I} \sum_{j=0}^{(N/2)-2} \frac{1}{D^j (1+T_{CA})^{j+1}} \right] \quad (2-27)$$

$$P_F^{GO} = \frac{D^{\frac{N}{2}-2}}{I} \cdot \left\{ \frac{1+I}{1+(1+I)T_{GO}} - \sum_{j=0}^{(N/2)-1} \frac{1}{(2+T_{GO})^{j+1}} \right. \\ \left. - \sum_{j=0}^{(N/2)-2} \frac{1}{D^j (1+T_{GO})^j} \right. \\ \left. + \sum_{j=0}^{(N/2)-2} \sum_{k=0}^{(N/2)-1} \frac{(j+k)!}{j! k!} \cdot \frac{1}{D^j (2+T_{GO})^{j+k+1}} \right\} + \frac{1}{(1+T_{GO})^{N/2}} \\ - \frac{D^{\frac{N}{2}-1} (1+I)^{N/2}}{[2+I+(1+I)T_{GO}]^{N/2}} + \frac{1}{I} \cdot \frac{1}{\Gamma(\frac{N}{2})} \sum_{j=0}^{(N/2)-2} \sum_{k=0}^{(N/2)-2-j} \frac{\Gamma(\frac{N}{2}+k)}{k!} \frac{D^j}{(2+T_{GO})^{\frac{N}{2}+k}} \quad (2-28)$$

$$P_F^{SO} = \frac{D^{\frac{N}{2}-2}}{I} \left\{ \sum_{j=0}^{(N/2)-1} \left[\frac{1+I}{2+I+(1+I)T_{SO}} \right]^{j+1} - \right. \\ \left. \sum_{j=0}^{(N/2)-2} \sum_{k=0}^{(N/2)-1} \frac{(j+k)!}{j! k!} \cdot \frac{1}{D^j (2+T_{SO})^{j+k+1}} \right\} + \frac{D^{\frac{N}{2}-1} (1+I)^{\frac{N}{2}}}{[2+I+(1+I)T_{SO}]^{N/2}} \\ - \frac{1}{I} \cdot \frac{1}{\Gamma(\frac{N}{2})} \sum_{j=0}^{(N/2)-2} \sum_{k=0}^{(N/2)-2-j} \frac{\Gamma(\frac{N}{2}+k)}{k!} \cdot \frac{1}{D^j (2+T_{SO})^{\frac{N}{2}+k}} \quad (2-29)$$

where,

$$D = \frac{1+I}{I}$$

Next, we present the weighted CA-CFAR detector.

2.4 Weighted Cell-Averaging CFAR Detector

The proposed weighted cell-averaging constant false-alarm rate detector, WCA-CFAR, for multiple target situations is shown in Figure 2-1. The output from the square law detector is fed into a tapped delay line forming the reference cells. The set of the leading reference cells form the reference window U , while the set of the lagging reference cells form the reference window V . The reference window U is multiplied by the weighting coefficient α , while the lagging reference window V is multiplied by another weighting coefficient, β . These weighted means of the leading cells and the lagging cells are added to yield the adaptive threshold, Q . The output, q_0 , of the test cell from the center tap is compared with the adaptive threshold where a detection decision is made.

An intuitive justification for using a weighted cell-averaging approach is the following. While computing an estimate of the background noise from the reference cells, we should assign more weight to those cells that do not contain interference. Thus, if interference is present in the leading cells, then the weight α assigned to the reference window U should be smaller than the weight β assigned to the reference window V . The relative values of α and β depend upon the level of interference in the reference cells. It should be mentioned that α and β should be such that the desired probability of false-alarm is maintained.

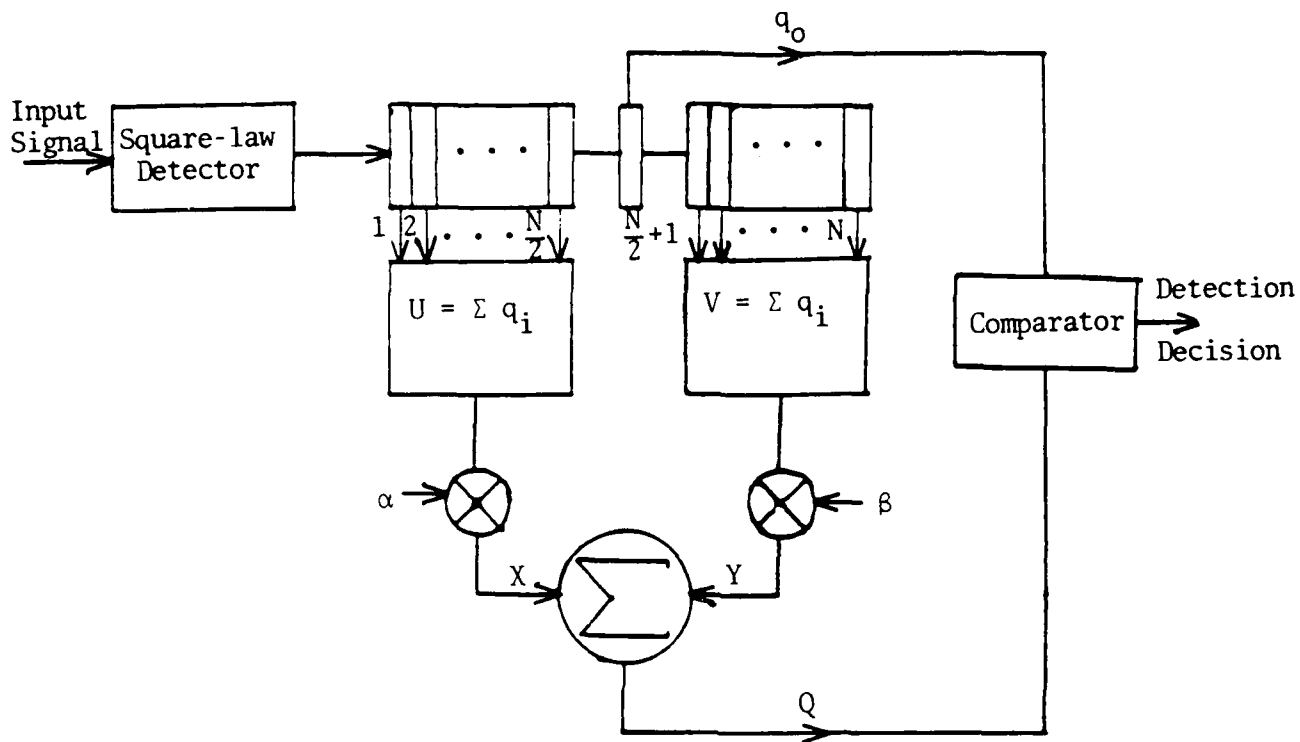


Fig. 2-1. Weighted Cell-Averaging CFAR Detector.

We assume that the primary target at the test cell has a signal-to-noise ratio, S , and the secondary target, or interference has an SNR, I . Without loss of generality, we assume that the interference is in the leading cells only. The primary target and the interfering target are assumed to be fluctuating in accordance with the Swerling target model I. The total noise power in the background is assumed to be white Gaussian. The reference windows U and V are statistically independent random variables. Rescaling U and V by the constants α and β , respectively, we obtain two new independent random variables X and Y , where,

$$P_X(x) = \frac{1}{|\alpha|} P_U\left(\frac{x}{\alpha}\right), \quad \alpha \neq 0 \quad (2-30)$$

and

$$P_Y(y) = \frac{1}{|\beta|} P_V\left(\frac{y}{\beta}\right), \quad \beta \neq 0 \quad (2-31)$$

Substituting equations (1-8) and (2-1) into equations (2-30) and (2-31), we obtain the probability density functions of X and Y to be

$$P_X(x) = \frac{1}{I} \cdot \left[\frac{1+I}{I}\right]^{\frac{N}{2}} \cdot \frac{1}{|\alpha|} \cdot \left\{ e^{-\frac{x}{\alpha(1+I)}} - e^{-\frac{x}{\alpha}} \sum_{j=0}^{(N/2)-2} \frac{1}{j!} \left[\frac{I}{1+I}\right]^j \frac{x^j}{\alpha^j} \right\} \quad \begin{array}{l} x \geq 0 \\ \alpha \neq 0 \end{array} \quad (2-32)$$

$$P_Y(y) = \frac{1}{\Gamma\left(\frac{N}{2}\right)} \cdot \frac{1}{|\beta|} \cdot \frac{1}{\beta^{\frac{N}{2}-1}} y^{\frac{N}{2}-1} e^{-y/\beta}, \quad \begin{array}{l} y \geq 0 \\ \beta \neq 0 \end{array} \quad (2-33)$$

The adaptive threshold, Q , of the weighted cell-averaging detector is the sum of X and Y , i.e.,

$$Q = X + Y \quad (2-34)$$

Since the adaptive threshold Q is the sum of the two independent random variables X and Y , the probability density function, $P_Q^W(q)$ is the convolution of X and Y , i.e.,

$$P_Q^W(q) = P_X(x) * P_Y(y) = \int_{-\infty}^{\infty} P_Y(y) P_X(q-y) dy \quad (2-35)$$

Using the constraints ($X, Y, \geq 0$), the probability density function of the adaptive threshold becomes

$$P_Q^W(q) = \int_0^q P_Y(y) P_X(q-y) dy \quad (2-36)$$

The probability of detection for this WCA-CFAR detector is defined as

$$P_D^W = \int_0^{\infty} \Pr(Q_o > q | Q, H_1) P_Q^W(q) dq \quad (2-37)$$

where

$$\Pr(Q_o > q | Q, H_1) = \int_q^{\infty} P_{Q_o | H_1}(q_o | H_1) dq_o = \exp \left[-\frac{q}{1+S} \right] \quad (2-38)$$

Now, substituting equations (2-36) and (2-38) into (2-37), P_D^W becomes

$$P_D^W = \int_0^\infty e^{-\frac{q}{1+S}} \int_0^q P_Y(y) P_X(q-y) dy \quad (2-39.a)$$

This results in

$$P_D^W = \gamma \int_0^\infty e^{-\frac{q}{1+S}} \int_0^q y^{\frac{N}{2}-1} e^{-y/\beta} \cdot \left\{ e^{-\frac{q-y}{\alpha(1+I)}} - e^{-\frac{q-y}{\alpha}} \sum_{j=0}^{(N/2)-2} \frac{1}{j!} \left[\frac{I}{\alpha(1+I)} \right]^j (q-y)^j \right\} dy dq \quad (2-39.b)$$

where,

$$\gamma = \frac{1}{|\alpha|} \cdot \frac{1}{|\beta|} \cdot \frac{1}{\Gamma(\frac{N}{2})} \cdot \frac{1}{I} \left[\frac{1+I}{I} \right]^{\frac{N}{2}-2}$$

Using the identity (2-9), the probability of detection can be rewritten as

$$P_D^W = \gamma \int_0^\infty y^{\frac{N}{2}-1} e^{-y \left[\frac{1}{\beta} - \frac{1}{\alpha(1+I)} \right]} \int_0^\infty e^{-q \left[\frac{1}{1+S} + \frac{1}{\alpha(1+I)} \right]} dq dy - \gamma \sum_{j=0}^{(N/2)-2} \frac{1}{j!} \left[\frac{I}{\alpha(1+I)} \right]^j \int_0^\infty e^{-y \left[\frac{1}{\beta} - \frac{1}{\alpha} \right]} \int_y^\infty e^{-q \left[\frac{1}{1+S} + \frac{1}{\alpha} \right]} (q-y)^j dq dy \quad (2-40)$$

Solving the double integrals, the probability of detection is given by

$$P_D^W = \frac{\alpha}{|\alpha|} \cdot \frac{\beta}{|\beta|} \cdot \frac{C}{(1+S+\beta)^{N/2}} \cdot \left[\frac{C'}{\{1+S+\alpha(1+I)\}} - \frac{1}{I} \sum_{j=0}^{(N/2)-2} \frac{C_j}{(1+S+\alpha)^{j+1}} \right] \quad (2-41)$$

where C , C' , and C_j are as defined in (2-11).

The goal of our WCA-CFAR detector is to obtain the weights α and β so as to obtain the best P_D^W while keeping the false-alarm probability, P_F^W , to be a constant ν . This can be achieved by using the calculus of extrema, for which we form the following objective function.

$$J(\alpha, \beta) = P_D^W(\alpha, \beta) + \xi [P_F^W(\alpha, \beta) - \nu] \quad (2-42)$$

where ν is the desired false-alarm probability and ξ is the Lagrange multiplier. To obtain the optimum values of α and β , we maximize the objective function $J(\alpha, \beta)$, i.e., we take the derivatives of $J(\alpha, \beta)$ with respect to α and β , set them equal to zero, and solve for α and β . The derivatives are

$$\frac{\partial J(\alpha, \beta)}{\partial \alpha} = \frac{C}{(1+S+\beta)^{\frac{N}{2}}} \cdot \left[\frac{-C'(1+I)}{\{1+S+\alpha(1+I)\}^2} + \frac{1}{I} \sum_{j=0}^{(N/2)-2} \frac{(j+1) C_j}{(1+S+\alpha)^{j+2}} \right] -$$

$$\xi \frac{D^{\frac{N}{2}-2}}{(1+\beta)^{N/2}} \cdot \left[\frac{-D(1+I)}{\{1+\alpha(1+I)\}^2} + \frac{1}{I} \sum_{j=0}^{(N/2)-2} \frac{j+1}{D^j (1+\alpha)^{j+2}} \right] = 0 \quad (2-43)$$

and

$$\frac{\partial J(\alpha, \beta)}{\partial \beta} = \frac{C}{(1+S+\beta)^{\frac{N+1}{2}}} \cdot \left[\frac{C'}{1+S+\alpha(1+I)} - \frac{1}{I} \sum_{j=0}^{(N/2)-2} \frac{C_j}{(1+S+\alpha)^{j+1}} \right] +$$

$$\xi \frac{D^{\frac{N}{2}-2}}{(1+\beta)^{\frac{N}{2}+1}} \cdot \left[\frac{D}{1+\alpha(1+I)} - \frac{1}{I} \sum_{j=0}^{(N/2)-2} \frac{1}{D^j (1+\alpha)^{j+1}} \right] = 0 \quad (2-44)$$

where,

$$D = \frac{1+I}{I}$$

We obtain ξ from equation (2-43), substitute for it in equation (2-44), and solve for β in terms of α . We obtain

$$\beta = \frac{(1+S) H_2 - H_1}{H_1 - H_2} \quad (2-45.a)$$

where

$$H_1 = \left[\frac{C'}{1+S+\alpha(1+I)} - \frac{1}{I} \sum_{j=0}^{(N/2)-2} \frac{C_j}{(1+S+\alpha)^{j+1}} \right] \cdot \left[\frac{-D(1+I)}{\{1+\alpha(1+I)\}^2} + \frac{1}{I} \sum_{j=0}^{(N/2)-2} \frac{(j+1)}{D^j (1+\alpha)^{j+2}} \right] \quad (2-45.b)$$

and

$$H_2 = \left[\frac{-C'(1+I)}{\{1+S+\alpha(1+I)\}^2} + \frac{1}{I} \sum_{j=0}^{(N/2)-2} \frac{(j+1)C_j}{(1+S+\alpha)^{j+2}} \right] \cdot \left[\frac{D}{1+(1+I)\alpha} - \frac{1}{I} \sum_{j=0}^{(N/2)-2} \frac{1}{D^j (1+\alpha)^{j+1}} \right] \quad (2-45.c)$$

Knowing the fact that the probability of false-alarm is

$$P_F^W = \frac{\alpha}{|\alpha|} \cdot \frac{\beta}{|\beta|} \cdot \frac{D^{\frac{N}{2}-2}}{(1+\beta)^{N/2}} \left[\frac{D}{1+\alpha(1+I)} - \frac{1}{I} \sum_{j=0}^{(N/2)-2} \frac{1}{D^j (1+\alpha)^{j+1}} \right], \quad (2-46)$$

we substitute for β from equation (2-45) into equation (2-46), and obtain a nonlinear equation in terms of α only. Using an iterative procedure, we solve for α and β . Since the equations are nonlinear, more than one solution may be obtained. Only those solutions which satisfy the given constraints of the problem are kept.

We obtain some numerical results to illustrate the performance of the WCA-CFAR detector. The desired P_F^W is assumed to be 10^{-4} . In Figures 2-2, 2-3, 2-4, we compare the performance of the WCA-CFAR with the CA-CFAR, GO-CFAR, SO-CFAR detectors in terms of P_D^N versus SNR curves for different interference levels. We notice that the WCA-CFAR detector performs better than the other three. In Figure 2-5, we show the performance of the WCA-CFAR detector as a function of the interference level. In Figures 2-6, 2-7, and 2-8 we also observe the performance of the WCA-CFAR detector as a function of the interference level. As expected, in Figures 2-6, 2-7, and 2-8 we observe that the performance of the WCA-CFAR improves when the number of reference cells is increased.

2.5 Summary and Conclusions

In this chapter, we proposed a weighted cell-averaging CFAR detector for multiple target situations. In this detector, the weighted leading and lagging reference windows are added to obtain the adaptive threshold. The weights are selected so that CFAR is achieved while maximizing the probability of detection. It results in a smaller weight being assigned to the window where interference occurs and more weight is assigned to the window without interference. This weighting procedure prevents the adaptive threshold from becoming too high and resulting in a severe degradation of the probability of detection. For Swerling target model I embedded in a white Gaussian noise of unknown level, we showed that the WCA-CFAR detector performs better than the CA-CFAR, GO-CFAR and SO-CFAR detectors.

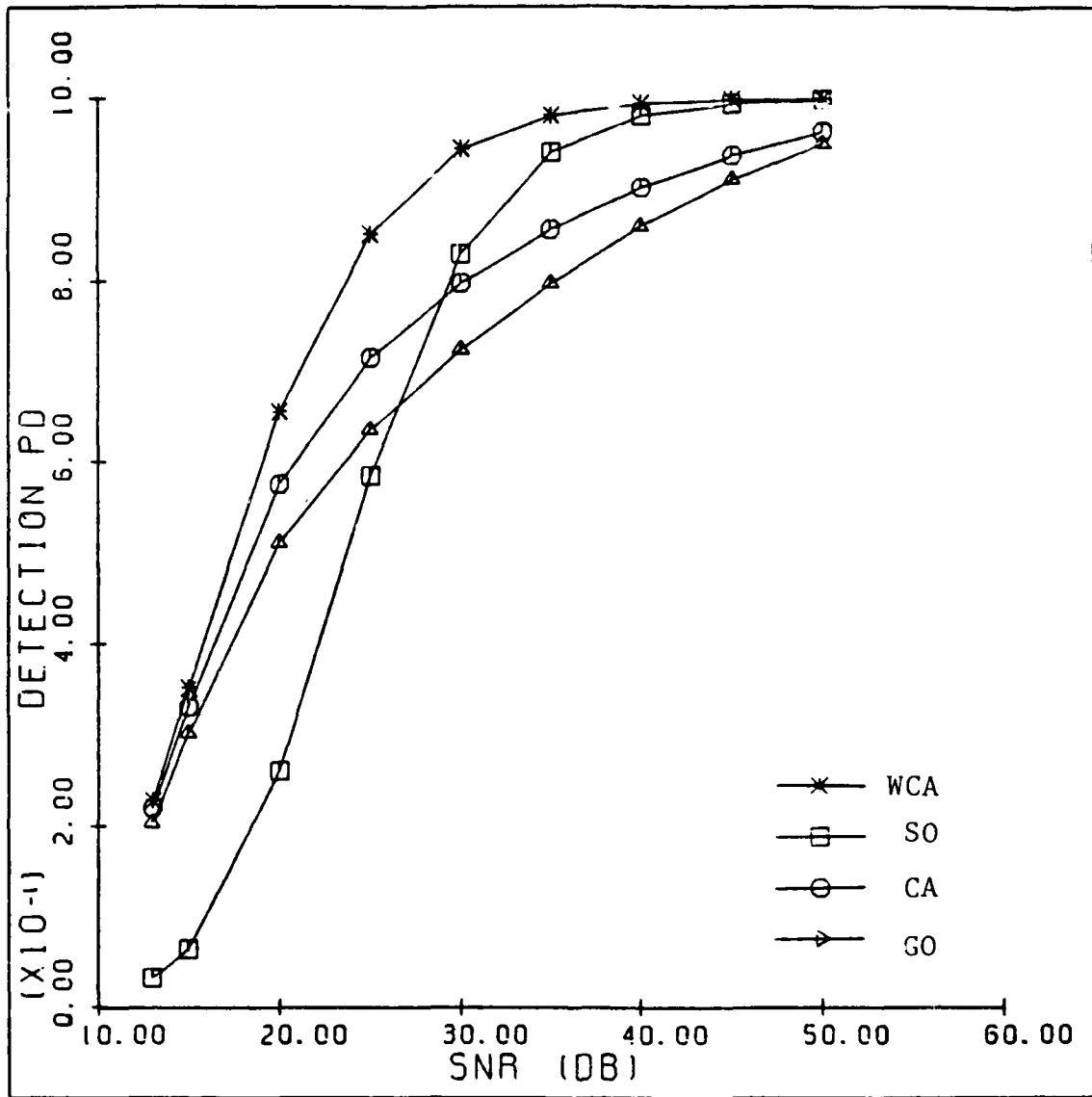


Fig.2-2. Detection Probability for CA, GO, SO and WCA-CFAR Detectors for $N=4$, $P_F = 10^{-4}$, and $I=S \div 10$.

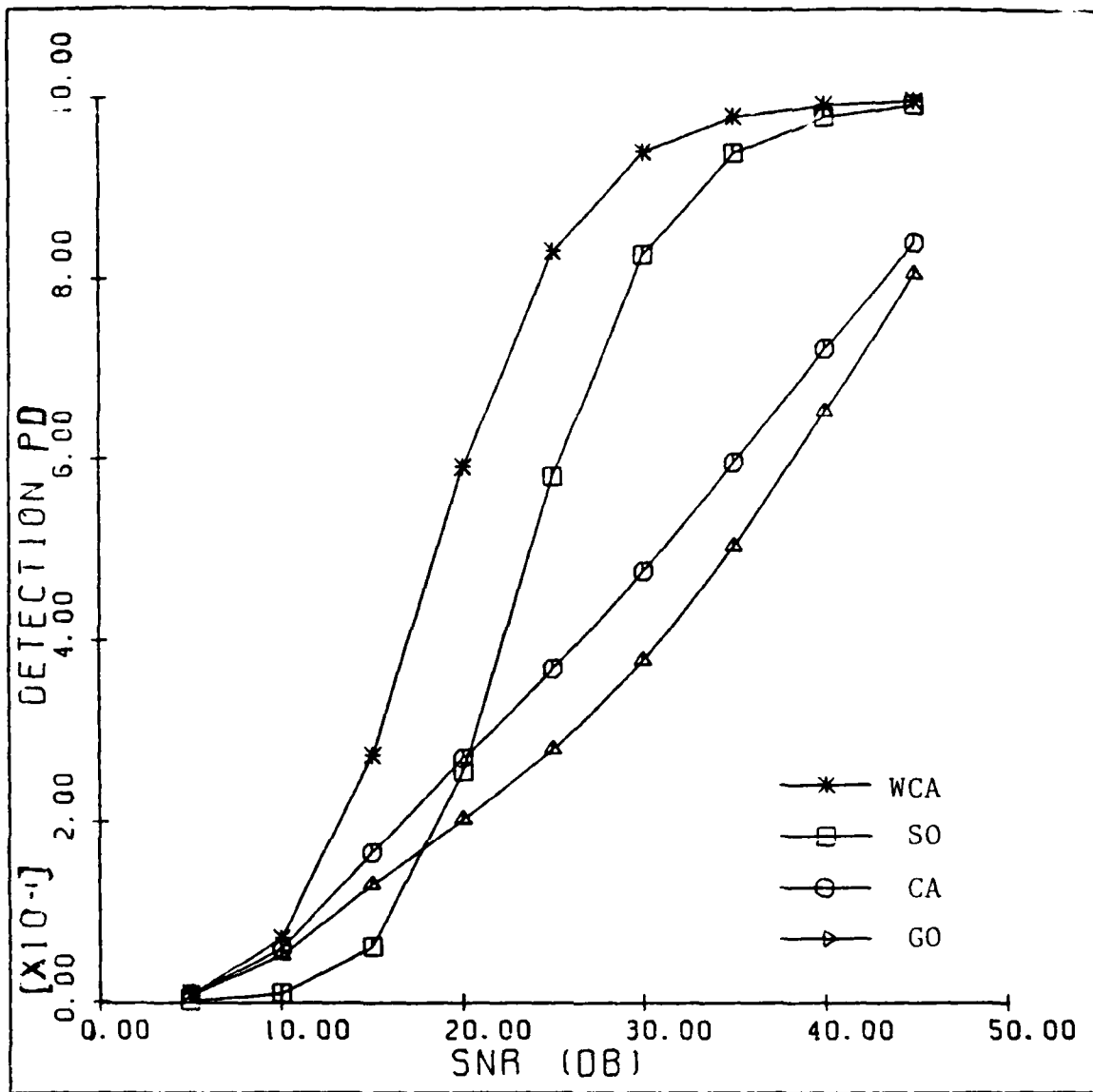


Fig. 2-3. Detection Probability for CA, SO, GO, and WCA-CFAR Detectors for $N=4$, $P_F = 10^{-4}$, and $I=S$.

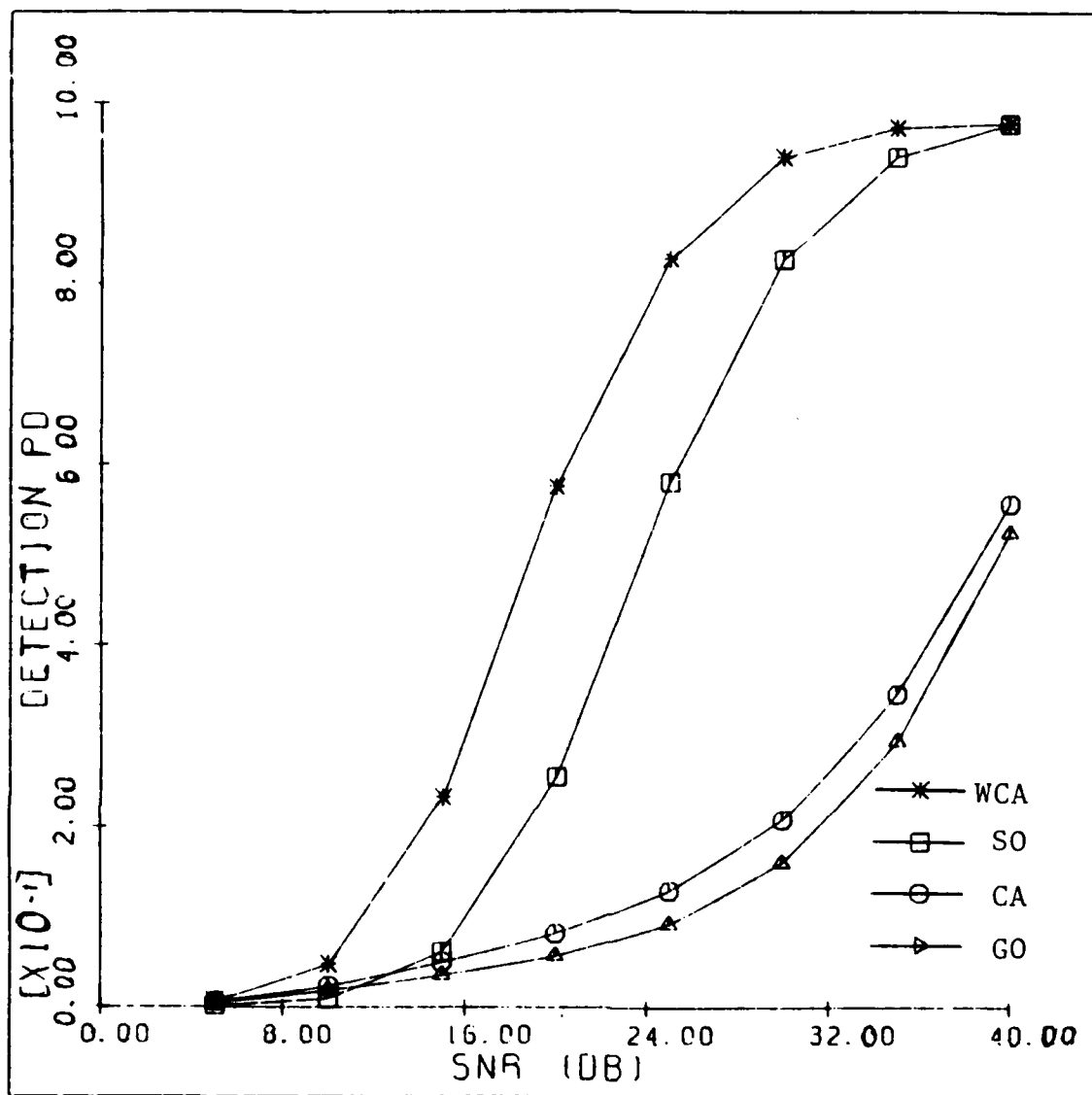


Fig.2-4. Detection Probability for CA, GO, SO, and WCA-CFAR Detectors for $N=4$, $P_F = 10^{-4}$, and $I=S \times 10$.

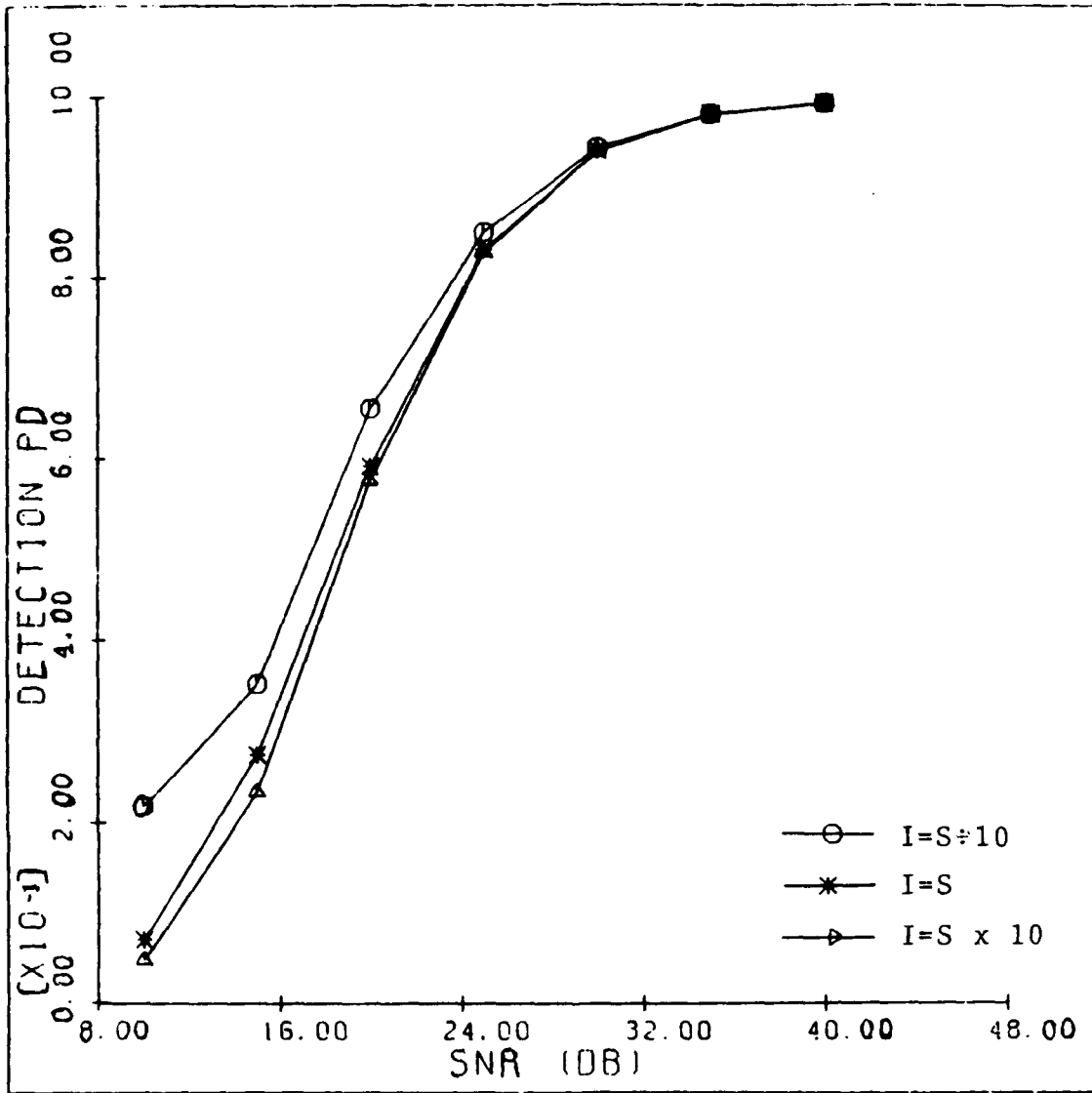


Fig. 2-5. Detection Probability for WCA-CFAR Detector when $N=4$, $P_F = 10^{-4}$, $I=S \div 10$, $I=S$ and $I=S \times 10$.

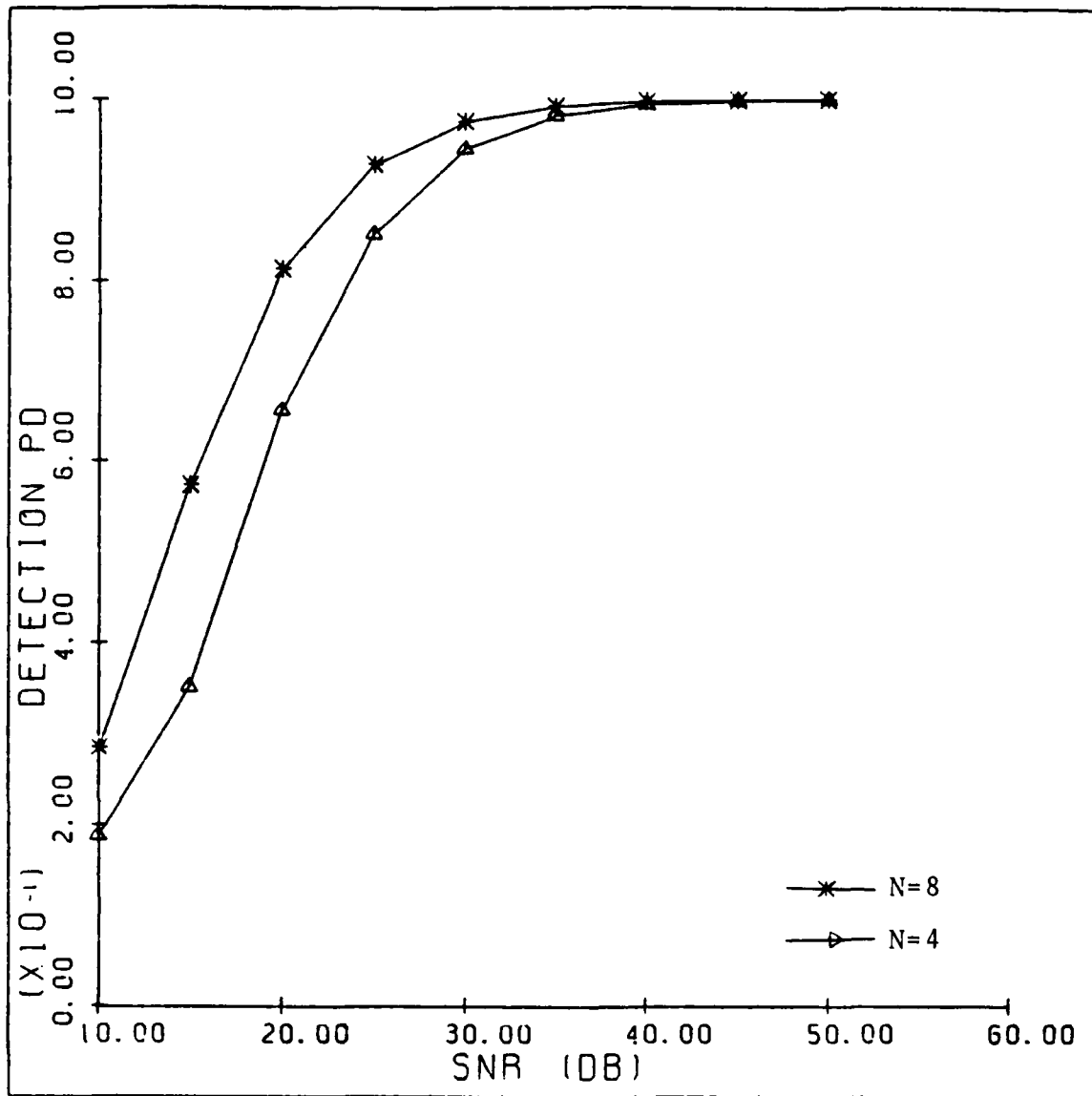


Fig.2-6. Detection Probability for WCA-CFAR Detector when $P_F = 10^{-4}$, $I=S \div 10$, $N=4$ and $N=8$.

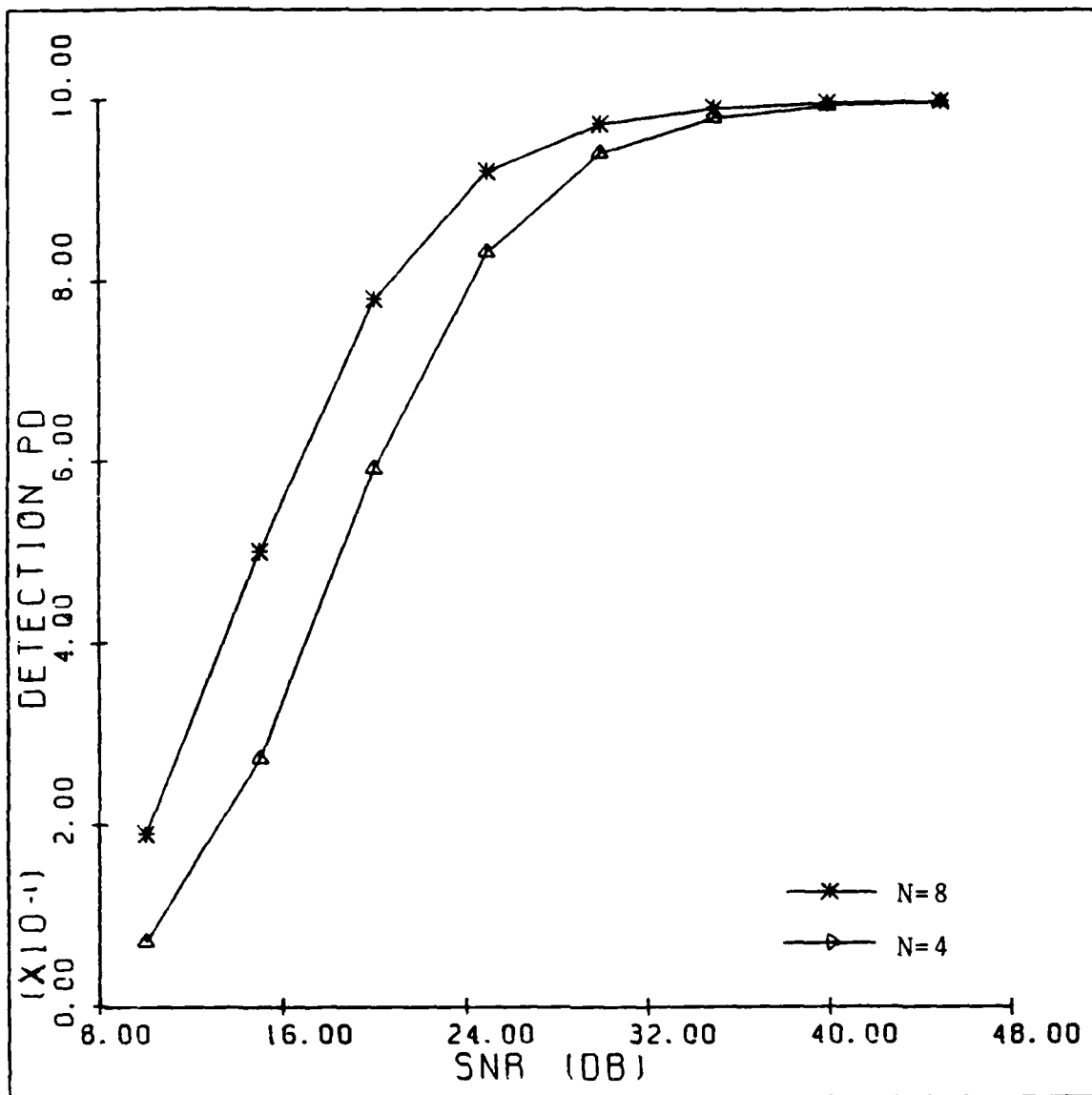


Fig. 2:7. Detection Probability for WCA-CFAR Detector when $P_F = 10^{-4}$, $I=S$, $N=4$ and $N=8$.

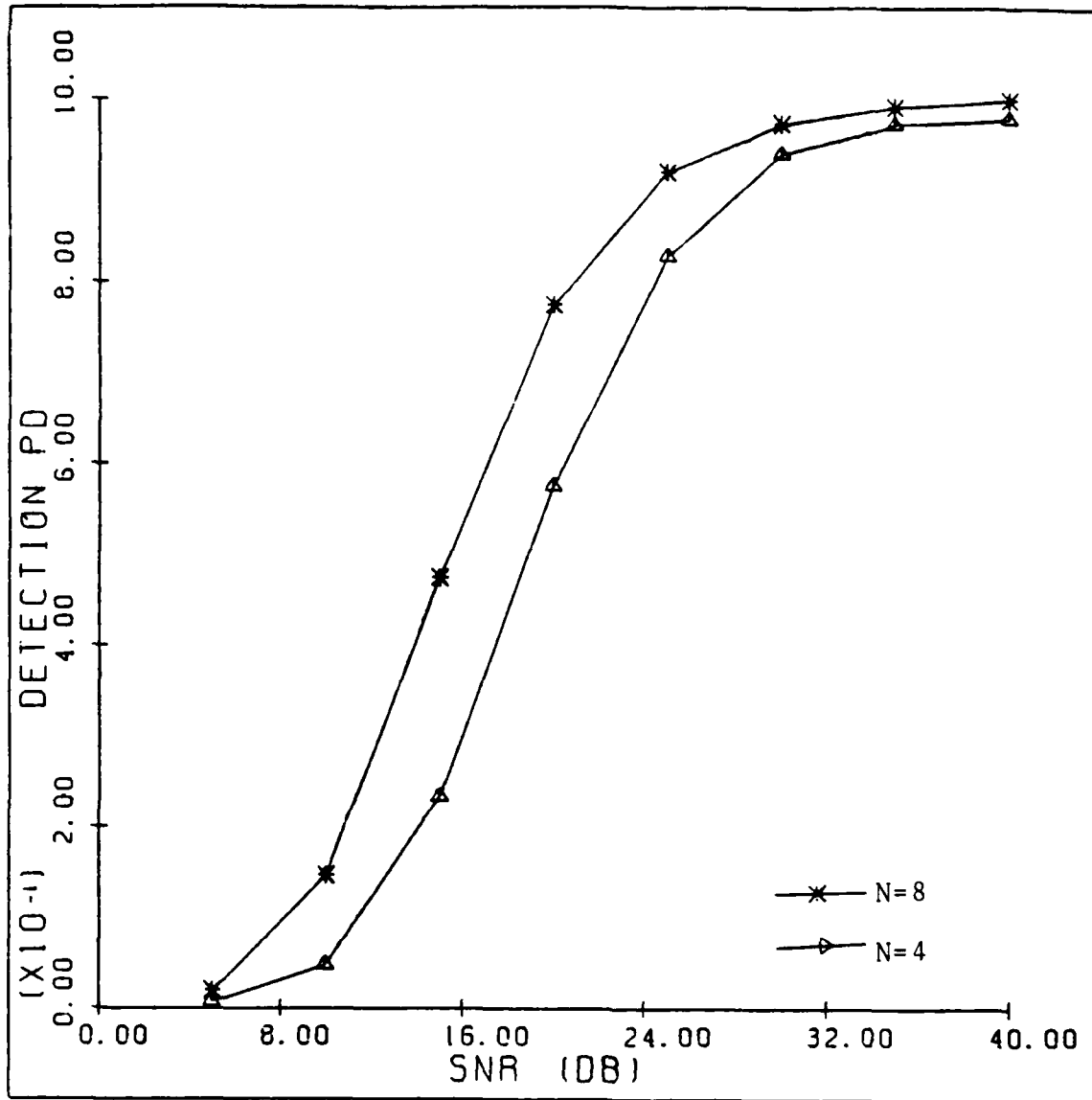


Fig. 2-8. Detection Probability for WCA-CFAR Detector when $P_F = 10^{-4}$, $I=S \times 10$, $N=4$ and $N=8$.

CHAPTER III
A CELL-CENSORED CFAR DETECTOR FOR
MULTIPLE TARGET SITUATIONS

3.1. Introduction

In the previous chapter, we proposed and analyzed the WCA-CFAR detector, which was shown to perform better than the CA-CFAR, GO-CFAR and SO-CFAR detectors for multiple target situations. In this chapter, we propose another scheme for adaptive cell-averaging CFAR detection for multiple target situations, where we censor those cells which may contain interference or noise spikes in them. In Section 3.2, we formulate the problem and study the performance of the proposed CFAR detector. In Section 3.3, we present a summary along with a discussion.

3.2. Cell-Censored CFAR Detection

The cell-censored mean-level detector considered in this chapter is shown in Figure 3-1. In this detector, the idea is to delete those cells, which may contain interference, while estimating the background noise. The output of each range cell is compared to a predetermined fixed threshold, λ , to determine the presence or absence of interference in that

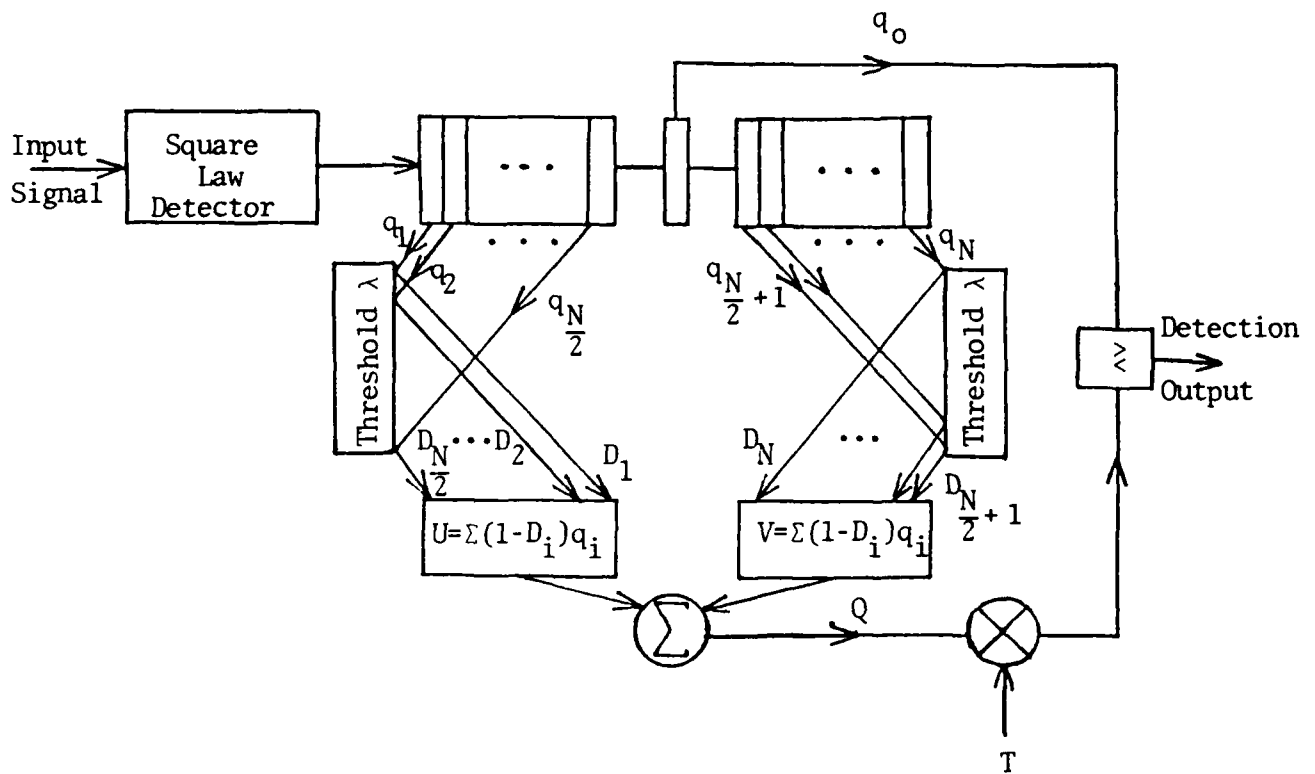


Fig. 3-1. Cell-Censored CFAR Detector.

range cell. The desired probability of false-alarm at the range cells determines the fixed threshold λ . The comparison of each range cell to λ yields a decision, D_i , $i=1,2,\dots,N$, where $D_i \in \{0,1\}$. When D_i , $i=1,2,\dots,N$, is one, it indicates the presence of interference in the i th cell. This cell is then censored and is not used while computing the estimate of the background noise. However, when D_i , $i=1,2,\dots,N$, is zero, it indicates the absence of interference in the i th cell and this cell is used in the estimation of the background. The estimate of the background noise is used to set the adaptive threshold, Q . As before, Q is scaled by a threshold multiplier, T , prior to comparison with the output of the center tap to yield the desired overall probability of false-alarm at the output. As seen in the previous chapters, presence of interference in the range cells raises the threshold unnecessarily and consequently, it reduces the probability of detection and the probability of false-alarm drastically. The proposed cell-censoring scheme prevents the adaptive threshold from becoming too high by eliminating the cells which may contain interference and thereby improves the system performance.

The leading range cells, for which an absence of interference is decided, form the leading reference window U , while the lagging range cells, for which an absence of interference is decided, form the lagging reference window V , i.e.,

$$U = \sum_{i=1}^{N/2} (1 - D_i) q_i \quad (3-1)$$

and

$$V = \sum_{i=(N/2)+1}^N (1 - D_i) q_i \quad (3-2)$$

Clearly, when D_i is one, the corresponding q_i drops out of the summation. As in the conventional cell-averaging CFAR detector, the adaptive threshold, Q , is obtained by summing the reference windows U and V . Q is then scaled by the threshold multiplier, T , in order to achieve CFAR at the desired value. The output, q_o , from the cell under test (center tap) is compared to the threshold, TQ , to yield the final decision D_o , $D_o \in \{0,1\}$.

We assume that the target to be detected, or the primary target at the test cell, is slowly fluctuating in accordance with Swerling target model I. We also assume that the interfering targets are of Swerling type I. Then, the probability density function of the normalized output of a range cell without interference is

$$P_{Q_i}(q_i) = e^{-q_i}, \quad q_i \geq 0, \quad (3-3)$$

$$i=1,2,\dots,N$$

and the probability density function of the normalized output of a range cell with interference is given by

$$P_{Q_i}^I(q_i) = \frac{1}{1+I_i} e^{-\frac{q_i}{1+I_i}}, \quad q_i \geq 0, \quad (3-4)$$

$$i=1,2,\dots,N$$

where I_i , $i=1,2,\dots,N$, denotes the SRN of the interference (if present) in the i th range cell and the superscript I in $P_{Q_i}^I(q_i)$ indicates the presence of interference in the i th range cell.

Next, we evaluate the performance of the proposed system when there might be only one interfering target with an SNR I in one of the taps of the leading reference window U . Without loss of generality, we assume that it is in the first cell. Then U and V are expressed as

$$U = \sum_{i=2}^{N/2} q_i + Z \quad (3-5)$$

and

$$V = \sum_{i=(N/2)+1}^N q_i \quad (3-6)$$

where Z corresponds to the output of the first cell which may contain interference, i.e.,

$$Z = (1 - D_1) q_1 \quad (3-7)$$

The discrete probability density function of the random variable D_1 is given by

$$P_{D_1}(d_1) = P_1^C \delta(d_1 - 1) + (1 - P_1^C) \delta(d_1) \quad (3-8)$$

where, $\delta(x)$ is the Kronecker delta function such that,

$$\delta(x - x_0) = \begin{cases} 1, & \text{if } x = x_0 \\ 0, & \text{if } x \neq x_0 \end{cases} \quad (3-9)$$

P_1^C is the probability that the decision D_1 is one, and $(1 - P_1^C)$ the probability that D_1 is zero. The superscript c in P_1^C indicates that it is the probability associated with an individual cell. We may express P_1^C as

$$\begin{aligned} P_1^C &= \Pr(D_1 = 1 | H_1^I) P(H_1^I) + \Pr(D_1 = 1 | H_0^I) P(H_0^I) \\ &= P_{D_1}^C P_1^I + P_{F_1}^C P_0^I \end{aligned} \quad (3-10)$$

where H_0^I is the hypothesis that no interference is present in the first cell while the hypothesis H_1^I indicates that interference is present in the first cell. $P_{F_1}^C$ is the pre-specified probability of false-alarm at the first cell which determines the fixed threshold λ . P_0^I and P_1^I are the prior probabilities indicating the absence and presence of the interfering target of SNR I at the first cell, respectively. The random variable Z of equation (3-7) is defined as

$$Z = GQ_1 \quad (3-11)$$

where

$$G = 1 - D_1, \quad G \in \{0,1\} \quad (3-12)$$

If D_1 is one, G is zero and thereby implying that Z is zero.

Since P_1^C represents the probability that D_1 is one, the probability that Z is zero is also P_1^C . When D_1 is zero, then due to the independence of the random variables G and Q_1 , the probability density function of Z is

$$P_Z(z) = \int_{-\infty}^{\infty} (1-P_1^C) \delta(g-1) e^{-z/g} \frac{1}{|g|} dg \quad (3-13)$$

Solving the integral, we can write the probability density function of Z as

$$P_Z(z) = \begin{cases} P_1^C & , \quad z = 0 \\ (1 - P_1^C) e^{-z} & , \quad z > 0 \end{cases} \quad (3-14)$$

From equation (3-10), we know that P_1^C is a function of $P_{D_1}^C$ and $P_{F_1}^C$, where $P_{F_1}^C$ and $P_{D_1}^C$ are

$$\begin{aligned} P_{F_1}^C &= \text{Pr}(\text{decide interference in the first cell} | \text{no} \\ &\quad \text{interference present}) \\ &= \int_{\lambda}^{\infty} e^{-q_1} dq_1 = e^{-\lambda} \end{aligned} \quad (3-15)$$

and

$$\begin{aligned} P_{D_1}^C &= \text{Pr}(\text{decide interference in the first cell} | \text{in-} \\ &\quad \text{terference present}) \\ &= \int_{\lambda}^{\infty} \frac{1}{1+I} e^{-\frac{q_1}{1+I}} dq_1 = e^{-\frac{\lambda}{1+I}} \end{aligned} \quad (3-16)$$

Let

$$U_1 = \sum_{i=2}^{N/2} q_i \quad (3-17)$$

then from Appendix A,

$$P_{U_1}(u_1) = \frac{1}{\Gamma(\frac{N}{2} - 1)} u_1^{\frac{N}{2} - 1} e^{-u_1}, \quad u_1 \geq 0 \quad (3-18)$$

The probability density function of V is as defined in equation (1-8). The adaptive threshold Q is the sum of U_1 , V and Z , i.e.,

$$Q = U_1 + V + Z \quad (3-19)$$

Then, the probability density function of the adaptive threshold, Q , is the convolution of the probability density functions of U_1 , V and Z , i.e.,

$$P_Q(q) = P_{U_1}(u_1) * P_V(v) * P_Z(z) \quad (3-20)$$

where $*$ denotes convolution as before. If we define R as

$$R = U_1 + V, \quad (3-21)$$

then the probability density function of R is (see Appendix A)

$$P_R(r) = \frac{1}{\Gamma(N-1)} r^{N-2} e^{-r}, \quad r \geq 0 \quad (3-22)$$

The probability density function of the adaptive threshold, Q , becomes

$$\begin{aligned}
P_Q(q) &= P_R(r) * P_Z(z) \\
&= \int_0^{\infty} P_R(r) P_Z(q-r) dr \quad (3-23)
\end{aligned}$$

Substituting equations (3-14) and (3-22) into equation (3-23) and solving the integral, we obtain

$$\begin{aligned}
P_Q(q) &= \frac{P_1^C}{\Gamma(N-1)} q^{N-2} e^{-q} + \frac{1-P_1^C}{\Gamma(N)} q^{N-1} e^{-q}, \quad (3-24) \\
&q \geq 0
\end{aligned}$$

To obtain the expression for the probability of detection, we substitute equation (3-24) into equation (1-4) and solve the integral to obtain the probability of detection, P_D , to be

$$P_D = P_1^C \left[\frac{1+S}{1+S+T} \right]^{N-1} + (1 - P_1^C) \left[\frac{1+S}{1+S+T} \right]^N \quad (3-25)$$

The probability of false-alarm is

$$P_F = \frac{P_1^C}{(1+T)^{N-1}} + \frac{1 - P_1^C}{(1+T)^N} \quad (3-26)$$

To evaluate the performance of the proposed cell-censored CFAR detector, we obtain some numerical results. We assume that the desired overall probability of false-alarm, P_F , is 10^{-5} ; the number of range cells, N , is 4; while the SNR of the interfering target is one tenth of the SNR of the primary target. From Figure 3-2, we observe that as λ is

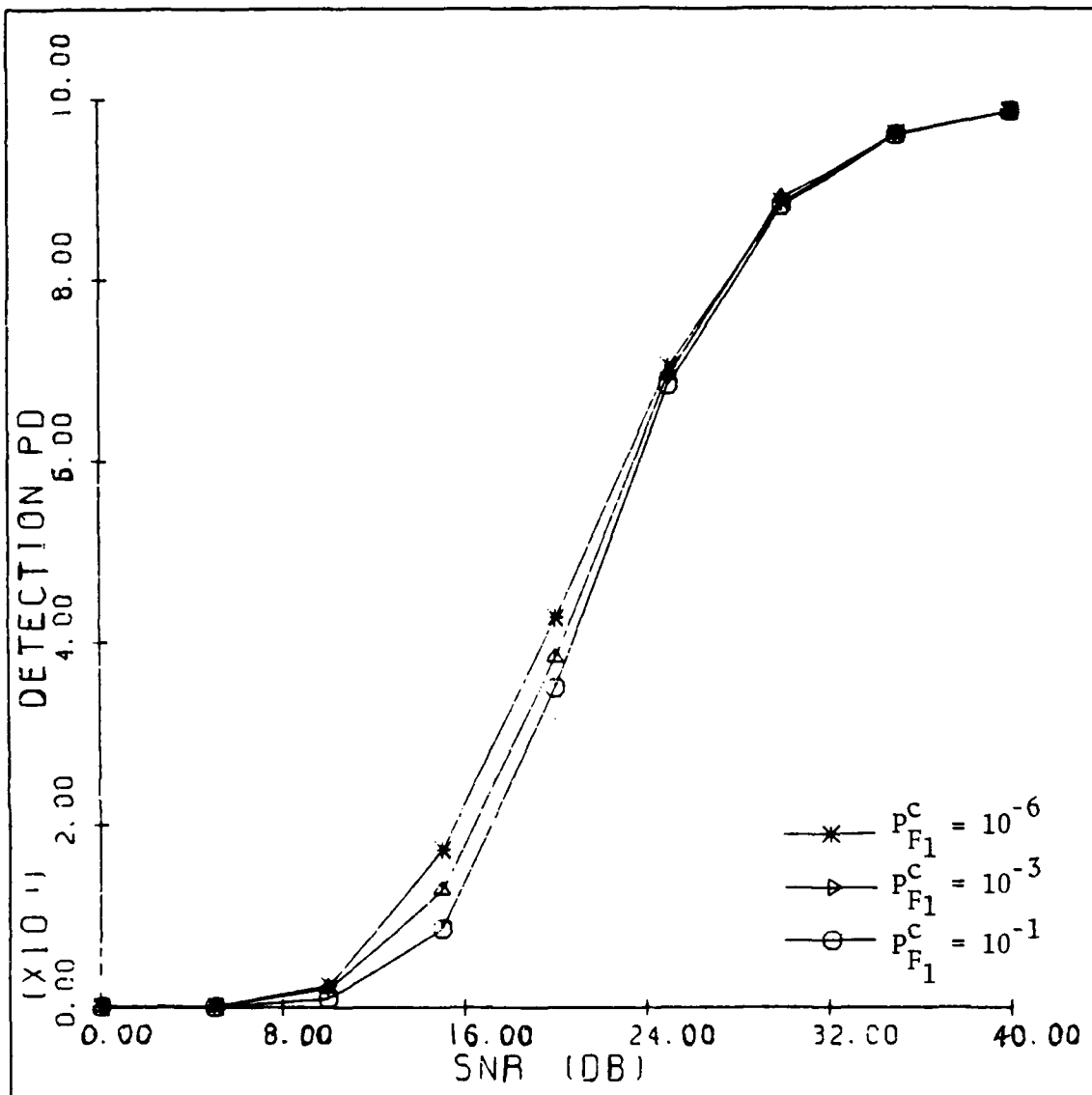


Fig. 3-2. Performance of the Cell-Censored CFAR Detector
 $P_F = 10^{-5}$, $P_O = 0.5$ and $I = S \div 10$.

increased ($P_{F_1}^C$ is reduced), the probability of detection, P_D , improves. We also notice from Figures 3-3, 3-4 and 3-5 that the performance of the conventional cell-averaging CFAR detector is better than the performance of the cell-censored CFAR detector for small values of the target SNR. As the SNR of the interfering target increases, at a certain point the cell with the interfering target is censored and the performance of the cell-censored CFAR detector becomes better than that of the CA-CFAR detector. The point at which this crossover takes place depends upon the value of $P_{F_1}^C$. It should be noted that if we make $P_{F_1}^C$ smaller, the crossover point would occur at a smaller value of the SNR of the interfering target.

3.3. Summary and Conclusions

In this chapter, we have proposed a CFAR detector using a cell-censoring scheme for multiple target situations. We analyzed the system for the case when no more than one interfering target may be present. The analysis for situations when more than one interfering targets are present can be carried out in a similar manner. Numerical results indicate that the proposed scheme is effective in a multiple target environment.

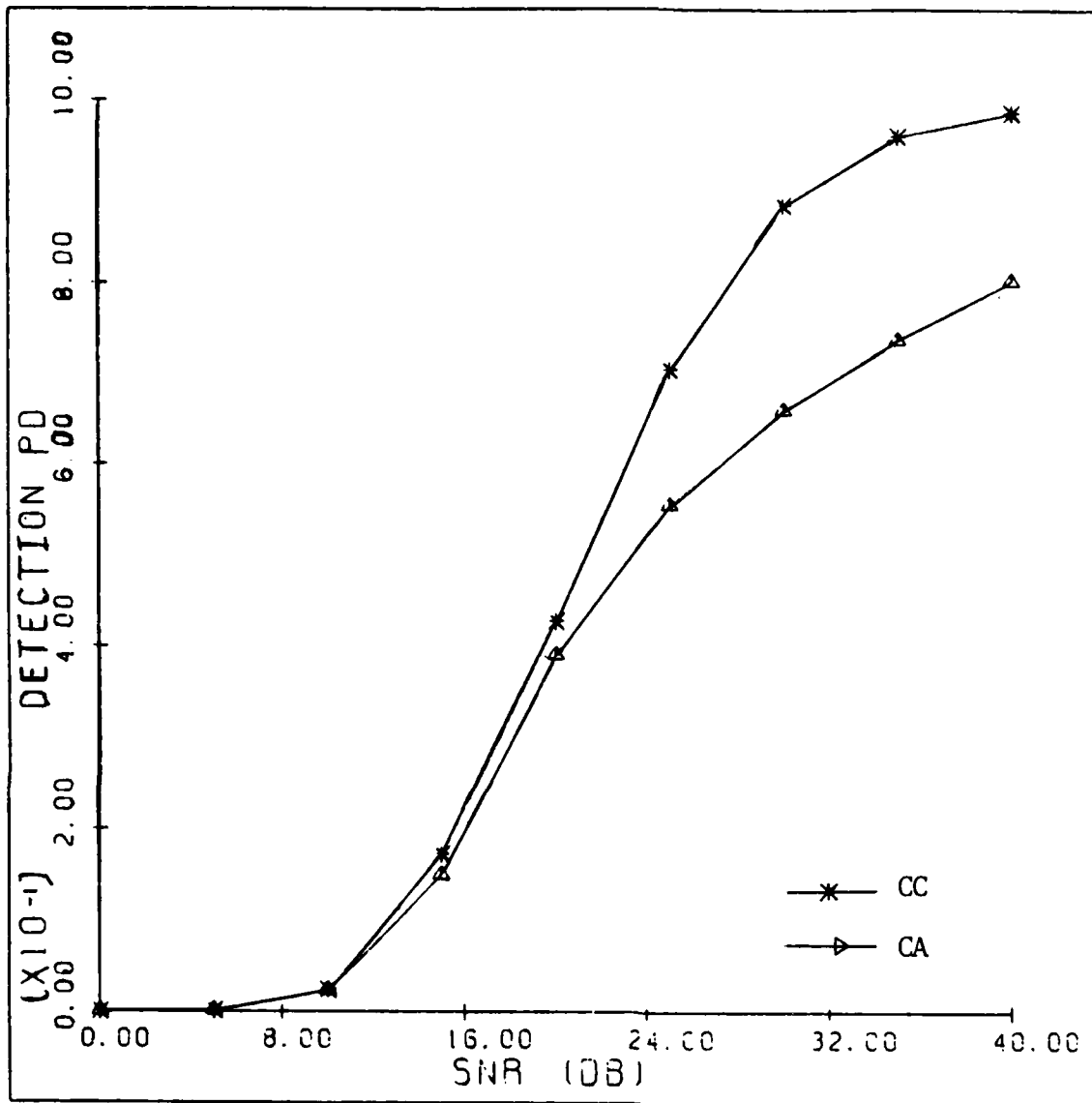


Fig. 3 - 3. A Performance Comparison of the Cell-Censored (CC) CFAR Detector and the CA-CFAR Detector.

$P_F = 10^{-5}$, $P_{F_1}^C = 10^{-6}$, $P_O = 0.5$ and $I = S \div 10$.

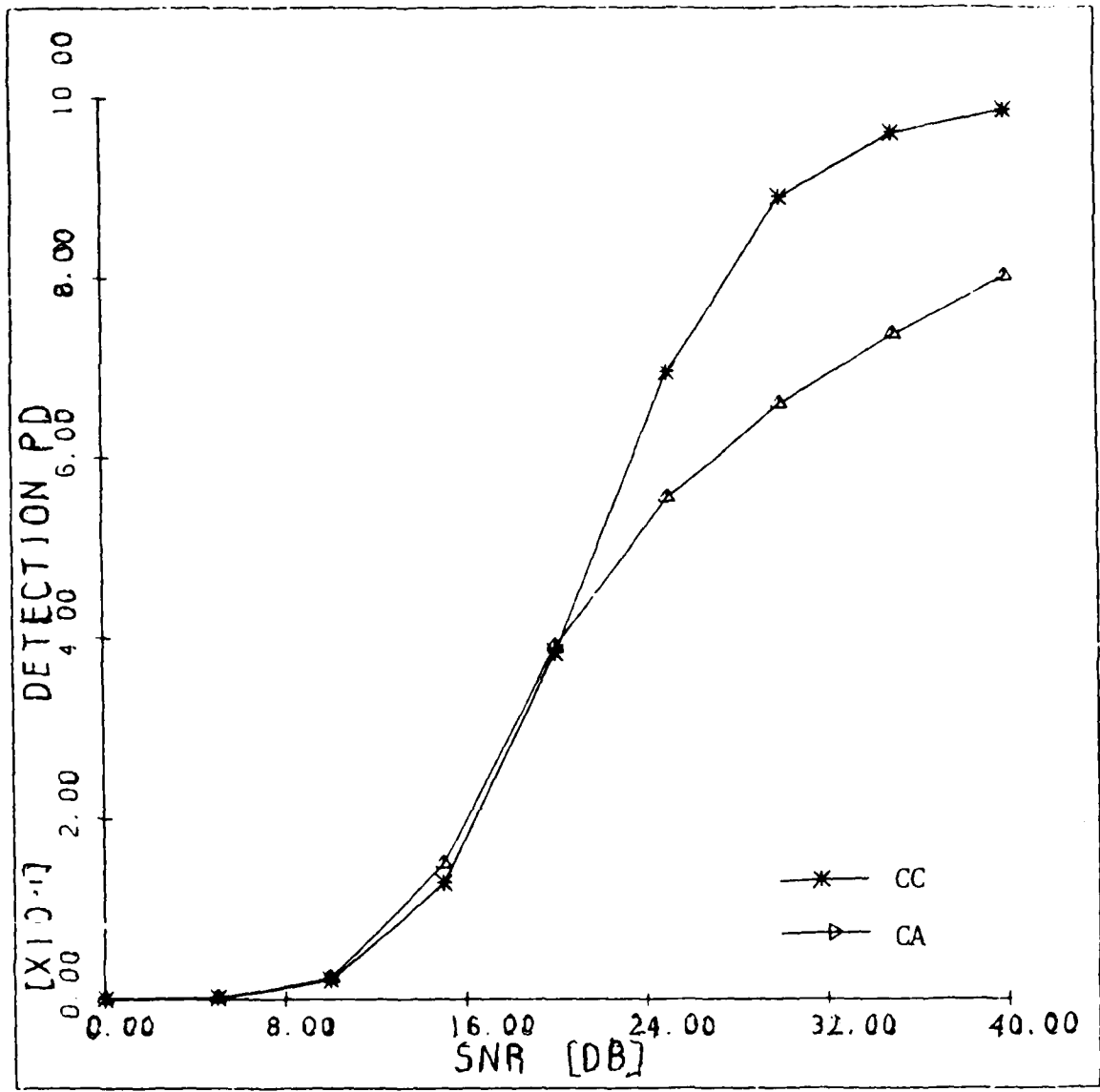


Fig. 3-4. A Performance Comparison of the Cell-Censored (CC) CFAR Detector and the CA-CFAR Detector.
 $P_F = 10^{-5}$, $P_{F_1}^C = 10^{-3}$, $P_0 = 0.5$ and $I = S \div 10$.

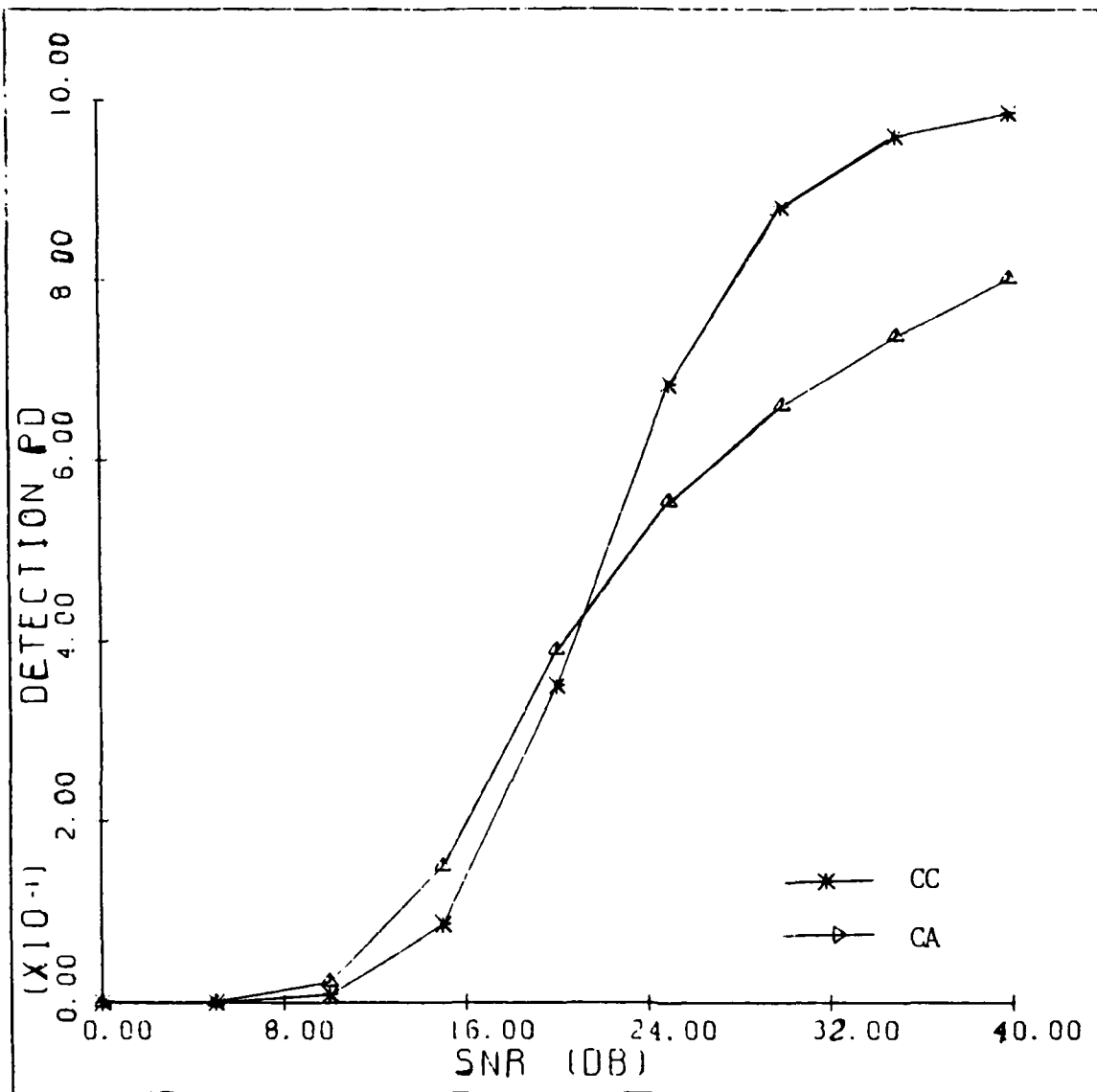


Fig. 3-5. A Performance Comparison of the Cell-Censored (CC) CFAR Detector and the CA-CFAR Detector.

$P_F = 10^{-5}$, $P_{F_1}^C = 10^{-1}$, $P_O = 0.5$ and $I = S \div 10$.

CHAPTER IV
CA-CFAR DETECTION WITH DISTRIBUTED RADARS
AND DATA FUSION

4.1. Introduction

As indicated in Chapter One, a lot of work on distributed detection has been reported in the literature [18-30]. Also, an extensive amount of research has been performed on cell-averaging CFAR detection using a single sensor [1-17]. To our knowledge, no work is reported on CFAR detection using multiple sensors and data fusion. The goal of this chapter is to develop the theory of cell-averaging CFAR detection using multiple sensors and data fusion. In Section 4.2, we formulate the problem of distributed CFAR detection with data fusion. In Section 4.3, we shall assume that the fusion rules at the fusion center are known. Specifically, we consider the "AND" and the "OR" fusion rules at the data fusion center. We obtain the optimum threshold multipliers of the individual detectors and derive an expression for the probability of detection at the data fusion center for the given fusion rules. As an illustration, we study the performance of a distributed CFAR detection system with two detectors and data fusion. Numerical results showing the improvement of the performance for the distributed

multiple sensor system with data fusion over a single sensor system are also presented. In Section 4.4, we consider the optimum design of the overall system, i.e., we obtain the optimum threshold multipliers at the individual detectors as well as the optimum fusion rule at the data fusion center. An example is also presented for illustration. In Section 4.5, we present a summary along with a discussion.

4.2. Distributed CFAR Detection with Data Fusion

We consider n distributed CA-CFAR detectors with a data fusion center as shown in Figure 4-1. It is assumed that the number of range cells at the i th detector is N_i , $i=1,2,\dots,n$. The target to be detected is a slowly fluctuating target model of Swerling type I. The target is embedded in a white Gaussian noise of unknown level. Let the probability of false-alarm and the probability of detection at the individual detectors be denoted by P_{F_i} and P_{D_i} , $i=1,2,\dots,n$, respectively. If the average noise power is σ^2 , then the conditional probability density function of the test statistic q_0^i from the test cell of detector i , $i=1,2,\dots,n$, is given by

$$P_{Q_0^i|H_j}(q_0^i|H_j) = \begin{cases} \frac{1}{2\sigma^2(1+S_i)} e^{-q_0^i/2\sigma^2(1+S_i)} & , \text{ for hypothesis } H_1 \\ \frac{1}{2\sigma^2} e^{-q_0^i/2\sigma^2} & , \text{ for hypothesis } H_0 \end{cases} \quad (4-1)$$

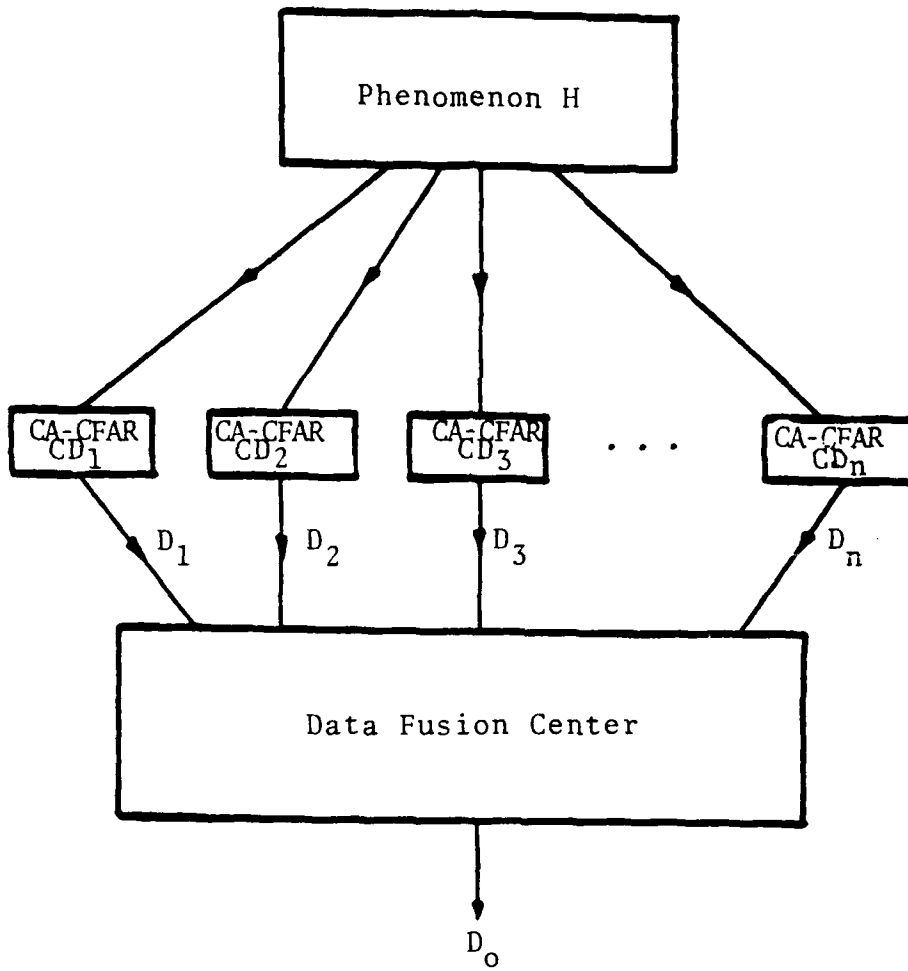


Fig. 4-1. Distributed CA-CFAR Detection with Data Fusion.

where S_i , $i=1,2,\dots,n$, is the target SNR at each CA-CFAR detector. The hypothesis H_0 represents the case of noise alone, while hypothesis H_1 represents the noise plus target signal case. To simplify the mathematical derivations, we assume $S_1 = S_2 = \dots = S_n = S$, where S is the target SNR. Results for the case of unequal target SNR's can be obtained in a straightforward manner. The probability of detection, P_{D_i} , for detector i , $i=1,2,\dots,n$, is given by

$$P_{D_i} = \int_0^{\infty} \Pr(Q_0^i > T_i q^i | Q^i, H_1) P_{Q^i}(q^i) dq^i \quad (4-2)$$

where T_i is the scaling factor at the CA-CFAR detector i , $i=1,2,\dots,n$, and $P_{Q^i}(q^i)$ denotes the probability density function of the adaptive threshold at the i th CA-CFAR detector. Also,

$$\Pr(Q_0^i > T_i q^i | Q^i, H_1) = \int_{T_i q^i}^{\infty} P_{Q_0^i | H_1}(q_0^i | H_1) dq_0^i = \exp \left[-\frac{T_i q^i}{1+S} \right] \quad (4-3)$$

Since the noise samples, for each CA-CFAR detector, are identically distributed, the probability of detection of the individual detectors can be written as (see Appendix A for details)

$$P_{D_i} = \frac{(1+S)^{N_i}}{(1+S+T_i)^{N_i}}, \quad i=1,2,\dots,n \quad (4-4)$$

Each CA-CFAR detector transmits its decision to the data fusion center. These local decisions of individual detectors are denoted by D_i , $i=1,2,\dots,n$, where

$$D_i = \begin{cases} 0, & \text{if detector } i \text{ decides } H_0 \\ 1, & \text{if detector } i \text{ decides } H_1 \end{cases} \quad (4-5)$$

In order to be able to express the overall probability of detection, P_D , the overall probability of false-alarm, P_F , and the overall probability of a miss, P_M , at the data fusion center, in terms of the probabilities of false-alarm and miss at the local detectors, i.e., P_{F_i} 's and P_{M_i} 's, we define the following quantities:

$$\underline{D} = (D_1, D_2, \dots, D_n)^T \quad (4-6.a)$$

$$M_{\underline{D}} = \prod_{S^0} P_{M_j} \prod_{S^1} (1 - P_{M_k}) = P(\underline{D}|H_1) \quad (4-6.b)$$

$$F_{\underline{D}} = \prod_{S^0} (1 - P_{F_j}) \prod_{S^1} P_{F_k} = P(\underline{D}|H_0) \quad (4-6.c)$$

$$P_{k\underline{D}} = \Pr(D_o = k | \underline{D}), \quad k=0,1 \quad (4-6.d)$$

$$D_o = \text{Global decision at the data fusion center} \quad (4-6.e)$$

$$S^0 = \text{Set of all } j, (j \neq 0), \text{ such that } D_j \text{ is an element of } \underline{D} \text{ and } D_j = 0 \quad (4-6.f)$$

$$S^1 = \text{Set of all } k, (k \neq 0), \text{ such that } D_k \text{ is an element of } \underline{D} \text{ and } D_k = 1 \quad (4-6.g)$$

Then, we may express P_D , P_M , and P_F as follows

$$P_M = \sum_{\underline{D}} P_{OD} M_{\underline{D}} \quad (4-7)$$

$$P_F = \sum_{\underline{D}} P_{1D} F_{\underline{D}} \quad (4-8)$$

and,

$$P_D = 1 - P_M \quad (4-9)$$

where,

$$\sum_{\underline{D}} = \text{summation over all possible values of } \underline{D}.$$

The transition probabilities P_{OD} and P_{1D} are determined by the given fusion rule. Since \underline{D} can take 2^n possible values, there are 2^n possibilities for P_{OD} and P_{1D} . The goal is to maximize the overall probability of detection while keeping the overall probability of false-alarm constant. To do this, we use the calculus of extrema and form the objective function

$$J(T_1, T_2, \dots, T_n) = P_D(S, T_1, \dots, T_n) + \xi [P_F(T_1, T_2, \dots, T_n) - \nu] \quad (4-10)$$

where ν is the desired false-alarm probability at the data fusion center, ξ is the Lagrange multiplier, and T_i , $i=1, 2, \dots, n$, are the threshold multipliers at each detector. To maximize $P_D(S, T_1, \dots, T_n)$, subject to the constraint that $P_F(T_1, T_2, \dots, T_n)$ is a constant, we must maximize the objective function $J(T_1, T_2, \dots, T_n)$. We set the derivative of $J(T_1, T_2, \dots, T_n)$ with respect to T_i , $i=1, 2, \dots, n$, equal to

zero and solve the following system of n nonlinear equations in n unknowns.

$$\frac{\partial J(T_1, T_2, \dots, T_n)}{\partial T_j} = 0, \quad j=1, 2, \dots, n \quad (4-11)$$

Once the threshold multipliers, T_i , $i=1, 2, \dots, n$, are obtained, all the P_{F_i} 's are fixed and the optimum P_D results. Now, we give specific results for the "AND" and the "OR" fusion rules. We also find the optimum threshold multipliers so as to maximize P_D while P_F is maintained at the desired value.

4.2-1 "AND" Fusion Rule

In Table 4-1, we present the "AND" fusion rule. From this table, we see that the global decision at the data fusion center is one only if all of the detectors decide a one. The transition probabilities are

$$P_{0\bar{D}} = \begin{cases} 0, & \text{if } \bar{D} = [1, 1, \dots, 1]^T \\ 1, & \text{otherwise} \end{cases} \quad (4-12.a)$$

and

$$P_{1\bar{D}} = \begin{cases} 1, & \text{if } \bar{D} = [1, 1, \dots, 1]^T \\ 0, & \text{otherwise} \end{cases} \quad (4-12.b)$$

Substituting equations (4-12.a), (4-12.b), and (4-9) into equations (4-7) and (4-8) and rearranging terms, P_D and P_F can be written as

| D_1 | D_2 | D_3 | \dots | D_{n-1} | D_n | D_0 |
|-------|-------|-------|----------|-----------|-------|-------|
| 0 | 0 | 0 | \dots | 0 | 0 | 0 |
| 0 | 0 | 0 | \dots | 0 | 1 | 0 |
| 0 | 0 | 0 | \dots | 1 | 0 | 0 |
| 0 | 0 | 0 | \dots | 1 | 1 | 0 |
| | | | \vdots | | | |
| 1 | 1 | 1 | \dots | 0 | 0 | 0 |
| 1 | 1 | 1 | \dots | 0 | 1 | 0 |
| 1 | 1 | 1 | \dots | 1 | 0 | 0 |
| 1 | 1 | 1 | \dots | 1 | 1 | 1 |

Table 4-1. "AND" Fusion Rule

$$P_D = \prod_{i=1}^n P_{D_i} \quad (4-13)$$

$$P_F = \prod_{i=1}^n P_{F_i} \quad (4-14)$$

That is,

$$P_D = \prod_{i=1}^n \frac{(1+S)^{N_i}}{(1+S+T_i)^{N_i}} \quad (4-15)$$

$$P_F = \prod_{i=1}^n \frac{1}{(1+T_i)^{N_i}} \quad (4-16)$$

Substituting equations (4-15) and (4-16) into equation (4-10), the objective function is,

$$J(T_1, T_2, \dots, T_n) = \prod_{i=1}^n \frac{(1+S)^{N_i}}{(1+S+T_i)^{N_i}} + \xi \left[\prod_{i=1}^n \frac{1}{(1+T_i)^{N_i}} - v \right] \quad (4-17)$$

Taking the derivative of $J(T_1, T_2, \dots, T_n)$ with respect to T_j , $j=1, 2, \dots, n$, and setting it equal to zero, we get

$$\frac{\partial J(T_1, T_2, \dots, T_n)}{\partial T_j} = \prod_{\substack{i=1 \\ i \neq j}}^n \frac{(1+S)^{N_i + N_j}}{(1+S+T_j)^{N_j+1} (1+S+T_i)^{N_i}} +$$

$$\prod_{\substack{i=1 \\ i \neq j}}^n \frac{1}{(1+T_j)^{N_j+1} (1+T_i)^{N_i}} = 0, \quad j=1, 2, \dots, n \quad (4-18)$$

The threshold multipliers, T_i 's, can be obtained by solving the above set of coupled nonlinear equations along with the constraint

$$P_F = \prod_{i=1}^n \frac{1}{(1+T_i)^{N_i}} = \nu \quad (4-19)$$

Numerical results will be obtained in Subsection 4.2-3.

4.2-2 "OR" Fusion Rule

In Table 4-2, we present the "OR" fusion rule. The global decision is zero only when all the detectors decide

| D_1 | D_2 | D_3 | \dots | D_{n-1} | D_n | D_0 |
|-------|-------|-------|----------|-----------|-------|----------|
| 0 | 0 | 0 | \dots | 0 | 0 | 0 |
| 0 | 0 | 0 | \dots | 0 | 1 | 1 |
| 0 | 0 | 0 | \dots | 1 | 0 | 1 |
| 0 | 0 | 0 | \dots | 1 | 1 | 1 |
| | | | \vdots | | | \vdots |
| | | | \vdots | | | \vdots |
| 1 | 1 | 1 | \dots | 0 | 0 | 1 |
| 1 | 1 | 1 | \dots | 0 | 1 | 1 |
| 1 | 1 | 1 | \dots | 1 | 0 | 1 |
| 1 | 1 | 1 | \dots | 1 | 1 | 1 |

Table 4-2. "OR" Fusion Rule.

a zero. The transition probabilities are:

$$P_{O\underline{D}} = \begin{cases} 1, & \text{if } \underline{D} = [0,0,\dots,0]^T \\ 0, & \text{otherwise} \end{cases} \quad (4-20.a)$$

and

$$P_{1\underline{D}} = \begin{cases} 0, & \text{if } \underline{D} = [0,0,\dots,0]^T \\ 1, & \text{otherwise} \end{cases} \quad (4-20.b)$$

Substituting equations (4-20.a) and (4-20.b) into equations (4-7) and (4-8) and rearranging terms, P_M and P_F can be written as

$$P_M = \prod_{i=1}^n P_{M_i} \quad (4-21)$$

and

$$P_F = \sum_{\substack{\underline{D} \\ \underline{D} \neq 0}} F_{\underline{D}} \quad (4-22.a)$$

$$= \sum_{\substack{\underline{D} \\ \underline{D} \neq 0}} \pi_{S^0} (1 - P_{F_j}) \pi_{S^1} P_{F_k} \quad (4-22.b)$$

The objective function then becomes

$$J(T_1, T_2, \dots, T_n) = \prod_{i=1}^n P_{M_i} + \xi \left\{ \sum_{\substack{\underline{D} \\ \underline{D} \neq 0}} F_{\underline{D}} - \nu \right\} \quad (4-23)$$

Note that in this case we have to minimize $J(T_1, T_2, \dots, T_n)$ since we are minimizing the overall probability of a miss, which is equivalent to maximizing P_D at the data fusion center as defined by equation (4-9). Taking the derivative of the objective function with respect to T_j , $j=1, 2, \dots, n$, and setting it equal to zero, we obtain

$$\begin{aligned} \frac{\partial J(T_1, T_2, \dots, T_n)}{\partial T_j} &= \prod_{\substack{i=1 \\ i \neq j}}^n \left[1 - \frac{(1+S)^{N_i}}{(1+S+T_i)^{N_i}} \right] \cdot \frac{(1+S)^{N_j}}{(1+S+T_j)^{N_j+1}} \\ &+ \xi \sum_{\substack{\underline{D} \\ \underline{D} \neq 0}} \pi_{S^0} \frac{1}{(1+T_j)^{N_j+1}} \cdot \prod_{\substack{S^1 \\ k \neq j}} \frac{1}{(1+T_k)^{N_k}} = 0 \end{aligned} \quad (4-24)$$

$j=1, 2, \dots, n$

Hence, we obtain a system of n coupled nonlinear equations in $(n+1)$ unknowns. Then, we use the following constraint

$$\sum_{\substack{D \\ D \neq 0}} \pi_{S_0} (1 - P_{F_j}) \pi_{S_1} P_{F_k} = \nu \quad (4-25)$$

to solve for the (n+1) unknowns.

In the next subsection, as an illustration, we derive specific results for a system consisting of two detectors and a data fusion center as shown in Figure 4-2. The performance of the system is also investigated.

4.2-3 Example

The system under consideration is shown in Figure 4-2. For ease of understanding, we will use a more explicit notation. Let us denote the transition probabilities by

$$P_{kij} = \Pr(D_0 = k | D_1 = i, D_2 = j) \quad (4-26)$$

for $i, j, k=0,1$. Then the overall probability of a miss, P_M , is

$$\begin{aligned} P_M = & P_{000} P_{M_1} P_{M_2} + P_{001} P_{M_1} (1 - P_{M_2}) + P_{010} (1 - P_{M_1}) P_{M_2} \\ & + P_{011} (1 - P_{M_1}) (1 - P_{M_2}) \end{aligned} \quad (4-27)$$

and the overall probability of false-alarm, P_F , is

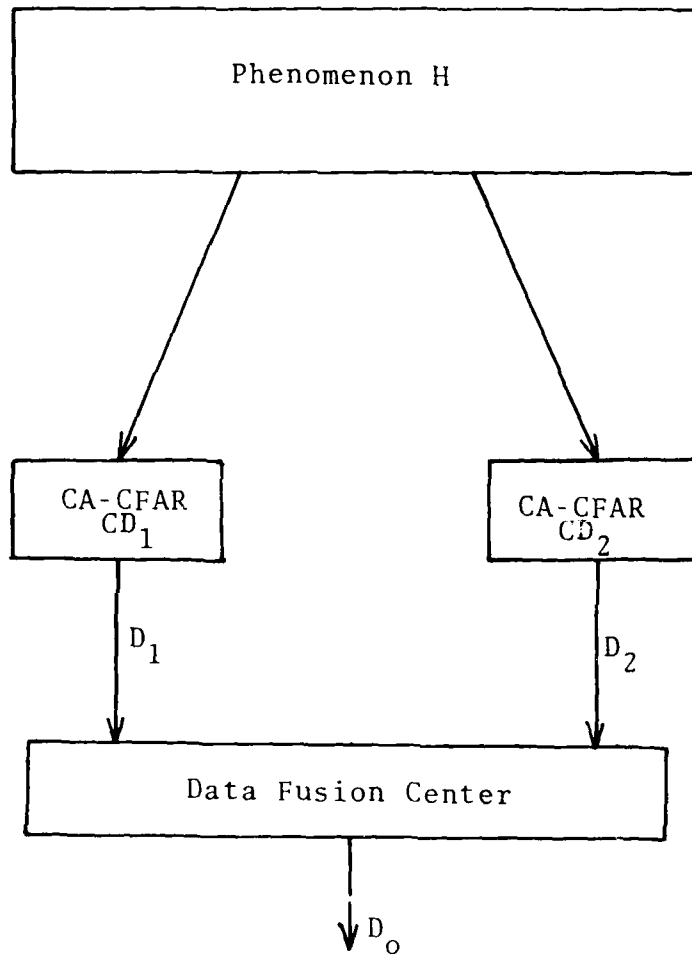


Fig. 4-2. Distributed CA-CFAR Detection with Data Fusion Using Two Detectors.

$$\begin{aligned}
P_F = & P_{100}(1-P_{F_1})(1-P_{F_2}) + P_{101}(1-P_{F_1})P_{F_2} + P_{110}P_{F_1}(1-P_{F_2}) \\
& + P_{111}P_{F_1}P_{F_2}
\end{aligned} \tag{4-28}$$

"AND" Fusion Rule

From the "AND" fusion rule at the data fusion center, the transition probabilities are

$$P_{011} = P_{100} = P_{101} = P_{110} = 0 \tag{4-29.a}$$

$$P_{000} = P_{001} = P_{010} = P_{111} = 1 \tag{4-29.b}$$

Thus, the overall probability of detection, P_D , and the overall false-alarm probability, P_F , become

$$P_D = P_{D_1} P_{D_2} \tag{4-30}$$

$$P_F = P_{F_1} P_{F_2} \tag{4-31}$$

The objective function is

$$J(T_1, T_2) = \frac{(1+S)^{N_1+N_2}}{(1+S+T_1)^{N_1}(1+S+T_2)^{N_2}} + \xi \left[\frac{1}{(1+T_1)^{N_1}(1+T_2)^{N_2}} - \nu \right] \tag{4-32}$$

where, N_1 and N_2 are the number of reference cells for detector one and detector two respectively. We maximize $J(T_1, T_2)$ with respect to T_1 and T_2 by setting the derivatives

equal to zero, i.e.,

$$\frac{\partial J(T_1, T_2)}{\partial T_1} = \frac{\partial J(T_1, T_2)}{\partial T_2} = 0 \quad (4-33)$$

The resulting equations are

$$\frac{(1+S)^{N_1+N_2}}{(1+S+T_1)^{N_1+1} (1+S+T_2)^{N_2}} + \xi \frac{1}{(1+T_1)^{N_1+1} (1+T_2)^{N_2}} = 0 \quad (4-34)$$

and

$$\frac{(1+S)^{N_1+N_2}}{(1+S+T_1)^{N_1} (1+S+T_2)^{N_2+1}} + \xi \frac{1}{(1+T_1)^{N_1} (1+T_2)^{N_2+1}} = 0 \quad (4-35)$$

Solving for T_1 and T_2 subject to the constraint

$$P_F = \frac{1}{(1+T_1)^{N_1} (1+T_2)^{N_2}} = \nu \quad (4-36)$$

we obtain,

$$T_1 = T_2 = -1 + \nu^{-\frac{1}{N_1+N_2}} \quad (4-37)$$

The performance of the system in terms of P_D versus the target SNR for $N_1 = 4$, $N_2 = 6$, and $P_F = 10^{-4}$ is plotted in Figure 4-3.

"OR" Fusion Rule

In this case, the transition probabilities are

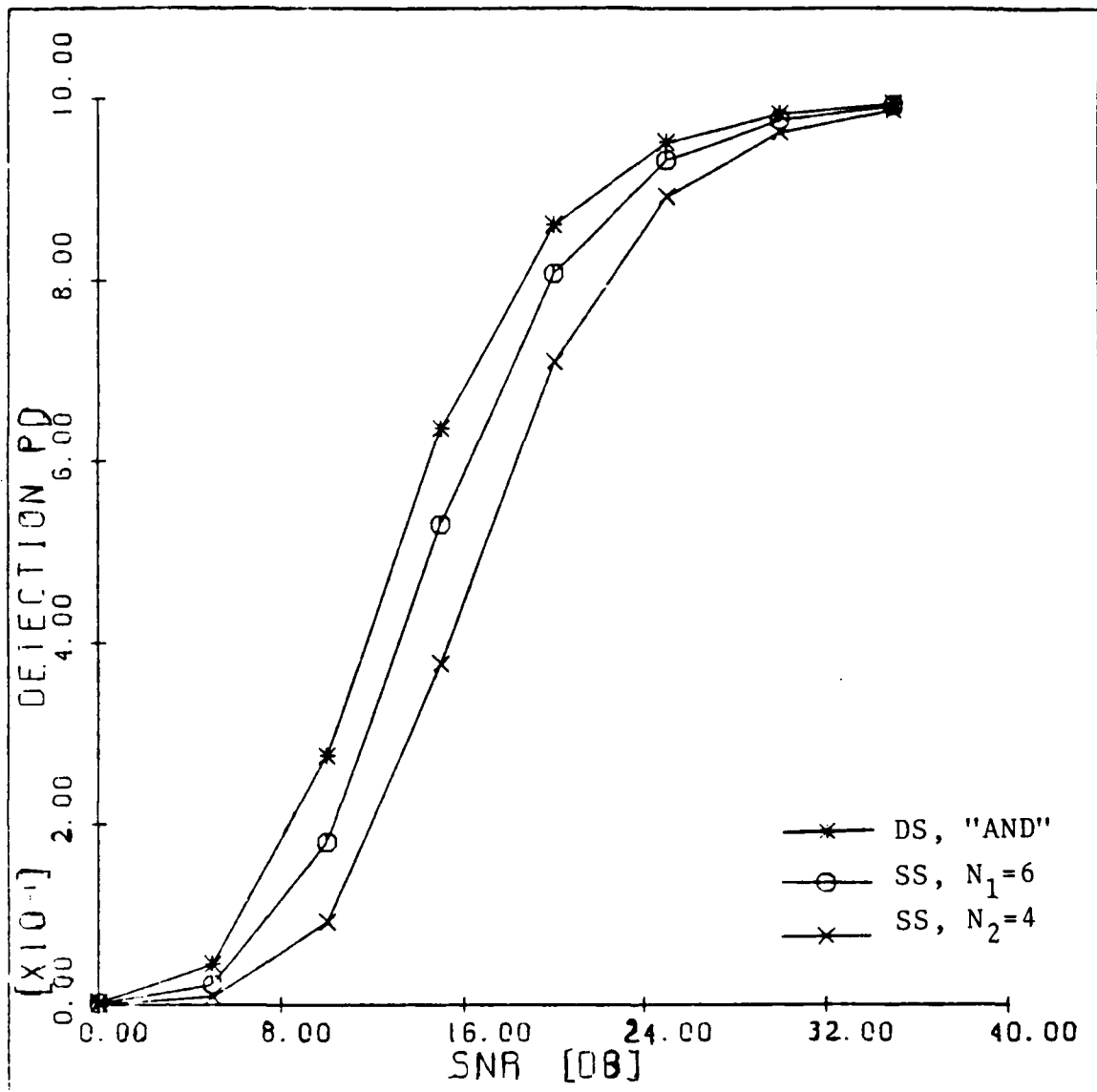


Fig. 4-3. Performance Comparison of the Two Sensor System (DS) Using the "AND" Fusion Rule with a Single Sensor System (SS).
 $P_F = 10^{-4}$, $N_1 = 6$ and $N_2 = 4$.

$$P_{011} = P_{010} = P_{100} = P_{011} = 0 \quad (4-38.a)$$

$$P_{000} = P_{110} = P_{101} = P_{111} = 1 \quad (4-38.b)$$

Thus, P_D and P_F become

$$P_D = P_{D1} + P_{D2} - P_{D1}P_{D2} \quad (4-39)$$

$$P_F = P_{F1} + P_{F2} - P_{F1}P_{F2} \quad (4-40)$$

The objective function is then

$$J(T_1, T_2) = \frac{(1+S)^{N_1}}{(1+S+T_1)^{N_1}} + \frac{(1+S)^{N_2}}{(1+S+T_2)^{N_2}} - \frac{(1+S)^{N_1+N_2}}{(1+S+T_1)^{N_1} (1+S+T_2)^{N_2}}$$

$$+ \xi \left\{ \frac{1}{(1+T_1)^{N_1}} + \frac{1}{(1+T_2)^{N_2}} - \frac{1}{(1+T_1)^{N_1} (1+T_2)^{N_2}} - v \right\} \quad (4-41)$$

We maximize $J(T_1, T_2)$ with respect to T_1 and T_2 by setting the derivatives equal to zero. After some manipulation, we obtain the following nonlinear equation.

$$(1+S)^{N_2} [(1+S)^{N_1} - (1+S+T_1)^{N_1}] (1+S+T_1) \cdot [(1+T_2)^{N_2} - 1] (1+T_2) =$$

$$(1+S)^{N_1} \cdot [(1+S)^{N_2} - (1+S+T_2)^{N_2}] \cdot [(1+T_1)^{N_1} - 1] (1+T_1) (1+S+T_2) \quad (4-42)$$

Using the constraint that

$$P_F = \frac{1}{(1+T_1)^{N_1}} + \frac{1}{(1+T_2)^{N_2}} - \frac{1}{(1+T_1)^{N_1}(1+T_2)^{N_2}} = \nu \quad (4-43)$$

we obtain T_1 in terms of T_2 as

$$T_1 = -1 + \left[\frac{(1+T_2)^{N_2} - 1}{\nu(1+T_2)^{N_2} - 1} \right] \frac{1}{N_1} \quad (4-44)$$

Substituting equation (4-44) into equation (4-43) and using an iterative procedure, we obtain a value for T_2 and then T_1 . For $N_1 = 4$, $N_2 = 6$, and $P_F = 10^{-4}$, the values of T_1 and T_2 are 11.597 and 4.050, respectively. The numerical results showing the performance are plotted in Figure 4-4. In the next subsection, we comment on the performance of the "AND" and the "OR" fusion rules.

4.2-4. A Comment on the Performance of the "AND and "OR" Fusion Rules

In Figure 4-5, we plot the system performance for the "AND" and the "OR" fusion rules. As evident from the figure, when the target SNR exceeds 14.5 dB (approximately), the performance of the "OR" fusion rule becomes better than the performance of the "AND" fusion rule. This is easily demonstrated analytically. Let the overall probabilities of detection at the data fusion center for the "AND" and the "OR" fusion rules be denoted by P_D^A and P_D^O , respectively. Then,

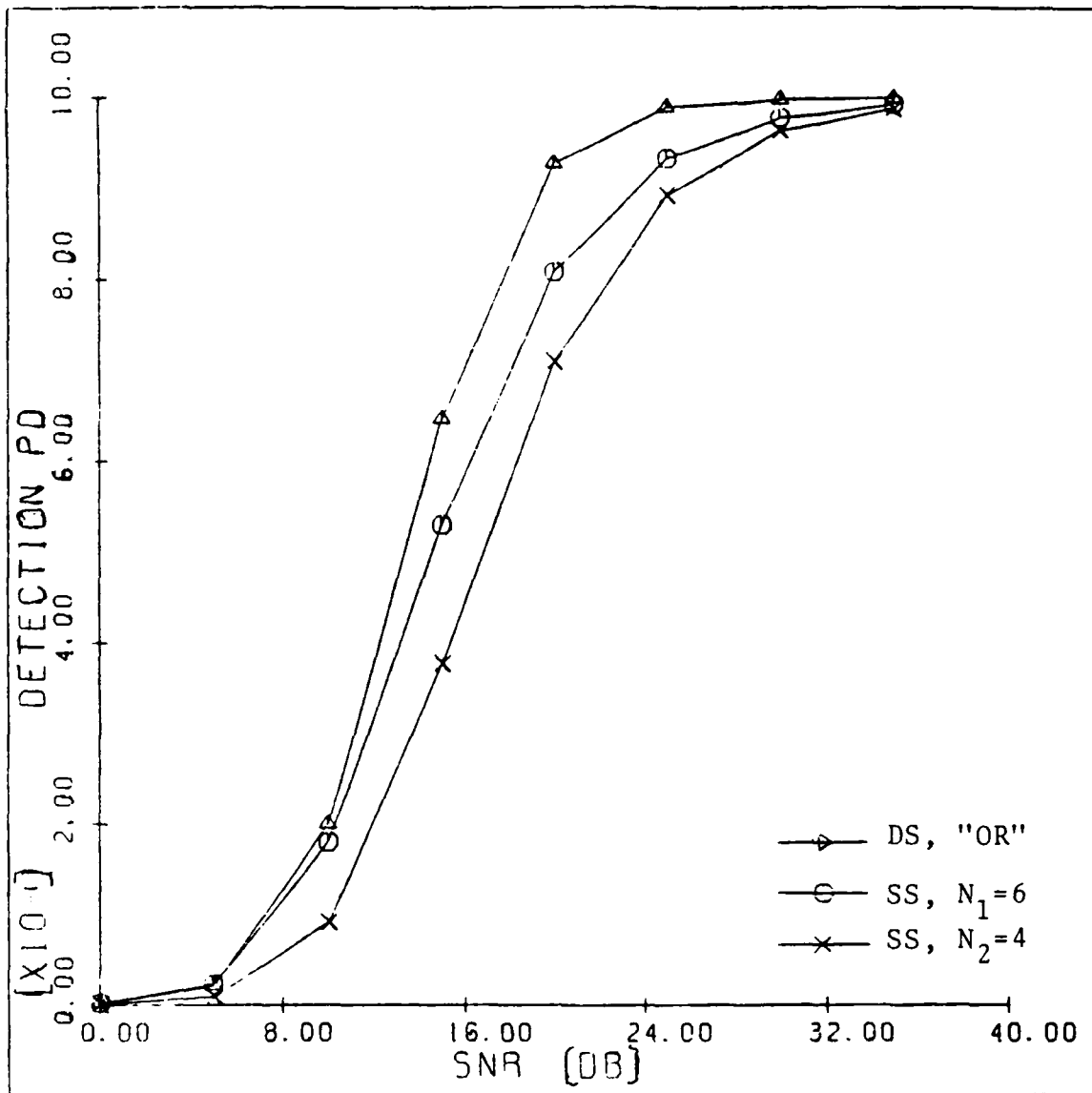


Fig. 4-4. Performance Comparison of the Two Sensor System (DS) Using the "OR" Fusion Rule with a Single Sensor System (SS).

$P_F = 10^{-4}$, $N_1 = 6$ and $N_2 = 4$.

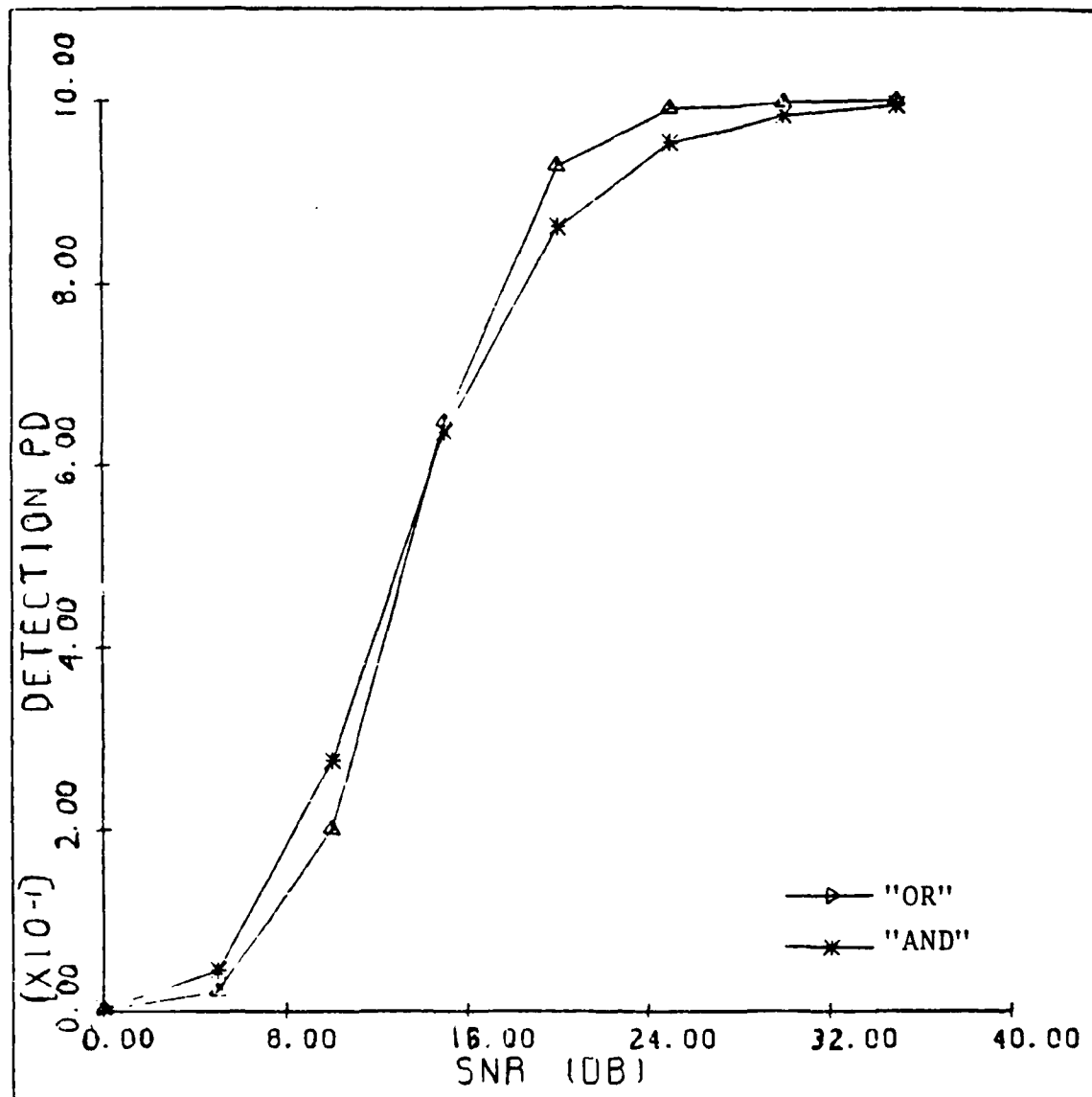


Fig. 4-5. Performance of the Two Sensor System for the "AND" and the "OR" Fusion Rule.
 $P_F = 10^{-4}$, $N_1 = 6$ and $N_2 = 4$.

$$P_D^O \geq P_D^A \quad (4-45)$$

if and only if,

$$\frac{(1+S)^{N_1}}{(1+S+T_1)^{N_1}} + \frac{(1+S)^{N_2}}{(1+S+T_2)^{N_2}} - \frac{(1+S)^{N_1+N_2}}{(1+S+T_1)^{N_1}(1+S+T_2)^{N_2}} \geq \frac{(1+S)^{N_1+N_2}}{(1+S+T_1)^{N_1}(1+S+T_2)^{N_2}} \quad (4-46)$$

Solving this nonlinear equation, we obtain $S=14.57$ which agrees with the graphical result.

4.3. Optimization of the Overall System

In the previous section, we studied the problem of CA-CFAR detection with multiple sensors and data fusion. Given the fusion rule at the data fusion center, we maximized the overall probability of detection by obtaining the optimum threshold multipliers at the individual CA-CFAR detectors, while the overall probability of false-alarm was maintained at the desired value. In this section, we will also consider the design of the optimum fusion rule. Again, the goal will be to maximize the overall probability of detection while the overall probability of false-alarm is kept at a desired value. While maximizing the overall probability of detection, we will derive the optimum fusion rule at the data fusion center as well as the optimum threshold multipliers at the individual CA-CFAR detectors. We will use an approach similar to the one in [35].

The decision output, D_o , at the data fusion center is a function of the incoming decisions D_i , $i=1,2,\dots,n$, i.e.,

$$D_o = f(D_1, D_2, \dots, D_n) \quad (4-47.a)$$

and

$$D_o \in \{0, 1\} \quad (4-47.b)$$

For ease in handling, we use the following notation for quantities defined in equations (4-6.b), (4-6.c) and (4-6.d),

$$P_{1\underline{D}} = \Pr(D_o = 1 | \underline{D}) \quad (4-48.a)$$

$$P_{\underline{D}1} = M_{\underline{D}} \quad (4-48.b)$$

$$P_{\underline{D}0} = F_{\underline{D}} \quad (4-48.c)$$

Then, the overall probability of detection, P_D , and the overall probability of false-alarm, P_F , at the output of the data fusion center can be written as

$$P_D = \sum_{\underline{D}} P_{1\underline{D}} P_{\underline{D}1} \quad (4-49)$$

$$P_F = \sum_{\underline{D}} P_{\underline{D}0} P_{1\underline{D}} \quad (4-50)$$

The optimization process for the overall system will be carried out in two steps. First, we optimize the fusion rule at the data fusion center assuming that the threshold multipliers are known. This yields a set of equations. Then, we obtain the optimum threshold multipliers assuming that the optimum fusion rule is known, which gives another set of equations to be solved. These two sets of nonlinear equations are then solved simultaneously to yield the optimum threshold multipliers and the optimum fusion rule.

Again, using the calculus of extrema, we form the objective function,

$$J = P_D + \xi (P_F - v) \quad (4-51)$$

where, ξ is the Lagrange multiplier and v is the desired probability of false-alarm at the data fusion center. Substituting equations (4-49) and (4-50) into equation (4-51), we obtain

$$J = \sum_{\underline{D}} P_{1\underline{D}} P_{\underline{D}1} + \xi \left\{ \sum_{\underline{D}} P_{1\underline{D}} P_{\underline{D}0} - v \right\} \quad (4-52)$$

The vector \underline{D} whose elements are the decisions D_i , $i=1,2,\dots,n$, can take 2^n values. For a specific value of \underline{D} given by

$$\underline{D}^* = (D_1^*, D_2^*, \dots, D_n^*)^T, \quad (4-53)$$

equation (4-52) can be rewritten as

$$J = P_{1\underline{D}^*} P_{\underline{D}^*1} + \xi \{ P_{1\underline{D}^*} P_{\underline{D}^*0} - v^* \} + K(\underline{D}^*) \quad (4-54)$$

where,

$$v^* = v - \sum_{\underline{D} \neq \underline{D}^*} P_{1\underline{D}} P_{\underline{D}0}$$

$$K(\underline{D}^*) = \sum_{\underline{D} \neq \underline{D}^*} P_{1\underline{D}} P_{\underline{D}1}$$

and

$$\sum_{\underline{D} \neq \underline{D}^*} = \text{Summation over all possible values of } \underline{D} \text{ except } \underline{D}^*$$

Our goal is to maximize J . This maximization is equivalent to maximizing $P_{1D^*} P_{D^*1}$ subject to the constraint $P_{1D^*} P_{D^*0} = v^*$. Dividing equation (4-54) by P_{D^*1} we obtain

$$J^* = P_{1D^*} + \xi^* \{P_{1D^*} - vv^*\} + KK(D^*) \quad (4-55)$$

where

$$J^* = \frac{J}{P_{D^*1}}$$

$$\xi^* = \xi \frac{P_{D^*0}}{P_{D^*1}}$$

$$vv^* = \frac{v^*}{P_{D^*0}}$$

and

$$KK(D^*) = \frac{K(D^*)}{P_{D^*1}}$$

Since $KK(D^*)$ does not depend on P_{1D^*} , equation (4-55) represents the equation of a straight line in terms of P_{1D^*} . Thus, as in [35], we obtain the conditions which the transition probabilities must satisfy to yield the optimum fusion rule.

$$P_{1D^*} = \min \{vv^*, 1\}$$


$$P_{1D^*} = 0$$

$$(4-56)$$

The next step is to find the optimum threshold multipliers, T_i , $i=1,2,\dots,n$. The probabilities of detection, P_{D_i} , and the probabilities of false-alarm, P_{F_i} , $i=1,2,\dots,n$, at each CA-CFAR detector are functions of the threshold

multipliers, T_i , $i=1,2,\dots,n$. Therefore, maximizing P_D , while P_F is fixed at the desired value v , is equivalent to maximizing J with respect to the threshold multipliers T_i 's. We take the derivative of J with respect to T_i , $i=1,2,\dots,n$, and set them equal to zero to yield the following set of equations which the optimum T_i 's must satisfy.

$$\frac{\partial J}{\partial T_i} = 0, \quad i=1,2,\dots,n \quad (4-57)$$

It should be emphasized that the set of equations (4-56) and (4-57) are to be solved simultaneously in order to obtain the optimum threshold multipliers as well as the best fusion rule. The computations involved are overwhelming and it will require an extensive computer iterative procedure. This point will become evident in the simple example we consider next.

Example

We consider the system of two CA-CFAR detectors with data fusion. For the sake of simplicity, let the transition probabilities of equation (4-26) be denoted by α_i , $i=1,2,3,4$. i.e.,

$$\alpha_1 = P_{100} \quad (4-58.a)$$

$$\alpha_2 = P_{101} \quad (4-58.b)$$

$$\alpha_3 = P_{110} \quad (4-58.c)$$

$$\alpha_4 = P_{111} \quad (4-58.d)$$

Using the same notation as in the example presented in Section 4.2, we can write the overall probability of detec-

tion, P_D , and the overall probability of false-alarm, P_F , as

$$P_D = \alpha_1(1-P_{D_1})(1-P_{D_2}) + \alpha_2(1-P_{D_1})P_{D_2} + \alpha_3P_{D_1}(1-P_{D_2}) + \alpha_4P_{D_1}P_{D_2} \quad (4-59)$$

$$P_F = \alpha_1(1-P_{F_1})(1-P_{F_2}) + \alpha_2(1-P_{F_1})P_{F_2} + \alpha_3P_{F_1}(1-P_{F_2}) + \alpha_4P_{F_1}P_{F_2} \quad (4-60)$$

Assuming that the target SNR is the same at each CA-CFAR detector, denoted by S , the probabilities of detection and the probabilities of false-alarm at each CA-CFAR detector are (see Appendix A),

$$P_{D_1} = \left[\frac{1+S}{1+S+T_1} \right]^{N_1} \quad (4-61)$$

$$P_{D_2} = \left[\frac{1+S}{1+S+T_2} \right]^{N_2} \quad (4-62)$$

$$P_{F_1} = \frac{1}{(1+T_1)^{N_1}} \quad (4-63)$$

$$P_{F_2} = \frac{1}{(1+T_2)^{N_2}} \quad (4-64)$$

As discussed earlier, to optimize the entire system we need to maximize the objective function defined in equation (4-51). Substituting equations (4-59) and (4-60) into equation (4-52), we obtain

$$J = \alpha_1(1-P_{D_1}-P_{D_2}+P_{D_1}P_{D_2}) + \alpha_2(1-P_{D_1})P_{D_2} + \alpha_3P_{D_1}(1-P_{D_2}) + \alpha_4P_{D_1}P_{D_2} \\ + \xi\{\alpha_1(1-P_{F_1}-P_{F_2}+P_{F_1}P_{F_2}) + \alpha_2(1-P_{F_1})P_{F_2} + \alpha_3P_{F_1}(1-P_{F_2}) + \alpha_4P_{F_1}P_{F_2}\} \quad (4-65)$$

Dividing equation (4-65) by $(1 - P_{D_1} - P_{D_2} + P_{D_1} P_{D_2})$, we get a new objective function J_1 , i.e.,

$$J_1 = \alpha_1 + \xi_1 \{ \alpha_1 - v_1 \} + K_1 \quad (4-66)$$

where

$$\Delta D_1 = 1 - P_{D_1} - P_{D_2} + P_{D_1} P_{D_2}$$

$$\Delta F_1 = 1 - P_{F_1} - P_{F_2} + P_{F_1} P_{F_2}$$

$$J_1 = \frac{J}{\Delta D_1}$$

$$\xi_1 = \xi \frac{\Delta F_1}{\Delta D_1}$$

$$v_1 = \frac{\{ \alpha_2 (1 - P_{F_1}) P_{F_2} + \alpha_3 P_{F_1} (1 - P_{F_2}) \} + \alpha_4 P_{F_1} P_{F_2} - v}{\Delta F_1}$$

$$K_1 = \frac{\alpha_2 (1 - P_{D_1}) P_{D_2} + \alpha_3 P_{D_1} (1 - P_{D_2}) + \alpha_4 P_{D_1} P_{D_2}}{\Delta D_1}$$

Notice that equation (4-66) is the equation of a straight line in α_1 . In this case, the extrema are at the end points depending on whether the slope is positive or negative. Thus, at the data fusion center, the value of α_1 is given by

$$\xi_1 \begin{matrix} \alpha_1 = \min \{ v_1, 1 \} \\ \text{---} \\ \alpha_1 = 0 \end{matrix} \quad (4-67)$$

In an analogous manner, we obtain

$$\begin{array}{l} \alpha_2 = \min \{v_2, 1\} \\ \xi_2 \quad \begin{array}{c} \diagup \\ \diagdown \\ \diagup \\ \diagdown \end{array} \quad 1 \\ \alpha_2 = 0 \end{array} \quad (4-68)$$

$$\begin{array}{l} \alpha_3 = \min \{v_3, 1\} \\ \xi_3 \quad \begin{array}{c} \diagup \\ \diagdown \\ \diagup \\ \diagdown \end{array} \quad 1 \\ \alpha_3 = 0 \end{array} \quad (4-69)$$

$$\begin{array}{l} \alpha_4 = \min \{v_4, 1\} \\ \xi_4 \quad \begin{array}{c} \diagup \\ \diagdown \\ \diagup \\ \diagdown \end{array} \quad 1 \\ \alpha_4 = 0 \end{array} \quad (4-70)$$

where, v_2 , v_3 and v_4 have a definition similar to v_1

The next step is to find the optimum threshold multipliers. The optimum threshold multipliers are related to the transition probabilities through the objective function J . This relation is easily seen by rewriting the objective function as

$$\begin{aligned} J = & P_{D1}[\alpha_3 - \alpha_1 + P_{D2}(\alpha_1 - \alpha_2 - \alpha_3 + \alpha_4)] \\ & + \xi \{P_F[\alpha_3 - \alpha_1 + P_{F2}(\alpha_1 - \alpha_2 - \alpha_3 + \alpha_4)] + \alpha_1 - v + P_{F2}(\alpha_2 - \alpha_1)\} \\ & + \alpha_1 + P_{D2}(\alpha_2 - \alpha_1) \} = 0 \end{aligned} \quad (4-71)$$

Dividing equation (4-71) by $[\alpha_3 - \alpha_1 + P_{D2}(\alpha_1 - \alpha_2 - \alpha_3 + \alpha_4)]$ and rearranging terms, we obtain the objective function J_{11} to be

$$J_{11} = P_{D_1} + \xi_{11} \{P_{F_1} - v_{11}\} + K_{11} \quad (4-72)$$

where,

$$\xi_{11} = \xi \frac{\alpha_3 - \alpha_1 + P_{F_2} (\alpha_1 - \alpha_2 - \alpha_3 + \alpha_4)}{\alpha_3 - \alpha_1 + P_{D_2} (\alpha_1 - \alpha_2 - \alpha_3 + \alpha_4)}$$

$$v_{11} = \frac{\alpha_1 - v + P_{F_2} (\alpha_2 - \alpha_1)}{\alpha_3 - \alpha_1 + P_{D_2} (\alpha_1 - \alpha_2 - \alpha_3 + \alpha_4)}$$

$$K_{11} = \frac{\alpha_1 + P_{D_2} (\alpha_2 - \alpha_1)}{\alpha_3 - \alpha_1 + P_{D_2} (\alpha_1 - \alpha_2 - \alpha_3 + \alpha_4)}$$

In a similar manner, we can define J_{22} , ξ_{22} , v_{22} and K_{22} for the second threshold multiplier. Taking the derivatives of J_{11} and J_{22} with respect to T_1 and T_2 , respectively, and rearranging terms, we obtain

$$\frac{\partial P_{D_1}}{\partial P_{F_1}} = - \xi_{11} \quad (4-73)$$

$$\frac{\partial P_{D_2}}{\partial P_{F_2}} = - \xi_{22} \quad (4-74)$$

Substituting equations (4-61) to (4-64) into equations (4-73) and (4-74), we get

$$\xi_{11} = - \frac{(1+S)^{N_1} (1+T_1)^{N_1+1}}{(1+S+T_1)^{N_1}} \quad (4-75)$$

$$\xi_{22} = - \frac{(1+S)^{N_2} (1+T_2)^{N_2+1}}{(1+S+T_2)^{N_2}} \quad (4-76)$$

Solving equations (4-59) to (4-64), (4-67) to (4-70),

(4-73) and (4-74) by an extensive iterative procedure, for $N_1 = 6$, $N_2 = 4$, we obtain the optimum P_D versus P_F curves shown in Figures 4-6 and 4-7, for $S = 5$ dB and $S = 10$ dB, respectively. To obtain the overall probability of detection, P_D , for a specific probability of false-alarm at the data fusion center, we read it directly from the graphs. From Figure 4-6, we read that for $P_F = 10^{-4}$, P_D is .451, which is equal to the P_D obtained from the "AND" fusion rule.

4.4 Summary and Discussion

In this chapter, we have developed the concept of distributed CA-CFAR detection with data fusion, where detection decisions are transmitted from each CA-CFAR detector to the data fusion center. The overall decision is obtained at the data fusion center based on some "k out of n" fusion rule. In the first part of the chapter, we obtained the optimum threshold multipliers at each CA-CFAR detector, given the fusion rule at the data fusion center. In the latter part of the chapter, we optimized the entire system. That is, we obtained the optimum threshold multipliers at each CA-CFAR detector, as well as the optimum fusion rule at the data fusion center. Although the computations involved required an extensive iterative procedure, numerical results were obtained to show the performance of the systems proposed.

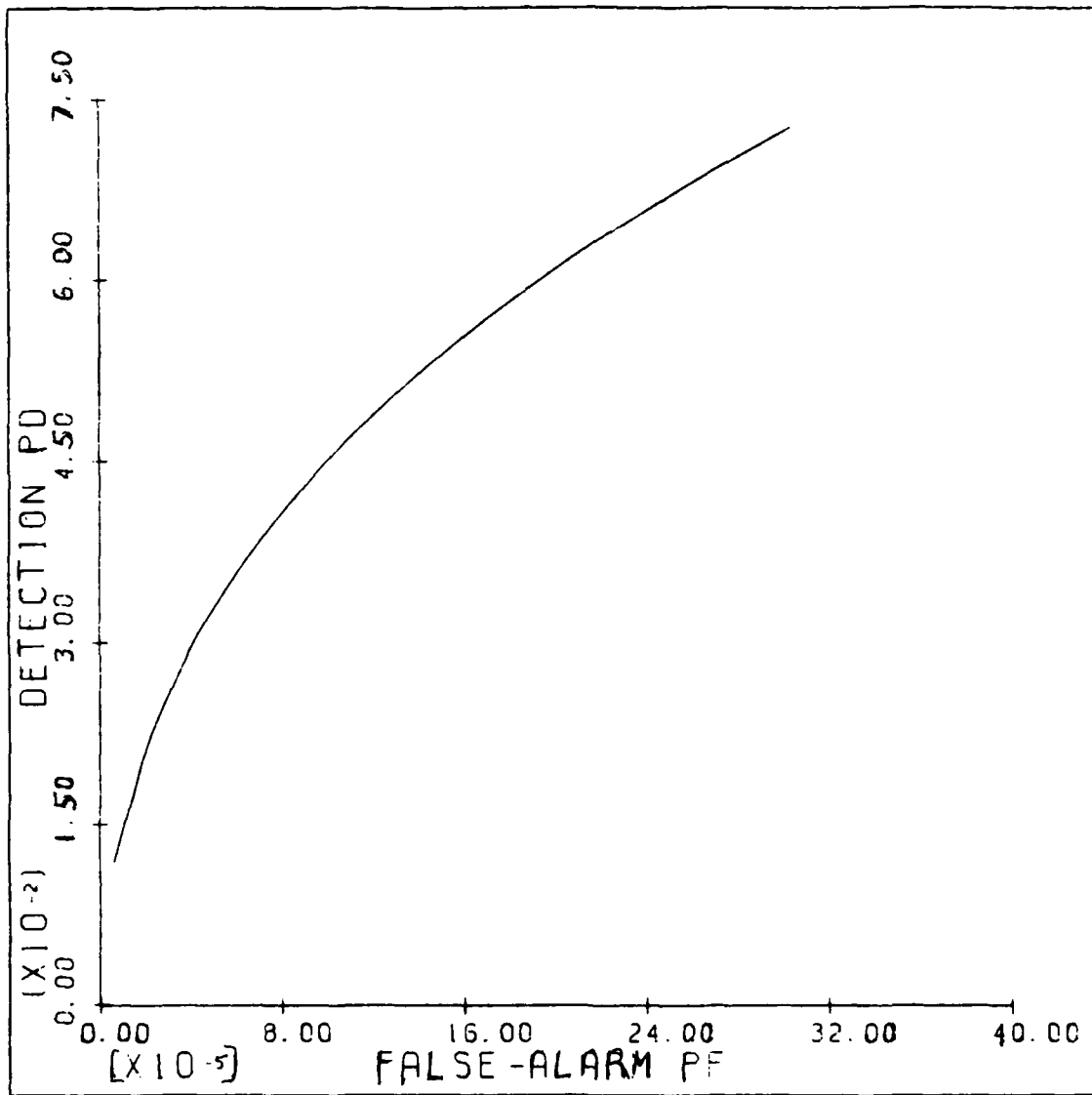


Fig. 4-6. P_D Versus P_F for the Overall Optimum System.
 $S = 5$ dB.

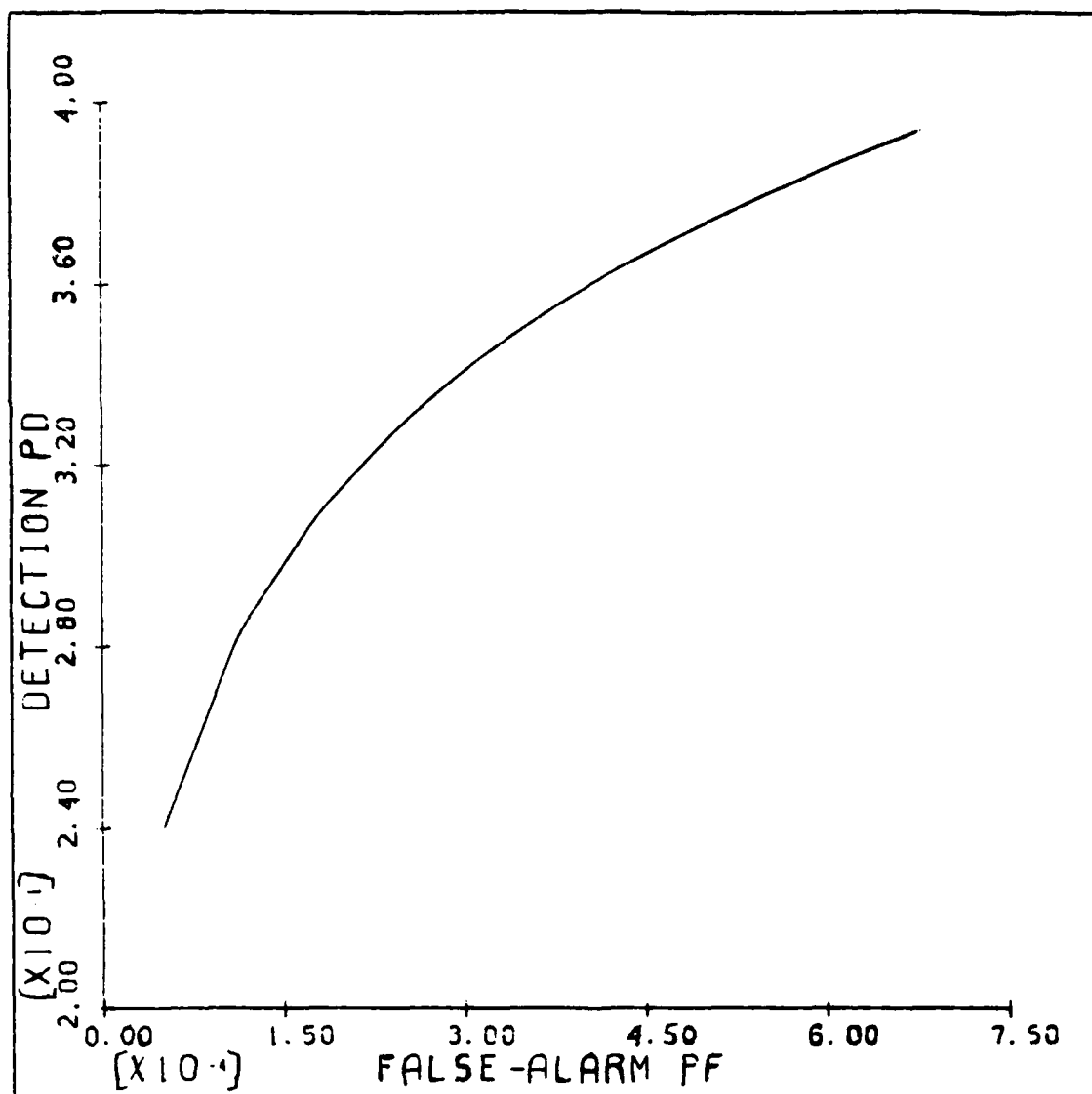


Fig. 4-7. P_D Versus P_F for the Overall Optimum System.
 $S = 10$ dB.

CHAPTER V
ADAPTIVE CFAR DETECTION WITH MULTIPLE
BACKGROUND ESTIMATORS

5.1 Introduction

In the last chapter, we studied the use of multiple sensors with data fusion for adaptive CFAR detection. Decisions of the individual CFAR detectors were transmitted to a data fusion center where they were combined according to some fusion rule to yield a final decision. In this chapter, we will still use multiple sensors as shown in Figure 5-1. However, rather than the detector decisions, the individual sensors compute and transmit estimates of the level of the background noise to the CFAR detector. These estimates are used to set the adaptive threshold required for the desired probability of false-alarm at the CFAR detector. In Section 5.2, we formulate the problem, discuss the operation of the system and derive expressions of the probability of detection for CA-CFAR, GO-CFAR, and SO-CFAR detection. An example is presented in Section 5.3. In Section 5.4, we suggest a hybrid system which combines the concept developed in Chapter four and the concept used here in Section 5.2.

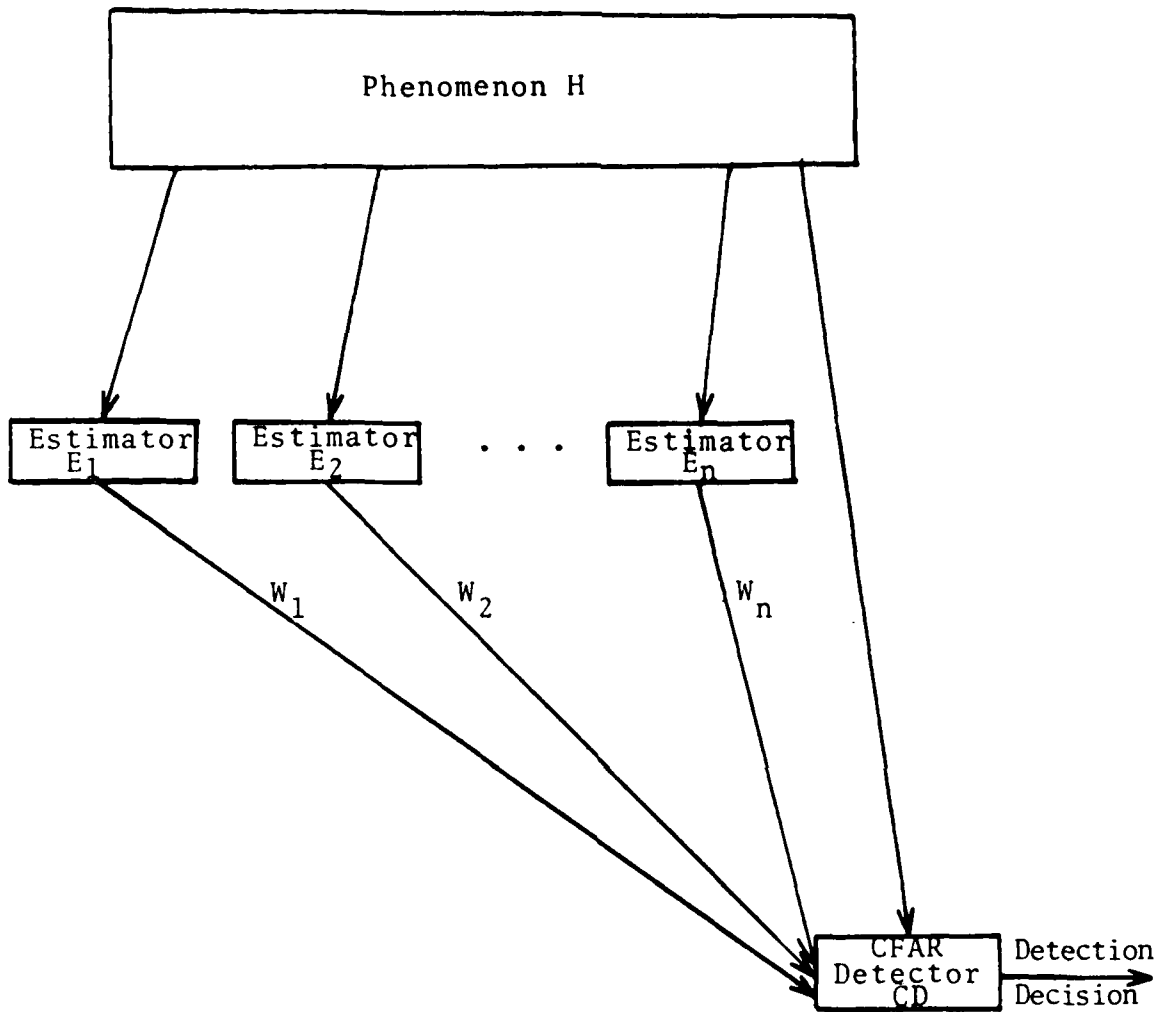
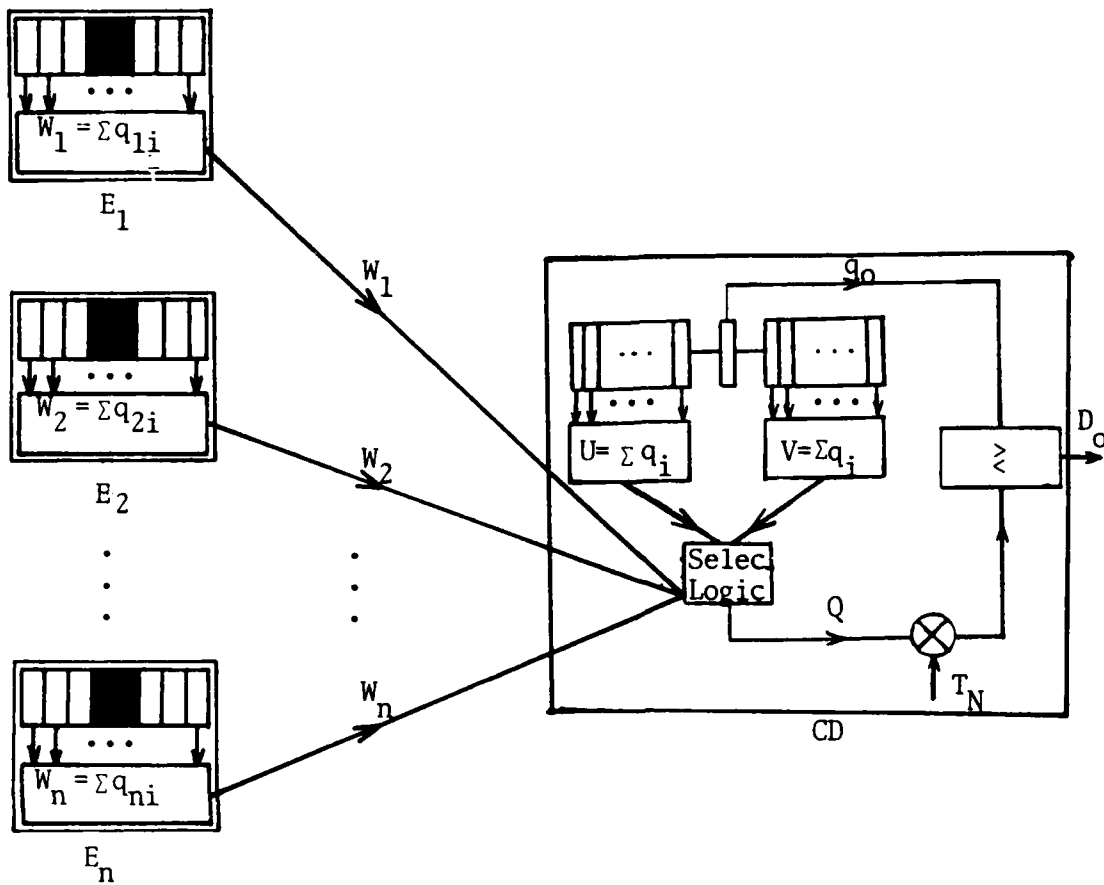


Fig. 5-1. CFAR Processor with Multiple Background Estimators.

5.2 Adaptive CFAR Detection with Multiple Background Estimators

A more detailed block diagram of the system under consideration is shown in Figure 5-2. It consists of $(n+1)$ sensors, n of which are used solely for the estimation of the unknown level of the white Gaussian background noise. These sensors are denoted by E_1, E_2, \dots, E_n . The sensor E_i , $i=1, 2, \dots, n$, obtains the maximum likelihood estimate (MLE), W_i , $i=1, 2, \dots, n$, of the unknown level of noise (we refer to W_i as the MLE even though strictly speaking it is N_i times the maximum likelihood estimate, where N_i is the number of range cells at the i th estimator). As indicated in Figure 5-2, the center tap and the guard cells are not used during the computation of W_i at the sensor E_i . After this data compression, the MLE W_i , $i=1, 2, \dots, n$, is transmitted to the CFAR detector CD. CD computes its own ML estimate of the background noise and obtains the reference windows U and V . The MLE's W_1, W_2, \dots, W_n are combined with the reference windows U and V at sensor CD where a decision about the target is to be made. The MLE's U, V and W_i , $i=1, 2, \dots, n$, are combined according to the desired selection logic CA, GO or SO to yield the adaptive threshold Q . Q is then scaled by the threshold multiplier, T_N , so that the probability of false-alarm at the output of the CFAR detector at CD is maintained at the desired value. The test statistic, q_0 , from the cell under test at the CFAR detector is compared to the threshold $T_N Q$ in order to make a decision.



$$\begin{aligned}
 Q &= U+V+W_1+\dots+W_n, \text{ CA-CFAR}; T_N \equiv T_{CA} \\
 Q &= \text{MAX}(U,V,W_1,\dots,W_n), \text{ GO-CFAR}; T_N \equiv T_{GO} \\
 Q &= \text{MIN}(U,V,W_1,\dots,W_n); \text{ SO-CFAR}; T_N \equiv T_{SO}
 \end{aligned}$$

Fig. 5-2. Cell-Averaging CFAR Processor with Multiple Background Estimators.

The target to be detected is assumed to be of Swerling type I with an SNR S embedded in a white Gaussian noise. The noise samples of the reference cells of the sensors are assumed to be independent, identically distributed with the probability density function defined as in equation (1-5). The probability density function and the cumulative distribution function of the estimates W_i , $i=1,2,\dots,n$, are (see Appendix A for details).

$$P_{W_i}(w_i) = \frac{1}{\Gamma(N_i)} w_i^{N_i-1} e^{-w_i}, \quad w_i \geq 0, \quad (5-1)$$

$i=1,2,\dots,n$

$$F_{W_i}(w_i) = 1 - e^{-w_i} \sum_{j=0}^{(N_i/2)-1} \frac{1}{j!} w_i^j, \quad w_i \geq 0, \quad (5-2)$$

$i=1,2,\dots,n$

where $N_i, i=1,2,\dots,n$, denotes the number of reference cells at the sensor E_i , $i=1,2,\dots,n$. The reference windows U and V at CD are assumed to have the same number of range cells equal to $\frac{N}{2}$. For ease of notation in deriving the adaptive threshold, we let

$$\frac{N}{2} = N_0 \quad (5-3)$$

Now, we obtain the probability of detection for the CFAR processor with multiple background estimators shown in Figure 5-2. The cell-averaging selection logics considered are the CA, GO and SO.

5.2-1 CA-CFAR Detection

In this case, the statistic Q is the sum of the MLE's i.e.,

$$Q = U + V + W_1 + W_2 + \dots + W_n \quad (5-4)$$

where U , V , and W_i , $i = 1, 2, \dots, n$, are statistically independent random variables. Let us define

$$W_0 = U + V \quad (5-5)$$

Then, the probability density function of W_0 is the convolution of the probability density functions of U and V . Using equations (1-7) and (1-8), and rewriting the convolution to obtain the probability density function of W_0 , we have

$$P_{W_0}(w_0) = \frac{1}{\Gamma(N_0) \Gamma(N_0)} e^{-w_0} \int_0^{w_0} u^{\frac{N}{2}-1} (u-w_0)^{\frac{N}{2}-1} du \quad (5-6)$$

Solving the integral and rearranging terms, we obtain

$$P_{W_0}(w_0) = \frac{1}{\Gamma(N_0)} e^{-w_0} w_0^{N_0-1}, \quad w_0 \geq 0 \quad (5-7)$$

The probability density function of Q , $P_Q^{CA}(q)$, is given by the following n -fold convolution.

$$P_Q^{CA}(q) = P_{W_0}(w_0) * P_{W_1}(w_1) * \dots * P_{W_n}(w_n) \quad (5-8)$$

For the sake of clarity, we define the following random variables.

$$Q_1 = W_0 + W_1$$

$$Q_i = Q_{i-1} + W_i, \quad i=2, 3, \dots, n-1$$

$$Q = Q_{n-1} + W_n \quad (5-9)$$

The probability density function of Q_1 is given by the following convolution

$$P_{Q_1}(q_1) = \int_0^{q_1} P_{W_0}(w_0) P_{W_1}(q_1 - w_0) dw_0 \quad (5-10)$$

Substituting equations (5-1) and (5-7) into equation (5-10), we obtain

$$P_{Q_1}(q_1) = \frac{e^{-q_1}}{\Gamma(N_1) \Gamma(N_0)} \int_0^{q_1} w_0^{-N_0-1} (q_1 - w_0)^{N_1-1} dw_0 \quad (5-11)$$

Solving the integral, we get

$$P_{Q_1}(q_1) = \frac{e^{-q_1}}{\Gamma(N_1) \Gamma(N_0)} q_1^{N_0+N_1-1} B(N_0, N_1) \quad (5-12)$$

where $B(x, y)$ is the incomplete Beta function. $B(x, y)$ can be defined in terms of the Gamma function, i.e.,

$$B(x, y) = \frac{\Gamma(x) \Gamma(y)}{\Gamma(x+y)} \quad (5-13)$$

Substituting equation (5-13) into equation (5-12), the probability density function of Q_1 becomes

$$P_{Q_1}(q_1) = \frac{1}{\Gamma(N_0+N_1)} e^{-q_1} q_1^{N_0+N_1-1}, \quad q_1 \geq 0 \quad (5-14)$$

Similarly, we can derive the probability density function of Q_2 , $P_{Q_2}(q_2)$. Since

$$Q_2 = Q_1 + W_2 \quad (5-15)$$

and Q_1 and W_2 are statistically independent,

$$P_{Q_2}(q_2) = \frac{e^{-q_2}}{\Gamma(N_2) \Gamma(N_0+N_1)} \int_0^{q_2} q_1^{N_2-1} (q_2 - q_1)^{N_0+N_1-1} dq_1 \quad (5-16)$$

Solving the integral and using equation (5-13), $P_{Q_2}(q_2)$ becomes

$$P_{Q_2}(q_2) = \frac{1}{\Gamma(N_0 + N_1 + N_2)} e^{-q_2} q_2^{N_0 + N_1 + N_2 - 1} \quad (5-17)$$

Continuing in this manner, the probability density function of the adaptive threshold, $P_Q^{CA}(q)$, can be seen to be

$$P_Q^{CA}(q) = \frac{1}{\Gamma(\psi)} e^{-q} q^{\psi-1} \quad (5-18)$$

where,

$$\psi = \sum_{i=0}^n N_i$$

Substituting equations (5-18) and (1-3) into equation (1-2), the probability of detection, P_D^{CA} , is

$$P_D^{CA} = \int_0^{\infty} e^{-\frac{T_{CA}q}{1+S}} \cdot \frac{1}{\Gamma(\psi)} e^{-q} q^{\psi-1} dq \quad (5-19)$$

This results in

$$P_D^{CA} = \left[\frac{1+S}{1+S+T_{CA}} \right]^{\psi} \quad (5-20)$$

The probability of false-alarm, P_F^{CA} , is obtained by just setting the target SNR S to be zero, i.e.,

$$P_F = \frac{1}{(1 + T_{CA})^{\psi}} \quad (5-21)$$

5.2-2 GO-CFAR Detection

In this case, the adaptive threshold Q is

$$Q = \text{MAX}(U, V, W_1, W_2, \dots, W_n)$$

Since the random variables U, V , and W_i , $i=1,2,\dots,n$, are independent of each other, the cumulative distribution function of Q is

$$\begin{aligned}
 F_Q^{GO}(q) &= \Pr \{ \text{Max}(U, V, W_1, W_2, \dots, W_n) \leq q \} \\
 &= \Pr \{ U \leq q, \quad V \leq q, \quad W_1 \leq q, \quad W_2 \leq q, \dots, W_n \leq q \} \\
 &= \Pr \{ U \leq q \} \cdot \Pr \{ V \leq q \} \cdot \Pr \{ W_1 \leq q \} \cdot \Pr \{ W_2 \leq q \} \dots \Pr \{ W_n \leq q \} \\
 &= F_U(q) F_V(q) F_{W_1}(q) F_{W_2}(q) \dots F_{W_n}(q) \quad (5-22)
 \end{aligned}$$

The probability density function and the cumulative distribution function of U and V are as defined in equations (1-7) to (1-10). We define the notation

$$U = W_0 \quad \text{and} \quad \frac{N}{Z} = N_0 \quad (5-23)$$

$$V = W_{n+1} \quad \text{and} \quad \frac{N}{Z} = N_{n+1} \quad (5-24)$$

Using equations (5-23) and (5-24) in equation (5-22), the cumulative distribution function becomes

$$F_Q^{GO}(q) = F_{W_0}(q) F_{W_1}(q) F_{W_2}(q) \dots F_{W_n}(q) F_{W_{n+1}}(q) \quad (5-25)$$

Then, the probability density function of the adaptive threshold is obtained by taking the derivative of equation (5-25) with respect to q , i.e.,

$$\begin{aligned}
P_Q^{GO}(q) &= P_{W_0}(q) F_{W_1}(q) F_{W_2}(q) \dots F_{W_n}(q) F_{W_{n+1}}(q) \\
&+ F_{W_0}(q) P_{W_1}(q) F_{W_2}(q) \dots F_{W_n}(q) F_{W_{n+1}}(q) \\
&+ F_{W_0}(q) F_{W_1}(q) P_{W_2}(q) \dots F_{W_n}(q) F_{W_{n+1}}(q) \\
&\vdots \\
&+ F_{W_0}(q) F_{W_1}(q) F_{W_2}(q) \dots P_{W_n}(q) F_{W_{n+1}}(q) \\
&+ F_{W_0}(q) F_{W_1}(q) F_{W_2}(q) \dots F_{W_n}(q) P_{W_{n+1}}(q) \quad (5-26)
\end{aligned}$$

Now, we substitute equations (1-7) to (1-10), (5-1), and (5-2) into equation (5-26) to obtain

$$\begin{aligned}
P_Q^{GO}(q) &= \frac{1}{\Gamma(N_0)} q^{N_0-1} e^{-q} \prod_{j=1}^{n+1} (1 - e^{-q} \sum_{i=0}^{N_j-1} \frac{1}{i!} q^i) \\
&+ \frac{1}{\Gamma(N_1)} q^{N_1-1} e^{-q} \prod_{\substack{j=0 \\ j \neq 1}}^{n+1} (1 - e^{-q} \sum_{i=0}^{N_j-1} \frac{1}{i!} q^i) \\
&\vdots \\
&+ \frac{1}{\Gamma(N_n)} q^{N_n-1} e^{-q} \prod_{\substack{j=0 \\ j \neq n}}^{n+1} (1 - e^{-q} \sum_{i=0}^{N_j-1} \frac{1}{i!} q^i) \\
&+ \frac{1}{\Gamma(N_{n+1})} q^{N_{n+1}-1} e^{-q} \prod_{j=0}^n (1 - e^{-q} \sum_{i=0}^{N_j-1} \frac{1}{i!} q^i) \quad (5-27)
\end{aligned}$$

Regrouping common terms, $P_Q^{GO}(q)$ becomes

$$P_Q^{GO}(q) = \sum_{k=0}^{n+1} \left\{ \frac{q^{N_k-1} e^{-q}}{\Gamma(N_k)} \prod_{\substack{j=0 \\ j \neq k}}^{n+1} (1 - e^{-q} \sum_{i=0}^{N_j-1} \frac{q^i}{i!}) \right\} \quad (5-28)$$

This can be substituted in equation (1-2) to obtain the probability of detection.

5.2-3 SO-CFAR Detection

In this case, the adaptive threshold Q is

$$Q = \text{MIN}(W_0, W_1, W_2, \dots, W_n, W_{n+1}) \quad (5-29)$$

where W_0 and W_{n+1} are as defined in equations (5-23) and (5-24). The cumulative distribution, $F_Q^{SO}(q)$, is

$$\begin{aligned} F_Q^{SO}(q) &= \text{Pr} \{ \min(W_0, W_1, W_2, \dots, W_n, W_{n+1}) \leq q \} \\ &= 1 - \text{Pr} \{ \min(W_0, W_1, W_2, \dots, W_n, W_{n+1}) > q \} \\ &= 1 - \text{Pr} \{ W_0 > q, W_1 > q, W_2 > q, \dots, W_n > q, W_{n+1} > q \} \\ &= 1 - [1 - F_{W_0}(q)] \cdot [1 - F_{W_1}(q)] \dots [1 - F_{W_n}(q)] \cdot [1 - F_{W_{n+1}}(q)] \end{aligned} \quad (5-30)$$

Taking the derivative with respect to q , the probability density function, $P_Q^{SO}(q)$, is

$$\begin{aligned}
P_Q^{SO}(q) = & - P_{W_0}(q) [1 - F_{W_1}(q)] \cdot [1 - F_{W_2}(q)] \dots [1 - F_{W_n}(q)] [1 - F_{W_{n+1}}(q)] \\
& - [1 - F_{W_0}(q)] P_{W_1}(q) [1 - F_{W_2}(q)] \dots [1 - F_{W_n}(q)] \cdot [1 - F_{W_{n+1}}(q)] \\
& - [1 - F_{W_0}(q)] [1 - F_{W_1}(q)] P_{W_2}(q) \dots [1 - F_{W_n}(q)] \cdot [1 - F_{W_{n+1}}(q)] \\
& \vdots \\
& - [1 - F_{W_0}(q)] [1 - F_{W_1}(q)] \cdot [1 - F_{W_2}(q)] \dots P_{W_n}(q) [1 - F_{W_{n+1}}(q)] \\
& - [1 - F_{W_0}(q)] [1 - F_{W_1}(q)] \cdot [1 - F_{W_2}(q)] \dots [1 - F_{W_n}(q)] P_{W_{n+1}}(q)
\end{aligned}
\tag{5-31}$$

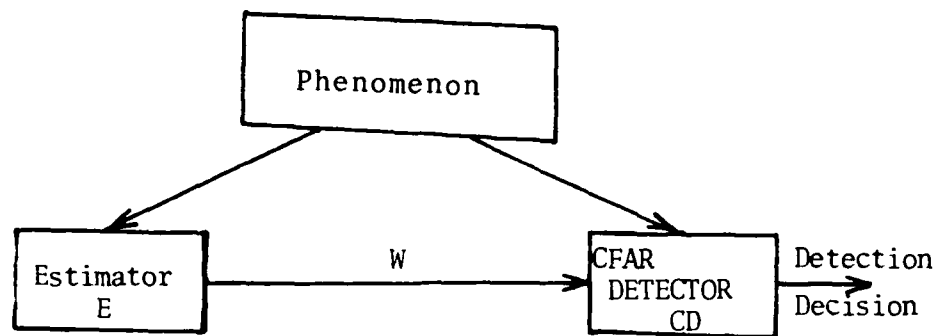
Substituting from equations (1-7), (1-8), (1-9), (1-10), (5-1) and (5-2) into equation (5-31), the probability density function is obtained to be

$$P_Q^{SO}(q) = - \sum_{k=0}^{n+1} \left\{ \frac{q^{N_k-1} e^{-q}}{\Gamma(N_k)} \prod_{\substack{j=0 \\ j \neq k}}^{n+1} \left(e^{-q} \sum_{i=0}^{N_j-1} \frac{q^i}{i!} \right) \right\}
\tag{5-32}$$

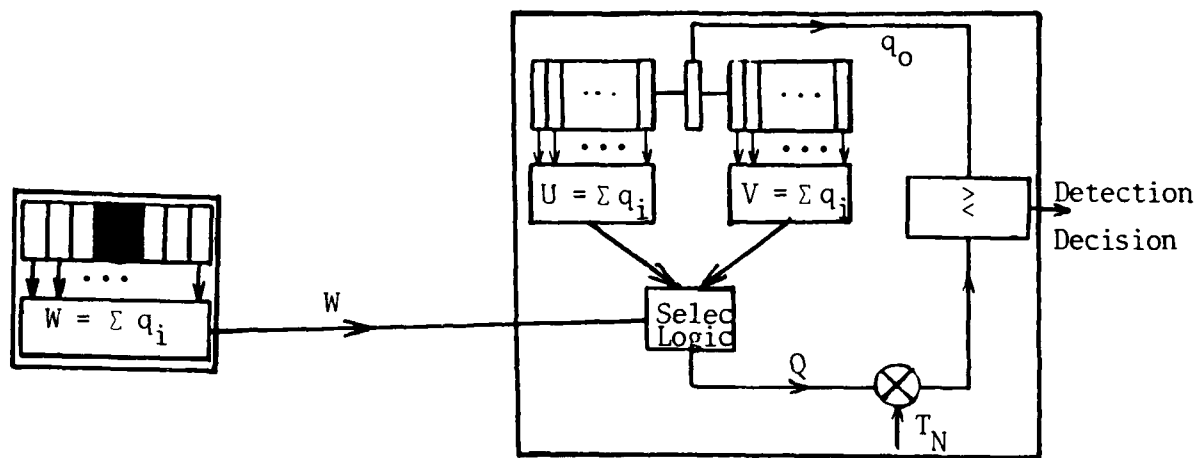
Again, we can use equation (5-32) in equation (1-2) to obtain the probability of detection. In the next section, we present an example for illustration.

5.3 Example

The two-sensor system under consideration is shown in Figure 5-3. The probability density functions of U and V



(a)



(b)

$$Q=U+V+W, \text{ CA-CFAR}; T_N \equiv T_{CA}$$

$$Q=\text{MAX}(U,V,W), \text{ GO-CFAR}; T_N \equiv T_{GO}$$

$$Q=\text{MIN}(U,V,W), \text{ SO-CFAR}; T_N \equiv T_{SO}$$

Fig. 5-3. A Two-Sensor CFAR Processor with One Background Estimator.

are defined in equations (1-7) and (1-8), and the probability density function of W is

$$P_W(w) = \frac{1}{\Gamma(N+2)} w^{N+1} e^{-w}, \quad w \geq 0 \quad (5-33)$$

Using these probability density functions, we derive expressions of the probability of detection for the three schemes, CA, GO and SO, discussed above.

CA-CFAR

The adaptive threshold Q is the sum of U, V , and W , i.e.,

$$Q = U + V + W \quad (5-34)$$

Thus,

$$P_Q^{CA}(q) = P_U(u) * P_V(v) * P_W(w) \quad (5-35)$$

Using the results derived in the previous section, $P_Q^{CA}(q)$ is

$$P_Q^{CA}(q) = \frac{1}{\Gamma(2N+2)} q^{2N+1} e^{-q}, \quad q \geq 0 \quad (5-36)$$

Substituting equations (5-36) and (1-3) into equation (1-2), we obtain the probability of detection P_D^{CA} to be

$$P_D^{CA} = \left[\frac{1 + S}{1 + S + T_{CA}} \right]^{2N+2} \quad (5-37)$$

while the probability of false-alarm is

$$P_F^{CA} = \frac{1}{(1 + T_{CA})^{2N+2}} \quad (5-38)$$

For a probability of false-alarm of 10^{-4} and $N=4$, we plot

P_D^{CA} versus the target SNR to study the improvement in the performance. In Figure 5-4, we plot the probability of detection of the two-sensor system of Figure 5-3, and the probability of detection of a single sensor system. The improvement in the performance is clearly noticeable.

GO-CFAR

In this case, the adaptive threshold is equal to the maximum of U, V, and W, i.e.,

$$Q = \text{MAX}(U, V, W) \quad (5-39)$$

The cumulative distribution of Q is

$$F_Q^{GO}(q) = F_U(q) F_V(q) F_W(q) \quad (5-40)$$

while the probability density is

$$P_Q^{GO}(q) = P_U(q)F_V(q)F_W(q) + F_U(q)P_V(q)F_W(q) + F_U(q)F_V(q)P_W(q) \quad (5-41)$$

Substituting equations (1-7) to (1-10), and (5-33) into equation (5-41), the probability density function of the adaptive threshold becomes

$$P_Q^{GO}(q) = \frac{2}{\Gamma(\frac{N}{2})} \left\{ q^{\frac{N}{2}-1} e^{-q} - 2q^{\frac{N}{2}-1} e^{-2q} \sum_{j=0}^{N+1} \frac{1}{j!} q^j \right. \\ \left. + q^{\frac{N}{2}-1} e^{-3q} \sum_{j=0}^{(N/2)-1} \sum_{k=0}^{N+1} \frac{1}{j!k!} q^{j+k} \right\} +$$

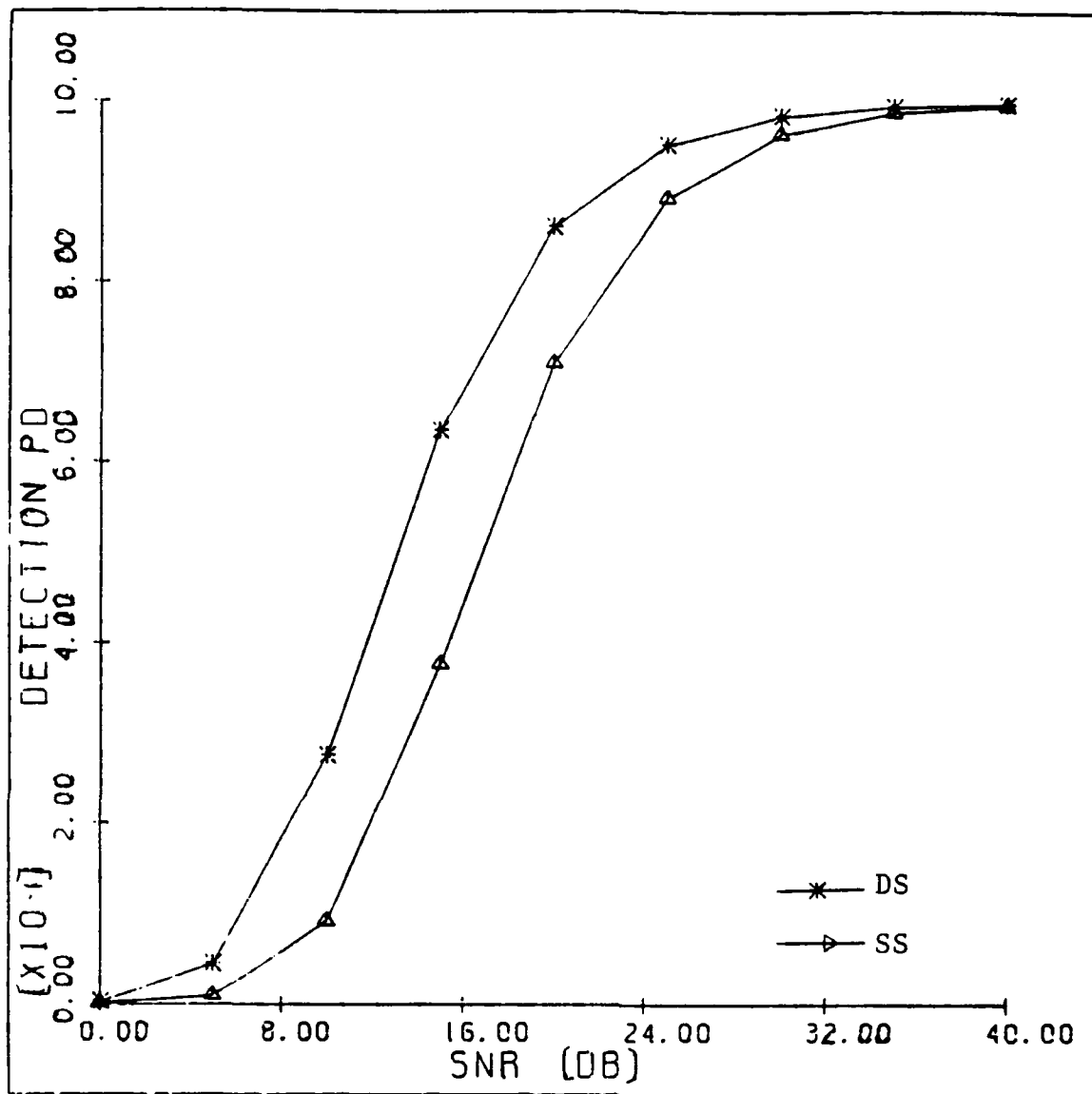


Fig. 5-4. Performance of the CA-CFAR Detectors for $P_F = 10^{-4}$ and $N=4$.
 DS \equiv CFAR Processor with a Background Estimator.
 SS \equiv Single Sensor CFAR Detector.

$$\begin{aligned} & \frac{1}{\Gamma(N+2)} \{ q^{N+1} e^{-q} - 2q^{N+1} e^{-2q} \sum_{j=0}^{(N/2)-1} \frac{1}{j!} q^j \\ & + q^{N+1} e^{-3q} \sum_{j=0}^{(N/2)-1} \sum_{k=0}^{(N/2)-1} \frac{1}{j!k!} q^{j+k} \} \end{aligned} \quad (5-42)$$

The probability of detection is obtained from equation (1-2) by using the results of equations (5-42) and (1-3). Solving the integral and rearranging terms, P_D^{GO} , can be written as

$$\begin{aligned} P_D^{GO} = & 2 \left[\frac{1+S}{1+S+T_{GO}} \right]^{\frac{N}{2}} - \frac{2}{\Gamma(\frac{N}{2})} \sum_{j=0}^{N+1} \frac{\Gamma(\frac{N}{2} + j)}{j!} \left[\frac{1+S}{2(1+S)+T_{GO}} \right]^{\frac{N}{2} + j} \\ & - \frac{2}{\Gamma(\frac{N}{2})} \sum_{j=0}^{(N/2)-1} \frac{\Gamma(\frac{N}{2} + j)}{j!} \left[\frac{1+S}{2(1+S)+T_{GO}} \right]^{\frac{N}{2} + j} \\ & + \frac{2}{\Gamma(\frac{N}{2})} \sum_{j=0}^{(N/2)-1} \sum_{k=0}^{N+1} \frac{\Gamma(\frac{N}{2} + j + k)}{j!k!} \left[\frac{1+S}{3(1+S)+T_{GO}} \right]^{\frac{N}{2} + j + k} \\ & + \left[\frac{1+S}{1+S+T_{GO}} \right]^{N+2} - \frac{2}{\Gamma(N+2)} \sum_{j=0}^{(N/2)-1} \frac{\Gamma(N+j)}{j!} \left[\frac{1+S}{2(1+S)+T_{GO}} \right]^{N+j+2} \\ & + \frac{1}{\Gamma(N+2)} \sum_{j=0}^{(N/2)-1} \sum_{k=0}^{(N/2)-1} \frac{(N+j+k+1)!}{j!k!} \left[\frac{1+S}{3(1+S)+T_{GO}} \right]^{N+j+k+2} \end{aligned} \quad (5-43)$$

The performance in terms of P_D^{GO} versus target SNR is shown in Figure 5-5. Again, the performance of the two-sensor system is compared to that of the single sensor system.

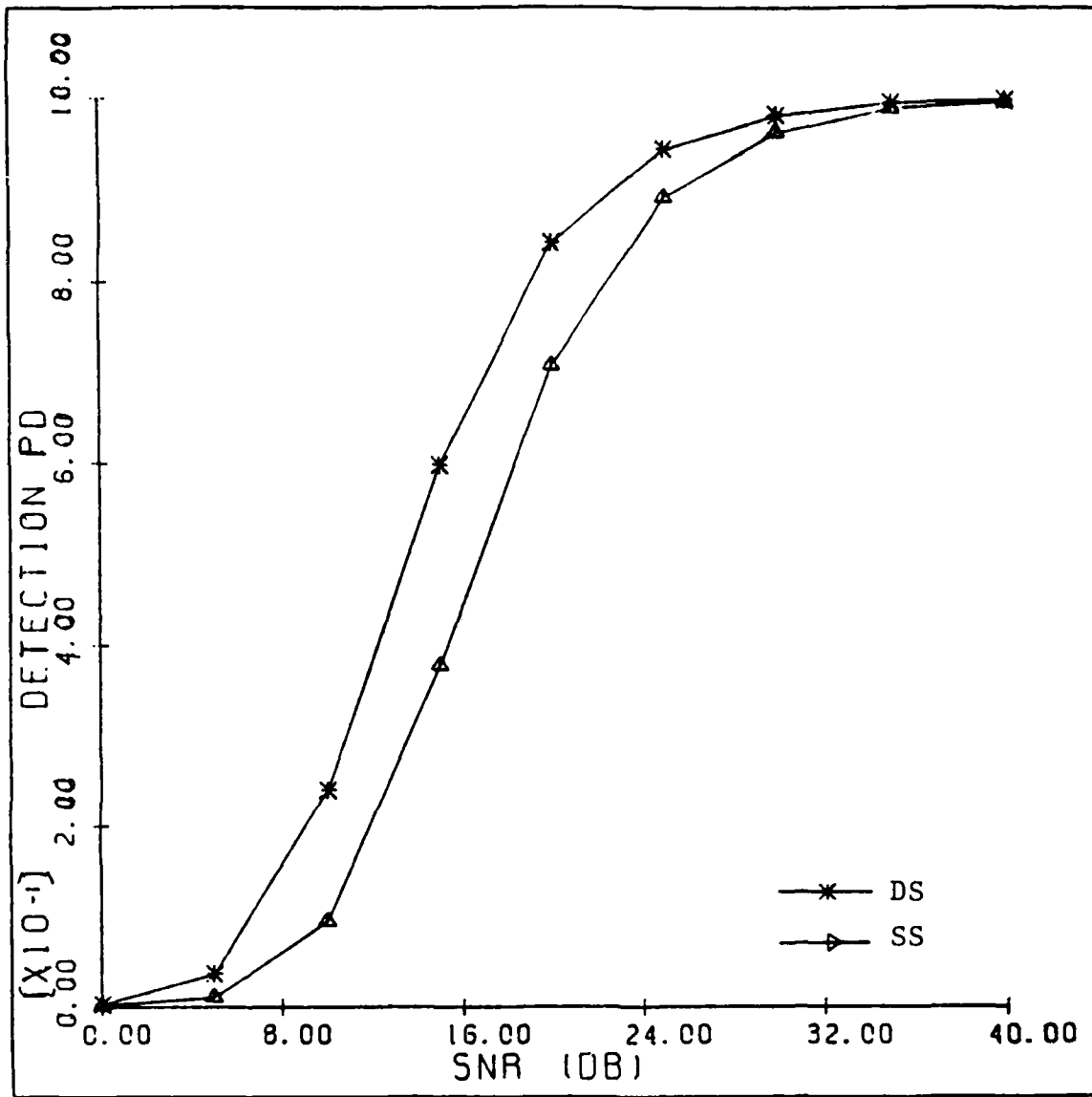


Fig. 5-5. Performance of the GO-CFAR Detectors for $P_F = 10^{-4}$ and $N=4$.
 DS \equiv CFAR Processor with a Background Estimator.
 SS \equiv single sensor CFAR Detector.

SO-CFAR

The threshold in this case, is the minimum of U, V, and W, i.e.,

$$Q = \text{MIN}(U, V, W) \quad (5-44)$$

The cumulative distribution of Q is given by

$$\begin{aligned} F_Q^{SO}(q) = & F_U(q) + F_V(q) + F_W(q) - F_{UV}(q, q) - F_{UW}(q, q) - F_{VW}(q, q) \\ & + F_{UVW}(q, q, q) \end{aligned} \quad (5-45)$$

The probability density function is, therefore,

$$\begin{aligned} f_Q^{SO}(q) = & 2P_U(q) [1 - F_V(q) - F_W(q)] + 2P_U(q) F_V(q) F_W(q) \\ & + P_W(q) [1 - 2F_U(q)] + P_W(q) F_U(q) F_V(q) \end{aligned} \quad (5-46)$$

Substituting equations (5-46), (1-3), (1-7), (1-8), (1-9), (1-10) and (5-33) into equation (1-2), and rearranging terms, the probability of detection is obtained to be

$$\begin{aligned} P_D^{SO} = & \frac{2}{\Gamma(\frac{N}{2})} \sum_{j=0}^{(N/2)-1} \sum_{k=0}^{N+1} \frac{\Gamma(\frac{N}{2} + j + k)}{j!k!} \left[\frac{1+S}{3(1+S)+T_{SO}} \right]^{\frac{N}{2}+j+k} \\ & + \frac{1}{\Gamma(N+2)} \sum_{j=0}^{(N/2)-1} \sum_{k=0}^{(N/2)-1} \frac{(N+j+k+1)!}{j!k!} \left[\frac{1+S}{3(1+S)+T_{SO}} \right]^{N+j+k+2} \end{aligned} \quad (5-47)$$

In Figure 5-6, we compare the performance of all of the

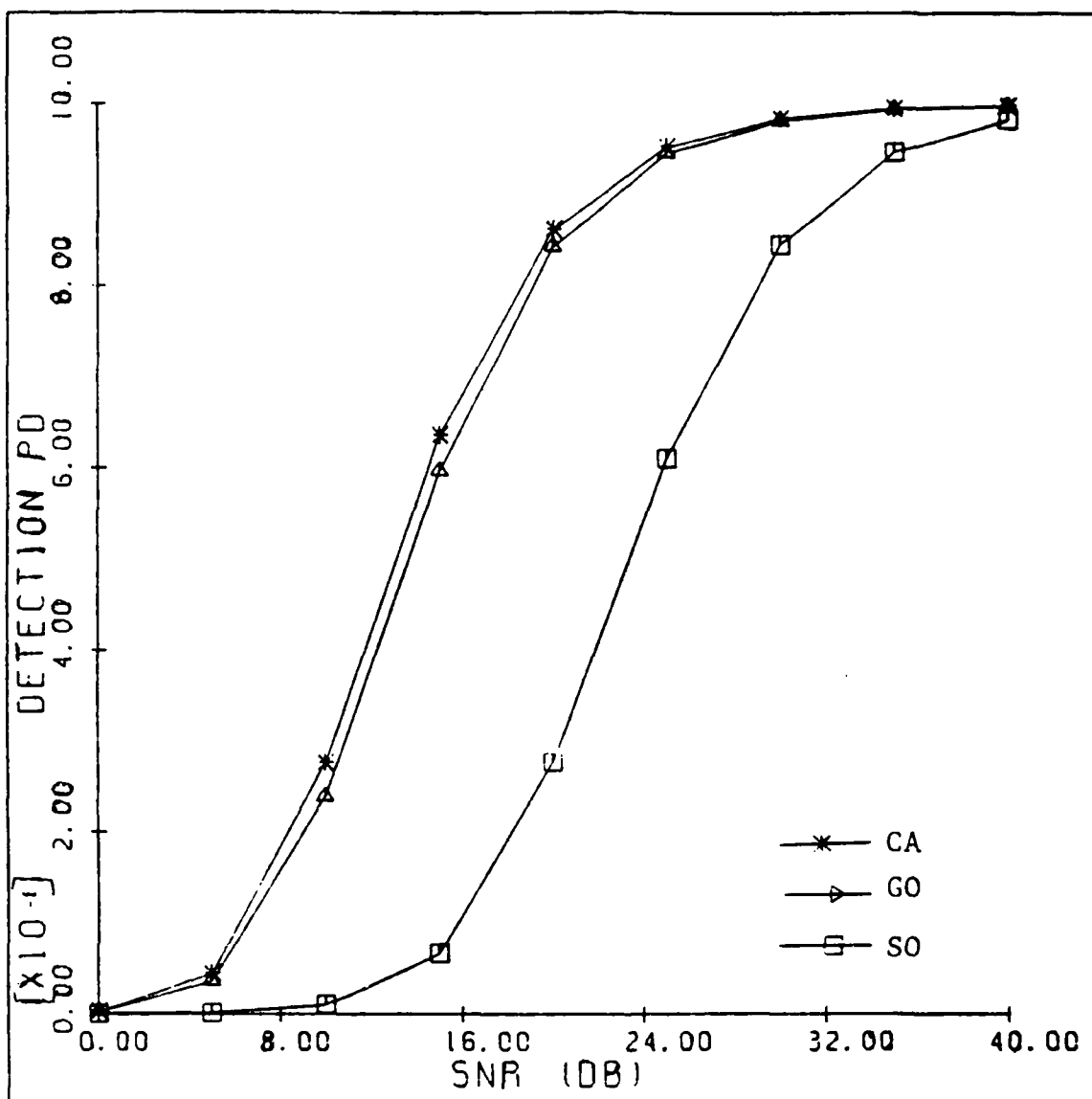


Fig. 5-6. Performance of the CA, GO and SO CFAR Detectors with a Background Estimator for $P_F = 10^{-4}$ and $N=4$.

three schemes for the two-sensor system considered in this example.

5.4. An Extension

In this section, the concept of using multiple background estimators is employed in conjunction with the concept of distributed detection with data fusion developed in Chapter four. The hybrid system that we consider is shown in Figure 5-7. The system consists of n background estimators E_1, E_2, \dots, E_n and a CFAR processor. Each background estimator E_i , $i=1, 2, \dots, n$, transmits the output q_{oi} from its test cell (center tap) as well as the MLE of the level of the background noise, W_i , to the CFAR processor. The MLE's are combined to obtain the adaptive threshold which is scaled by the threshold multiplier, T_N , to achieve the desired value of the probability of the false-alarm at the system output. At the CFAR processor, each test cell q_{oi} , $i=1, 2, \dots, n$, is compared to the above adaptive threshold to yield a decision D_i , $i=1, 2, \dots, n$, where $D_i \in \{0, 1\}$. In a manner analogous to Chapter four, the decisions D_i are combined according to a "k out of n" fusion rule to yield the final decision D_o . The performance of the system proposed in this section is expected to be better than the system discussed in Chapter four. This is due to the additional information about the background noise available at the CFAR processor while computing the adaptive threshold Q . To illustrate the above concepts, an example is presented.

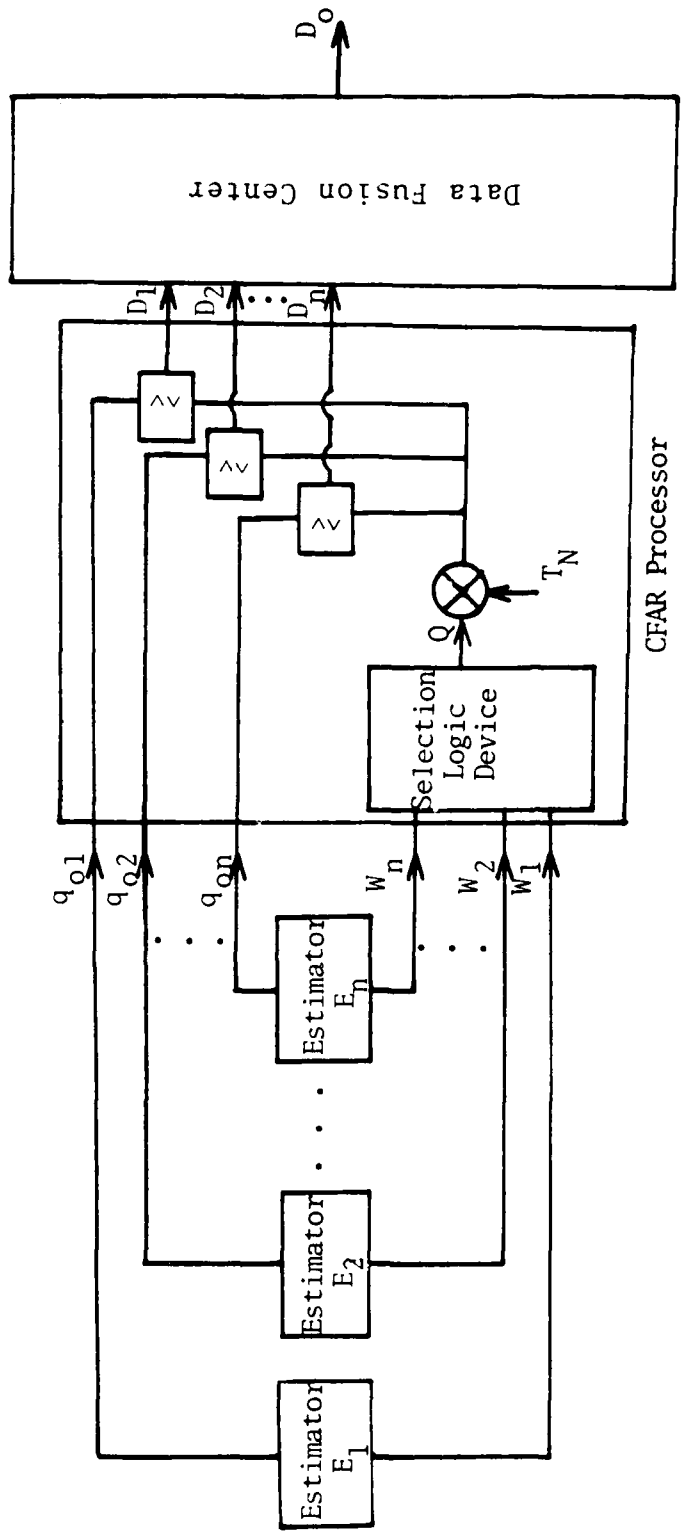


Fig. 5-7. Hybrid CFAR Processor with Data Fusion.

Example

In this example, we consider the system consisting of two background estimators and a CFAR processor as shown in Figure 5-8. At the CFAR processor, we use the CA-CFAR scheme and combine the individual decisions according to the "AND" fusion rule. The result is compared to the corresponding system discussed in Chapter four, i.e., CA-CFAR detection with the "AND" fusion rule. Let $P_{D_1}^h$ and $P_{D_2}^h$ denote the probabilities of detection corresponding to the decisions D_1 and D_2 , respectively, in the hybrid system. Let $P_{D_1}^d$ and $P_{D_2}^d$ be the probabilities of detection corresponding to the decisions D_1 and D_2 for the system shown in Figure 4-2. Let P_D^h and P_D^d represent the overall probabilities of detection for the hybrid system and the system of Figure 4-2, respectively. Then, as shown in Chapter four, the detection probabilities can be written as

$$P_{D_1}^h = \left[\frac{1 + S_1^h}{1 + S_1^h + T} \right]^{N_1 + N_2} \quad (5-48)$$

$$P_{D_2}^h = \left[\frac{1 + S_2^h}{1 + S_2^h + T} \right]^{N_1 + N_2} \quad (5-49)$$

$$P_{D_1}^d = \left[\frac{1 + S_1^d}{1 + S_1^d + T_1} \right]^{N_1} \quad (5-50)$$

$$P_{D_2}^d = \left[\frac{1 + S_2^d}{1 + S_2^d + T_2} \right]^{N_2} \quad (5-51)$$

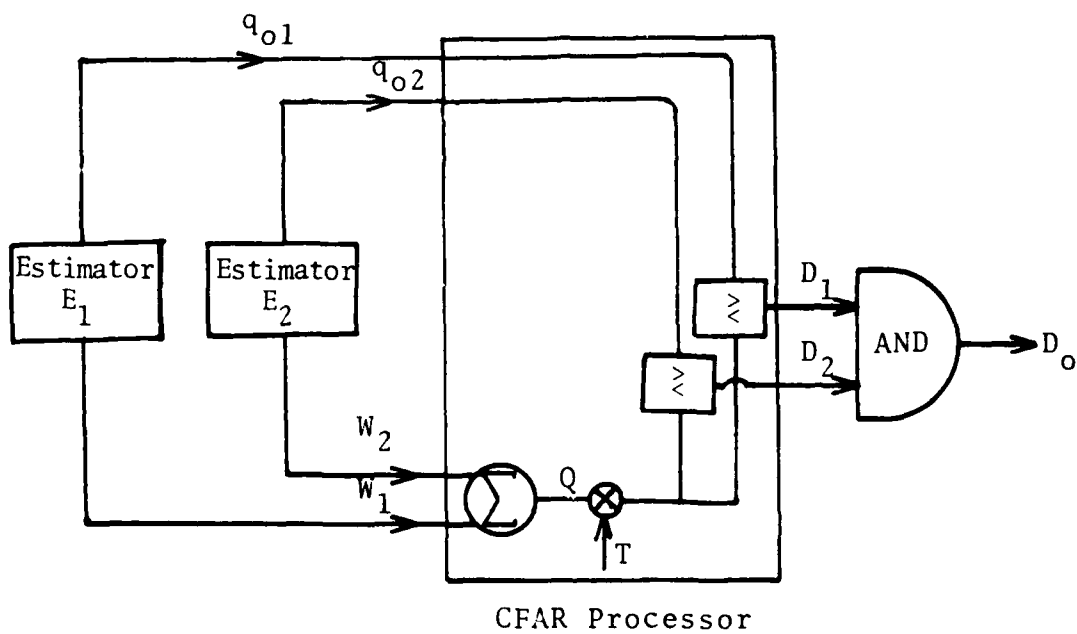


Fig. 5-8. Hybrid System with Two Background Estimators and a Data Fusion Center Using the "AND" Fusion Rule.

where S_1^h and S_2^h are the target SNR's at the two sensors of the hybrid system; S_1^d and S_2^d are the target SNR's at the system of Figure 4-2; T_1 and T_2 are the threshold multipliers of the system shown in Figure 4-2; and T is the threshold multiplier of the hybrid system. Substituting equations (5-48), (5-49), (5-50) and (5-51) into equation (4-13), the overall probabilities of detection P_D^h and P_D^d can be written as

$$P_D^h = \left\{ \frac{1 + S_1^h}{1 + S_1^h + T} \cdot \frac{1 + S_2^h}{1 + S_2^h + T} \right\}^{N_1 + N_2} \quad (5-52)$$

$$P_D^d = \left[\frac{1 + S_1^d}{1 + S_1^d + T_1} \right]^{N_1} \cdot \left[\frac{1 + S_2^d}{1 + S_2^d + T_2} \right]^{N_2} \quad (5-53)$$

In order to compare the two systems under the same conditions, we let $S_1^h = S_2^h = S_1^d = S_2^d = S$. Then, P_D^h and P_D^d become

$$P_D^h = \left[\frac{1 + S}{1 + S + T} \right]^{2(N_1 + N_2)} \quad (5-54)$$

$$P_D^d = \frac{(1 + S)^{N_1 + N_2}}{(1 + S + T_1)^{N_1} (1 + S + T_2)^{N_2}} \quad (5-55)$$

The probabilities of false-alarm are

$$P_F^h = \frac{1}{(1 + T)^{2(N_1 + N_2)}} \quad (5-56)$$

$$P_F^d = \frac{1}{(1 + T_1)^{N_1} (1 + T_2)^{N_2}} \quad (5-57)$$

Using $N_1 = 6$, $N_2 = 4$, and $P_F^h = P_F^d = P_F = 10^{-4}$, we plot P_D^h and P_D^d versus the target SNR S in Figure 5-9. As expected, the hybrid system performs better.

5.5. Summary and Discussion

In this chapter, we have developed the concept of using multiple background estimators for CFAR processing. Since the multiple background estimators provide more information about the level of noise in the background, the performance improved as expected. The model considered in this chapter is applicable to systems using frequency diversity. The model is also applicable to space diversity systems if we make idealized assumptions, i.e., perfect synchronization etc. We also discussed an extension of the work in Chapter four using multiple background estimators.

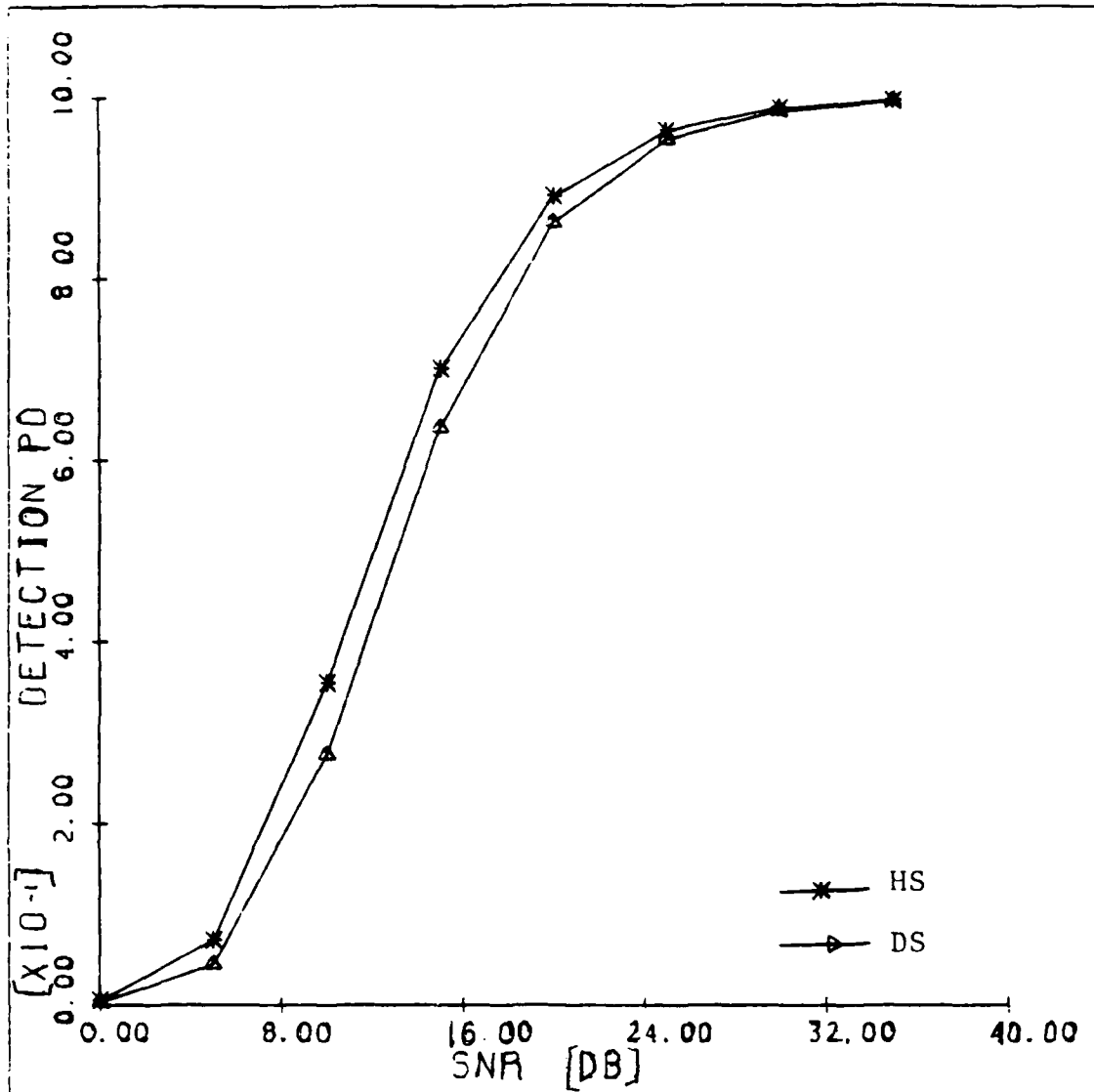


Fig. 5-9. Performance of the Hybrid System with Two Background Estimators (DS) and the Two-Sensor System of Figure 4-2 (DS) $P_F = 10^{-4}$, $N_1 = 6$, $N_2 = 4$.

CHAPTER VI
ADAPTIVE CFAR DETECTION WITH DIFFERENT
NETWORK TOPOLOGIES

6.1. Introduction

In the last two chapters, we have considered the problem of multisensor CFAR detection with data fusion. In Chapter four, the decisions from distributed CFAR processors were combined at the data fusion center according to a "k out of n" fusion rule to yield the overall decision. In Chapter five, multiple sensors transmitted the estimates of the background noise to the CFAR processor where an adaptive threshold based on these estimates was used to yield the final decision. In this chapter, we still consider the problem of multisensor CFAR detection with data fusion. However, the compressed data transmitted between sensors are decisions instead of estimates. In Section 6.2, we formulate the general problem of adaptive CFAR detection for two different network topologies. These systems are optimized and their performance is studied. In Section 6.3, we illustrate the performance by an example. In Section 6.4, we provide a summary along with a discussion.

6.2. System Optimization and Performance Analysis

The network topologies to be considered in this chapter are shown in Figures 6-1 and 6-2. In the first, decisions from individual CA-CFAR processors are transmitted in parallel to the CFAR processor where a final decision is to be made. In the second, the CFAR processors are connected in tandem. Decisions are transmitted from one CFAR processor to the next. At the last CFAR processor, the final decision is made.

The target to be detected is assumed to be of Swerling type I embedded in a white Gaussian noise of unknown level. At each CA-CFAR detector, CD_i , $i = 1, 2, \dots, n$, we denote the target SNR by S_i , $i=1, 2, \dots, n$. The target SNR at the final CA-CFAR detector, CD_0 , is denoted by S . For simplicity and without loss of generality, we let $S_1=S_2=\dots=S_n=S$. The number of range cells used by each CA-CFAR detector, CD_i is denoted by N_i , $i=1, 2, \dots, n$, and N denotes the number of range cells for detector CD_0 . Next, we consider the two networks topologies.

6.2-1. Adaptive CFAR Detection with Parallel Network Topology

The system under consideration is shown in Figure 6-1. It consists of $(n+1)$ CA-CFAR processors. Based on its observation, each CA-CFAR detector, CD_i , $i=1, 2, \dots, n$, makes a decision D_i , $i=1, 2, \dots, n$, where $D_i \in \{0, 1\}$. The adaptive threshold Q_i of CD_i is scaled by the threshold multiplier T_i , $i=1, 2, \dots, n$. As will be shown later, these T_i 's are

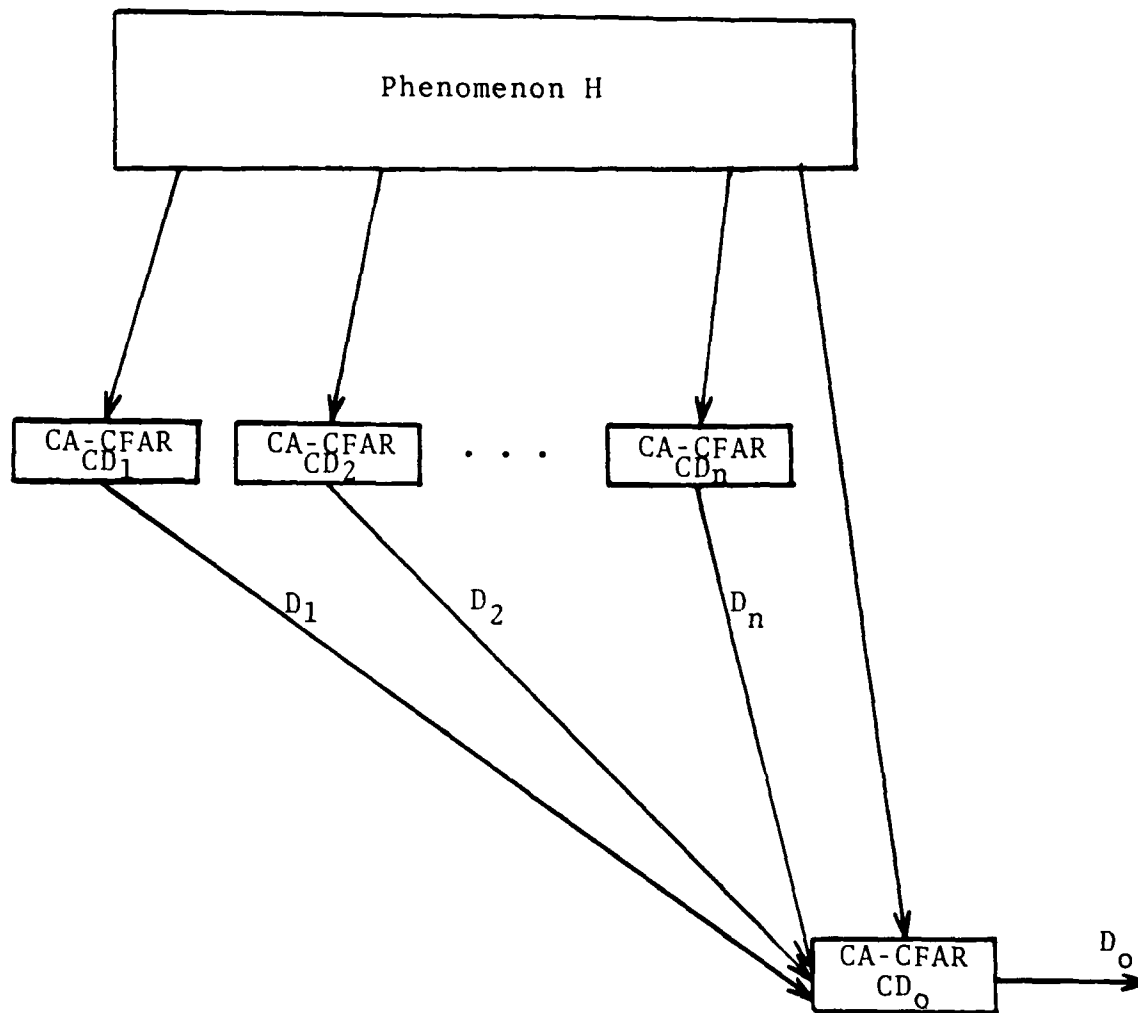


Fig. 6-1. Parallel Network Topology for Adaptive CFAR Detection.

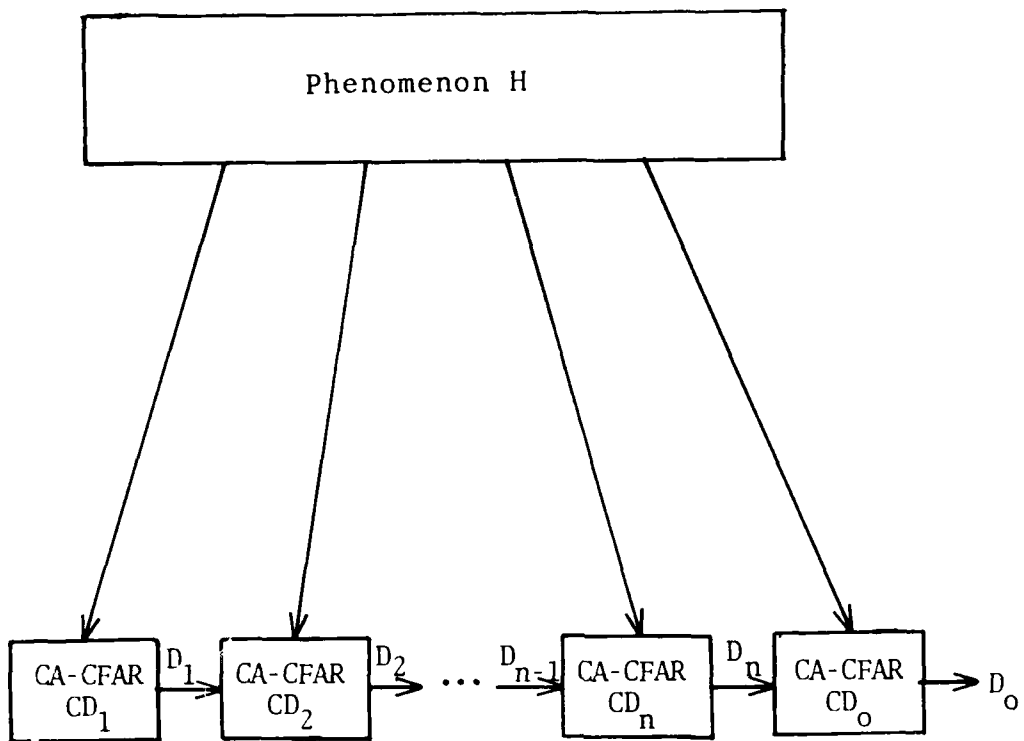


Fig. 6-2. Tandem Network Topology for Adaptive CFAR Detection.

obtained so as to maximize the overall probability of detection while maintaining the overall probability of false-alarm at the desired value. The CA-CFAR detector, CD_0 , combines the decisions D_i , $i=1,2,\dots,n$, with its own estimate of the level of the background noise to obtain the adaptive threshold Q . The threshold Q is scaled by a threshold multiplier, which is also obtained so as to maximize the overall probability of detection while CFAR is achieved. The threshold multiplier depends on the decisions D_i , $i=1,2,\dots,n$. We define the vector, DV_ℓ , consisting of decisions arriving at CD_0 as

$$DV_\ell = (D_1, D_2, \dots, D_n)^T, \quad \ell = 1, 2, \dots, 2^n \quad (6-1)$$

Since each D_i , $i = 1, 2, \dots, n$, takes the value zero or one, DV_ℓ can take 2^n possible values. For each value of DV_ℓ arriving at CD_0 , there is a corresponding threshold multiplier $T_{0\ell}$, $\ell = 1, 2, \dots, 2^n$, at CD_0 . These threshold multipliers, $T_{0\ell}$, $\ell = 1, 2, \dots, 2^n$, are obtained by optimizing the overall system, i.e., by maximizing the overall probability of detection, while the overall probability of false-alarm is kept constant. Thus, the threshold at CD_0 adapts to two types of information, its own estimate of the level of the background noise and the incoming decision vector DV_ℓ . Let P_{D_i} , P_{F_i} , and P_{M_i} be the probability of detection, the probability of false-alarm, and the probability of a miss at each CA-CFAR detector, CD_i , $i=1,2,\dots,n$, respectively. The overall probability of detection, the overall probability of a miss, and the overall probability

of false-alarm at the output of the CA-CFAR detector, CD_o , are denoted by P_D , P_M , and P_F , respectively. Then, P_D and P_F can be written as

$$P_D = \sum_{\ell=1}^{2^n} P_D^\ell \prod_{S_0} P_{M_j} \prod_{S_1} P_{D_k} \quad (6-2)$$

and

$$P_F = \sum_{\ell=1}^{2^n} P_F^\ell \prod_{S_0} (1 - P_{F_j}) \prod_{S_1} P_{F_k} \quad (6-3)$$

where from Appendix A,

$$P_D^\ell = \Pr(D_o = 1 | DV_\ell, H_1) \quad (6-4.a)$$

$$= \left[\frac{1+S}{1+S+T_{o\ell}} \right]^N \quad (6-4.b)$$

and

$$P_F^\ell = \Pr(D_o = 1 | DV_\ell, H_0) \quad (6-5.a)$$

$$= \frac{1}{(1 + T_{o\ell})^N} \quad (6-5.b)$$

The superscript, ℓ , in P_D^ℓ and P_F^ℓ indicates the correspondence between the probabilities of detection and false-alarm and the specific threshold multiplier, $T_{o\ell}$, obtained from the optimized system.

To optimize the overall system, we form the following objective function.

$$J = P_D + \xi [P_F - \nu] \quad (6-6)$$

Substituting equations (6-2), (6-3), (6-4.b) and (6-5.b) into equation (6-6), we get

$$\begin{aligned}
 J = & \sum_{\ell=1}^{2^n} \frac{(1+S)^N}{(1+S+T_{o\ell})^N} \cdot \prod_{S^0} \left[1 - \frac{(1+S)^{N_i}}{(1+S+TM_i^0)^{N_i}} \right] \cdot \prod_{S^1} \frac{(1+S)^{N_i}}{(1+S+TM_i^1)^{N_i}} \\
 & + \xi \left\{ \sum_{\ell=1}^{2^n} \frac{1}{(1+T_{o\ell})^N} \cdot \prod_{S^0} \left[1 - \frac{1}{(1+TM_i^0)^{N_i}} \right] \cdot \prod_{S^1} \frac{1}{(1+TM_i^1)^{N_i}} \right\}^{-v}
 \end{aligned}
 \tag{6-7}$$

where TM_i 's are the threshold multipliers of CD_i 's, $i=1,2,\dots,n$. The superscript zero in TM_i^0 indicates that the decision of the corresponding CD_i is zero, and the superscript one in TM_i^1 indicates that the decision of the corresponding CD_i is a one. In order to maximize P_D while P_F is fixed, for each value of DV_ℓ , we must find the best threshold multiplier, $T_{o\ell}$, at CD_o and the best set of threshold multipliers at the CD_i 's, $i=1,2,\dots,n$. Maximizing P_D for a fixed P_F is equivalent to maximizing the objective function J . Thus, we take the derivatives of J with respect to TM_i^0 and TM_i^1 , $\ell=1,2,\dots,2^n$, $i=1,2,\dots,n$ (the number of TM_i^0 's and TM_i^1 's add to n), and set them equal to zero. The resulting equations are

$$\begin{aligned}
 \frac{\partial J}{\partial T_{o\ell}} = & \sum_{\ell=1}^{2^n} \frac{(1+S)^N}{(1+S+T_{o\ell})^{N+1}} \cdot \prod_{S^0} \left[1 - \frac{(1+S)^{N_i}}{(1+S+TM_i^0)^{N_i}} \right] \cdot \prod_{S^1} \frac{(1+S)^{N_i}}{(1+S+TM_i^1)^{N_i}} \\
 & + \xi \left\{ \frac{1}{(1+T_{o\ell})^{N+1}} \cdot \prod_{S^0} \left[1 - \frac{1}{(1+TM_i^0)^{N_i}} \right] \cdot \prod_{S^1} \frac{1}{(1+TM_i^1)^{N_i}} \right\} = 0
 \end{aligned}
 \tag{6-8}$$

$$\frac{\partial J}{\partial TM_i^0} = \sum_{\ell=1}^{2^n} \frac{(1+S)^N}{(1+S+T_{o\ell})^N} \cdot \prod_{S^0} \frac{(1+S)^{N_i}}{(1+S+TM_i^0)^{N_i+1}} \cdot \prod_{S^1} \frac{(1+S)^{N_i}}{(1+S+TM_i^1)^{N_i}}$$

$$+ \xi \left\{ \sum_{\ell=1}^{2^n} \frac{1}{(1+T_{o\ell})^N} \cdot \prod_{S^0} \frac{1}{(1+TM_i^0)^{N_i+1}} \cdot \prod_{S^1} \frac{1}{(1+TM_i^1)^{N_i}} \right\} = 0$$

(6-9)

and

$$\frac{\partial J}{\partial TM_i^1} = \sum_{\ell=1}^{2^n} \frac{(1+S)^N}{(1+S+T_{o\ell})^N} \cdot \prod_{S^0} \left[1 - \frac{(1+S)^{N_i}}{(1+S+TM_i^0)^{N_i}} \right] \cdot \prod_{S^1} \frac{(1+S)^{N_i}}{(1+S+TM_i^1)^{N_i+1}}$$

$$+ \xi \left\{ \sum_{\ell=1}^{2^n} \frac{1}{(1+T_{o\ell})^N} \cdot \prod_{S^0} \left[1 - \frac{1}{(1+TM_i^0)^{N_i}} \right] \cdot \prod_{S^1} \frac{1}{(1+TM_i^1)^{N_i+1}} \right\} = 0$$

(6-10)

For each incoming DV_ℓ , we have to solve $(n+1)$ equations to obtain the multipliers at CD_i 's, $i=1,2,\dots,n$, and the threshold multiplier at CD_0 . Since DV_ℓ can take 2^n possible values, there are $(n+1)2^n$ equations in $(n+1)2^n$ unknowns to be solved. It should be noted that in using this procedure, we have optimized the entire system and therefore, the resulting nonlinear equations are coupled. The solutions to the nonlinear equations are the optimum threshold multipliers at all CD_i 's, $i=1,2,\dots,n$, which maximizes P_D while CFAR is achieved.

6.2-2. Adaptive CFAR Detection with Tandem Network Topology

In this case, the system considered is shown in Figure 6-2. The CA-CFAR detector, CD_1 , makes a decision, D_1 , and transmits it to the CA-CFAR detector CD_2 . Based on the decision D_1 and on its own estimate of the background noise, CA-CFAR detector CD_2 makes another decision, D_2 . The decision D_2 is transmitted to the next CA-CFAR detector CD_3 , and the process continues. At the last CA-CFAR detector, CD_0 , the final decision, D_0 , is made.

Let the threshold multipliers of detectors $CD_0, CD_1, CD_2, \dots, CD_n$, be denoted by T, T_1, T_2, \dots, T_n , respectively. We define P_{D_i}, P_{F_i} , and P_{M_i} , $i=1,2,\dots,n$, to be the probability of detection, the probability of false-alarm, and the probability of a miss at the individual CA-CFAR detectors CD_i , $i=1,2,\dots,n$. At CD_i , $i=2,3,\dots,n$, the threshold multiplier is represented by $T_i^0(T_i^1)$ if the decision received from CD_{i-1} is zero (one). Let N, N_1, N_2, \dots, N_n be the number of range cells used by CA-CFAR detectors $CD_0, CD_1, CD_2, \dots, CD_n$, respectively. As before, we assume that the target to be detected is of Swerling type I and has an SNR S for all of the detectors. Then, the probability of detection and the probability of false-alarm of CA-CFAR detector CD_1 are

$$P_{D_1} = \frac{(1+S)^{N_1}}{(1+S+T_1)^{N_1}} \quad (6-11)$$

$$P_{F_1} = \frac{1}{(1+T_1)^{N_1}} \quad (6-12)$$

The probability of detection and the probability of false-alarm at CA-CFAR detector CD_2 are

$$P_{D_2} = \Pr(D_2=1|D_1=1, H_1) \Pr(D_1=1|H_1) + \Pr(D_2=1|D_1=0, H_1) \Pr(D_1=0|H_1) \quad (6-13.a)$$

$$= \Pr(D_2=1|D_1=1, H_1)P_{D_1} + \Pr(D_2=1|D_1=0, H_1)(1-P_{D_1}) \quad (6-13.b)$$

$$P_{F_2} = \Pr(D_2=1|D_1=1, H_0) \Pr(D_1=1|H_0) + \Pr(D_2=1|D_1=0, H_0) \Pr(D_1=0|H_0) \quad (6-14.a)$$

$$= \Pr(D_2=1|D_1=1, H_0)P_{F_1} + \Pr(D_2=1|D_1=0, H_0)(1-P_{F_1}) \quad (6-14.b)$$

The resulting expressions for P_{D_2} and P_{F_2} are

$$P_{D_2} = \frac{(1+S)^{N_1+N_2}}{(1+S+T_2)^{N_2} (1+S+T_1)^{N_1}} + \frac{(1+S)^{N_2}}{(1+S+T_2^0)^{N_2}} \left[1 - \frac{(1+S)^{N_1}}{(1+S+T_1)^{N_1}} \right] \quad (6-15)$$

$$P_{F_2} = \frac{1}{(1+T_2^1)^{N_2} (1+T_1)^{N_1}} + \frac{1}{(1+T_2^0)^{N_2}} \left[1 - \frac{1}{(1+T_1)^{N_1}} \right] \quad (6-16)$$

For CA-CFAR detector CD_3 , we have

$$P_{D_3} = \Pr(D_3=1|D_2=1, H_1) \Pr(D_2=1|H_1) + \Pr(D_3=1|D_2=0, H_1) \Pr(D_2=0|H_1) \quad (6-17.a)$$

$$= \frac{(1+S)^{N_3}}{(1+S+T_3^1)^{N_3}} P_{D_2}^1 + \frac{(1+S)^{N_3}}{(1+S+T_3^0)^{N_3}} (1-P_{D_2}^0) \quad (6-17.b)$$

$$P_{F_3} = \Pr(D_3=1 | D_2=1, H_0) \Pr(D_2=1 | H_0) + \Pr(D_3=1 | D_2=0, H_0) \Pr(D_2=0 | H_0) \quad (6-18.a)$$

$$= \frac{1}{(1+T_3^1)^{N_3}} P_{F_2}^1 + \frac{1}{(1+T_3^0)^{N_3}} (1-P_{F_2}^0) \quad (6-18.b)$$

where, $P_{D_2}^1 = \Pr(D_2 = 1 | D_1, H_1)$, $P_{D_2}^0 = \Pr(D_2=0 | D_1, H_1)$, $P_{F_2}^1 = \Pr(D_2 = 1 | D_1, H_0)$ and $P_{F_2}^0 = \Pr(D_2 = 0 | D_1, H_0)$. $P_{D_2}^1$ and $P_{F_2}^1$ are equal to equations (6-15) and (6-16) respectively, while $P_{D_2}^0$ and $P_{F_2}^0$ can be expressed as

$$P_{D_2}^0 = \left[1 - \frac{(1+S)^{N_2}}{(1+S+T_2^1)^{N_2}}\right] P_{D_1} + \left[1 - \frac{(1+S)^{N_2}}{(1+S+T_2^0)^{N_2}}\right] (1-P_{D_1}) \quad (6-19)$$

$$P_{F_2}^0 = \left[1 - \frac{1}{(1+T_2^1)^{N_2}}\right] P_{F_1} + \left[1 - \frac{1}{(1+T_2^0)^{N_2}}\right] (1-P_{F_1}) \quad (6-20)$$

The superscript one (zero) in $P_{D_2}^1$ ($P_{D_2}^0$) and $P_{F_2}^1$ ($P_{F_2}^0$) indicates that the decision made by detector two is one (zero). Recall that the superscript one (zero) in T_2^1 (T_2^0) indicates that the received decision from D_1 is one (zero). Continuing in this manner, we can write the expressions of the probability of detection and the probability of false-alarm at the i th detector as,

$$P_{D_i} = \Pr(D_i=1 | D_{i-1}=1, H_1) \Pr(D_{i-1}=1 | H_1) + \Pr(D_i=1 | D_{i-1}=0, H_1) \Pr(D_{i-1}=0 | H_1) \quad (6-21.a)$$

$$= \frac{(1+S)^{N_i}}{(1+S+T_i^1)^{N_i}} P_{D_{i-1}}^1 + \frac{(1+S)^{N_i}}{(1+S+T_i^0)^{N_i}} (1-P_{D_{i-1}}^0) \quad (6-21.b)$$

$$P_{F_i} = \Pr(D_i=1|D_{i-1}=1, H_0) \Pr(D_{i-1}=1|H_0) + \Pr(D_i=1|D_{i-1}=0, H_0) \Pr(D_{i-1}=0|H_0) \quad (6-22.a)$$

$$= \frac{1}{(1+T_i^1)^{N_i}} P_{F_{i-1}}^1 + \frac{1}{(1+T_i^0)^{N_i}} (1-P_{F_{i-1}}^0) \quad (6-22.b)$$

where

$$P_{D_{i-1}}^j = \frac{(1+S)^{N_{i-1}}}{(1+S+T_{i-1}^j)^{N_{i-1}}}, \quad j=0,1. \quad (6-22.c)$$

$$P_{F_{i-1}}^j = \frac{1}{(1+T_{i-1}^j)^{N_{i-1}}}, \quad j=0,1 \quad (6-22.d)$$

The superscript j in $P_{D_{i-1}}^j$ and $P_{F_{i-1}}^j$ indicates whether the previous decision is zero or one. The general expressions for the overall probability of detection, P_D , and the overall probability of false-alarm, P_F , at the CA-CFAR detector CD_0 can then be written as

$$P_D = \frac{(1+S)^N}{(1+S+T^1)^N} P_{D_n}^1 + \frac{(1+S)^N}{(1+S+T^0)^N} (1-P_{D_n}^0) \quad (6-23)$$

$$P_F = \frac{1}{(1+T^1)^N} P_{F_n}^1 + \frac{1}{(1+T^0)^N} (1-P_{F_n}^0) \quad (6-24)$$

where, $P_{F_n}^j$ and $P_{D_n}^j$, $j=0,1$, are defined recursively in equation (6-22.c) and (6-22.d) and T^1 (T^0) is the threshold at detector CD_0 if the received decision D_n is one (zero).

We wish to maximize the probability of detection, P_D , at the output of CA-CFAR detector CD_0 , while the probability of false-alarm, P_F , is fixed at the desired value ν . Since the CA-CFAR detectors $CD_0, CD_1, CD_2, \dots, CD_n$ are coupled, the entire system is optimized. To achieve this, we form the objective function

$$J = P_D + \xi [P_F - \nu] \quad (6-25)$$

We take the derivatives of J with respect to T^j and T_k^j , $j=0,1$, and $k=1,2,\dots,n$, and set them equal to zero. This results in a system of $2(n+1)$ nonlinear equations in $2(n+1)$ unknowns to be solved. In the next section, we present an example to illustrate the effectiveness of the system under consideration.

6.3. Example

The system under consideration is shown in Figure 6-3. In order to avoid any ambiguity with the notation defined in the subsections 6.2-1 and 6.2-2, we define a more explicit notation that is used in this example.

D_0, D_1 = detection decisions at detectors CD_0 and CD_1 , respectively.

T_1 = threshold multiplier at CA-CFAR detector CD_1

T^0 = threshold multiplier at CA-CFAR detector CD_0
if the decision D_1 is zero.

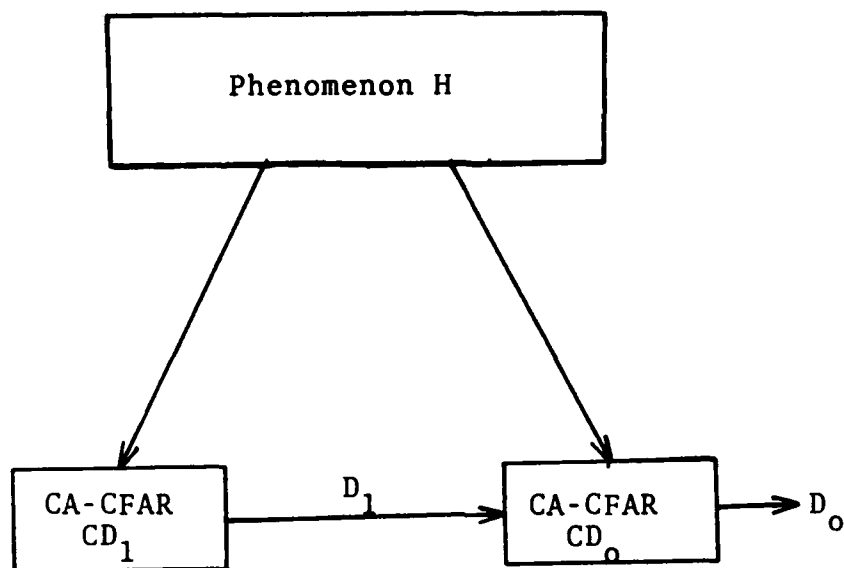


Fig. 6-3. A Two Sensor Network Topology for Adaptive CFAR Detection.

T^1 = threshold multiplier at CA-CFAR detector
 CD_0 if the decision D_1 is one.

P_D, P_{D_1} = probabilities of detection at CA-CFAR
detectors CD_0 and CD_1 , respectively.

P_F, P_{F_1} = probabilities of false-alarm at CA-CFAR
detectors CD_0 and CD_1 , respectively.

S = target SNR at CA-CFAR detectors CD_0
and CD_1

N, N_1 = number of reference cells at CA-CFAR
detectors CD_0 and CD_1 , respectively.

P_D and P_F can then be expressed as

$$P_D = \Pr(D_0=1|D_1=1, H_1) \Pr(D_1=1|H_1) + \\ \Pr(D_0=1|D_1=0, H_1) \Pr(D_1=0|H_1) \quad (6-26)$$

$$P_F = \Pr(D_0=1|D_1=1, H_0) \Pr(D_1=1|H_0) + \\ \Pr(D_0=1|D_1=0, H_0) \Pr(D_1=0|H_0) \quad (6-27)$$

Substituting the expressions of $\Pr(D_0=1|D_1=1, H_1)$,
 $\Pr(D_0=1|D_1=1, H_0)$, $\Pr(D_0=1|D_1=0, H_1)$, $\Pr(D_0=1|D_1=0, H_0)$,
 P_{D_1} , P_{F_1} , P_{F_2} and P_{D_2} into equations (6-26) and (6-27),
 P_D and P_F become

$$P_D = \frac{(1+S)^{N+N_1}}{(1+S+T^1)^N (1+S+T_1)^{N_1}} + \frac{(1+S)^N}{(1+S+T^0)^N} \left[1 - \frac{(1+S)^{N_1}}{(1+S+T_1)^{N_1}} \right] \quad (6-28)$$

$$P_F = \frac{1}{(1+T^1)^N (1+T_1)^{N_1}} + \frac{1}{(1+T^0)^N} \left[1 - \frac{1}{(1+T_1)^{N_1}} \right] \quad (6-29)$$

Substituting equations (6-28) and (6-29), and $P_F = v$ into equation (6-25), the objective function is

$$J(T^0, T^1, T_1) = \frac{(1+S)^{N+N_1}}{(1+S+T^1)^N (1+S+T_1)^{N_1}} + \frac{(1+S)^N}{(1+S+T^0)^N} \left[1 - \frac{(1+S)^{N_1}}{(1+S+T_1)^{N_1}} \right] \\ + \xi \left\{ \frac{1}{(1+T^1)^N (1+T_1)^{N_1}} + \frac{1}{(1+T^0)^N} \left[1 - \frac{1}{(1+T_1)^{N_1}} \right] - v \right\} \quad (6-30)$$

Maximizing P_D is equivalent to maximizing J . That is, we take the derivatives of $J(T^0, T^1, T_1)$ with respect to T^0 , T^1 , and T_1 , respectively, and set them equal to zero to obtain

$$\frac{\partial J}{\partial T^0} = \frac{(1+S)^N}{(1+S+T^0)^{N+1}} \left[1 - \frac{(1+S)^{N_1}}{(1+S+T_1)^{N_1}} \right] + \xi \frac{1}{(1+T^0)^{N+1}} \left[1 - \frac{1}{(1+T_1)^{N_1}} \right] = 0 \quad (6-31)$$

$$\frac{\partial J}{\partial T^1} = \frac{(1+S)^{N+N_1}}{(1+S+T^1)^{N+1} (1+S+T_1)^{N_1}} + \xi \frac{1}{(1+T^1)^{N+1} (1+T_1)^{N_1}} = 0 \quad (6-32)$$

and

$$\frac{\partial J}{\partial T_1} = \frac{-(1+S)^{N+N_1}}{(1+S+T^1)^N (1+S+T_1)^{N_1+1}} + \frac{(1+S)^{N+N_1}}{(1+S+T^0)^N (1+S+T_1)^{N_1+1}} + \\ \xi \left\{ \frac{-1}{(1+T^1)^N (1+T_1)^{N_1+1}} + \frac{1}{(1+T^0)^N (1+T_1)^{N_1+1}} \right\} = 0 \quad (6-33)$$

The equations (6-31), (6-32), (6-33) and $P_F = \nu$ form a set of four nonlinear equations in four unknowns to be solved. We first obtain the Lagrange multiplier, ξ , from equation (6-32), i.e.,

$$\xi = - \frac{(1+S)^{N+N_1} (1+T_1)^{N_1} (1+T^1)^{N+1}}{(1+S+T^1)^{N+1} (1+S+T_1)^{N_1}} \quad (6-34)$$

Substituting equation (6-34) into equations (6-31), (6-33) and $P_F = \nu$, and solving for T^0 in terms of T^1 and T_1 , we get the following system of three equations in three unknowns (T^0 , T^1 , T_1) to be solved.

$$T^0 = -1 + \left\{ \frac{(1+T^1)^N [(1+T_1)^{N_1} - 1]}{\nu(1+T_1)^{N_1} (1+T^1)^N - 1} \right\}^{\frac{1}{N}} \quad (6-35)$$

$$\begin{aligned} & [(1+S+T_1)^{N_1} - (1+S)^{N_1}] (1+S+T^1)^{N+1} (1+T^0)^{N+1} \\ & - [(1+T_1)^{N_1} - 1] (1+S+T^0)^{N+1} (1+S)^N (1+T^1)^{N+1} = 0 \end{aligned} \quad (6-36)$$

and

$$\begin{aligned} & [(1+S+T^1)^N - (1+S+T^0)^N] (1+S+T^1) (1+T_1) (1+T^0)^N - \\ & - [(1+T^1)^N - (1+T^0)^N] (1+S+T_1) (1+T^1) (1+S+T^1)^N = 0 \end{aligned} \quad (6-37)$$

For $N=6$, $N_1=4$, and $P_F=10^{-5}$, we obtain the results shown in Table 6-1. Note that the probability of detection, P_D^{DS} , of the two sensor system is much better than the probability

of detection, P_D^{SS} , of the single sensor system, for the same probability of false-alarm and the same target SNR.

| SNR S (DB) | T_1 | T^0 | T^1 | P_D^{DS} | P_D^{SS} |
|---------------|--------|-------|-------|------------|------------|
| 5 | 10.569 | 6.103 | 0.713 | .00687 | .00156 |
| 10 | 2.554 | 7.683 | 2.057 | .179 | .025 |
| 15 | 3.711 | 7.029 | 1.620 | .594 | .190 |

Table 6-1. Performance of Adaptive CFAR Detection with Two-Sensor System and a Single Sensor System.

$$P_F = 10^{-5}, N=6, N_1=4.$$

6.4. A Comparison

In this section, we present an example where we compare the performance of the three systems that we have developed and analyzed in Chapters four, five and six. We use two CA-CFAR detectors with a number of range cells equal to N_1 and N_2 for detectors one and two, respectively. The systems under consideration are shown in Figure 6-4. In Figure 6-4(a), we have two CA-CFAR detectors with a data fusion center. We assume that the fusion rule at the data fusion center is the "AND" rule. In Figure 6-4(b), we have a two-sensor system composed of a background estimator and a CA-CFAR detector as proposed in Chapter five, while in Figure 6-4(c), we have two

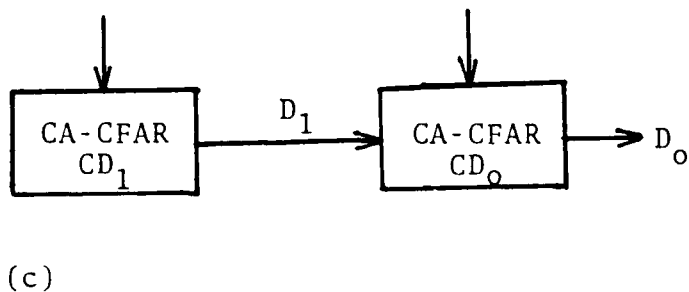
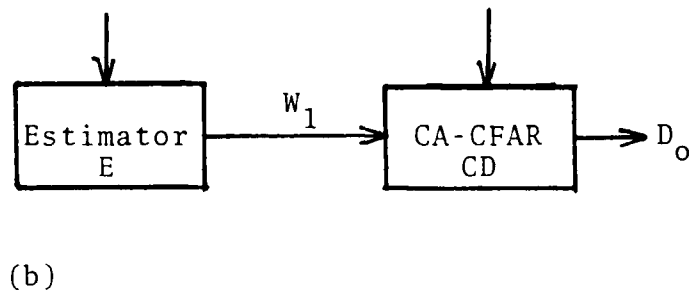
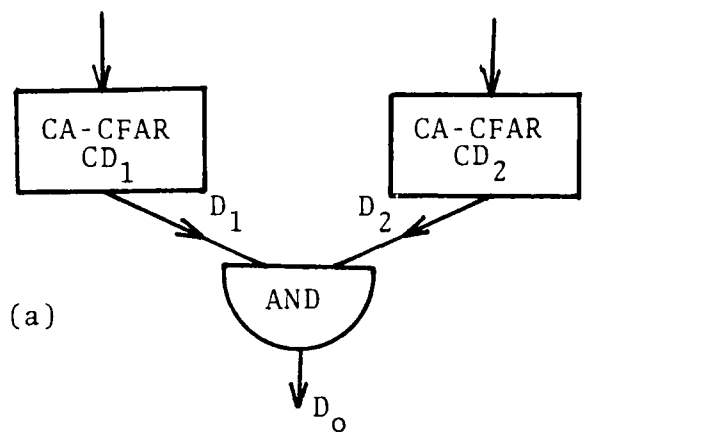


Fig. 6-4. Different Network Topologies for Two-Sensor CFAR Detection Systems.

CA-CFAR detectors whose operation is as described in this chapter. For the same cross sectional target SNR S , for an overall probability of false-alarm $P_F = 10^{-5}$, for $N_1=6$ and $N_2=4$, we compare the performance of the three networks in Table 6-2.

| S | P_D^a | P_D^b | P_D^c |
|-----|---------|---------|---------|
| 5 | 0.0152 | 0.0152 | 0.0687 |
| 10 | 0.166 | 0.166 | 0.179 |
| 15 | 0.526 | 0.526 | 0.594 |

Table 6-2. CA-CFAR Performance of the Two-Sensor Systems of Figure 6.4.

The superscripts a , b and c on the probabilities of detection of the entries in Table 6-2, represent the systems a , b , and c as shown in Figure 6-4, respectively. It should be noted that if we had used the "OR" fusion rule instead of the "AND" fusion rule in the system shown in Figure 6-4(a), the performance in terms of P_D would have been worse for the values of S considered here.

6.5. Summary and Conclusions

In this chapter, we have derived expressions for the probability of detection using n CA-CFAR detectors in parallel

and in tandem. In the parallel topology, n decisions from n CA-CFAR detectors arrived at the $(n+1)$ th CA-CFAR where the final decision was obtained. The entire system was optimized and the best threshold multipliers at the CA-CFAR detectors were obtained so that the overall probability of detection was maximum while the overall probability of false-alarm was maintained at the desired value. In the tandem topology, the detection decisions were transmitted from one CA-CFAR detector to the next in series and the entire system was optimized. The improvement in the performance was shown by an example. This procedure, in which the threshold is adaptive to two types of compressed data, the received decision and its own estimate of the level of the background noise, turned out to be very effective.

CHAPTER VII
SUMMARY AND SUGGESTIONS FOR FUTURE
RESEARCH WORK

7.1. Summary

New adaptive threshold techniques for CFAR processing were proposed and analyzed. In the first half of the report, we studied CFAR processors for multiple target situations. We proposed a weighted cell-averaging CFAR detector for multiple target situations. We obtained the optimum weights for the leading and the lagging reference windows so that the probability of detection was maximum while the probability of false-alarm was kept at the desired value. The performance of the WCA-CFAR detector was shown to be superior to that of the CA-CFAR, GO-CFAR and SO-CFAR detectors. The WCA-CFAR detector was shown to be especially effective when the interference is large.

The second CFAR detector proposed for a multiple target environment was a cell-censored CFAR detector. A predetermined fixed threshold at the level of each range cell was used to determine the presence or absence of interference in each range cell. The cells, for which interference was decided, were censored while others (cells without interference) were used in the estimation of the

background noise. The sum of the leading cells without interference, and the sum of the lagging cells without interference were added to yield the adaptive threshold, which in turn was scaled to achieve CFAR. The performance was studied and it was shown that the cell-censored CFAR detector was effective in a multiple target environment.

In the second part of the report, we developed the theory of distributed adaptive CFAR detection. CFAR detection with distributed detectors and data fusion was studied. Given a "k out of n" fusion rule at the data fusion center, the optimum threshold multipliers at the CFAR detectors were obtained so that the overall probability of detection at the output of the data fusion center was maximum, while the overall probability of false-alarm was fixed. Then, the entire system was optimized, i.e., the optimum threshold multipliers at the individual detectors were obtained as well as the optimum fusion rule at the data fusion center. In the optimization of the entire system, the overall probability of false-alarm was maintained at the desired value while the overall probability of detection was maximized at the data fusion center.

Due to the fact that more knowledge about the background noise improves the detection, adaptive CFAR detection with multiple background estimators was studied. Estimates of the background noise were transmitted from the estimators to the CFAR detector. The CFAR detector computed its own

estimate of the background noise and combined it with the received estimates to yield the adaptive threshold. The adaptive threshold was then scaled and was compared with the statistic of the output of the cell under test to make a decision. As expected, the performance improved. An extension using a hybrid system consisting of background estimators and a data fusion center was also considered. The performance of the hybrid system was also studied by means of an example.

Finally, adaptive CFAR detection for two different network topologies was considered. The two topologies considered were the parallel and the tandem topologies. In these cases, the compressed data that were transmitted from one CFAR detector to the next were decisions instead of estimates. The final decision at the last CFAR detector was based on two types of compressed data; namely, its own estimate of the background noise and the received decisions. In both cases, the entire system was optimized so that the probability of detection was maximum, while the probability of false-alarm was maintained at the desired values. In maximizing the probability of detection, optimum threshold multipliers were derived. Again, as expected the performance improved. In the next section, we provide some suggestions for future research work.

7.2. Suggestions for Future Research Work

As indicated earlier, no work has been reported in the literature on CFAR detection using distributed sensors. In this report, we make the first contribution in this area by developing the theory of distributed adaptive CFAR detection. We did not consider multiple target situations in our work. One obvious direction for future research is to extend the theory developed here for multiple target situations. Also, different network topologies, structures and implementations can be considered and analyzed for distributed adaptive CFAR detection.

Also, as shown in Chapters four and six, solving the nonlinear equations, to obtain the optimum threshold multipliers at the individual CFAR detectors and/or the optimum fusion rule at the data fusion center, required extensive computer iterative steps. These values may be computed and compiled in tables so that a table look-up procedure may be implemented. Development of more efficient numerical techniques for solving the above nonlinear equations is desirable.

APPENDIX A

A-1. Swerling Cross Section Models [12,36]

Case 1. In this case, the returned signal power per pulse on any one scan is assumed to be constant, but these echo pulses are independent (uncorrelated) from scan to scan. This assumption ignores factors such as the effect of the antenna beam shape on the amplitude of the returned signal. A returned signal of this type is referred to as scan-to-scan fluctuation. The probability density function for the cross section (input signal-to-noise power ratio, σ , is assumed to be

$$P(\sigma, \sigma_{av}) = \frac{1}{\sigma_{av}} \exp\left(-\frac{\sigma}{\sigma_{av}}\right), \quad \sigma \geq 0 \quad (A-1)$$

where σ_{av} is the average cross section (average of σ) over all target fluctuations.

Case 2. In this case, the fluctuations are more rapid than in case 1 and are assumed to be independent from pulse to pulse instead of from scan to scan. This type of fluctuation is referred to as pulse-to-pulse fluctuation. The probability density function for the target cross section is the same as given in equation (A-1).

Case 3. In this case, the fluctuation is as in Case 1, i.e. scan-to-scan fluctuation, but the probability density function is given by

$$P(\sigma, \sigma_{av}) = \frac{4\sigma}{\sigma_{av}^2} e^{-2\sigma/\sigma_{av}}, \quad \sigma \geq 0 \quad (A-2)$$

Case 4. In this case, the fluctuation is pulse-to-pulse as in case 2, but the probability density function is given by equation (A-2).

Only Case 1 is considered in this dissertation.

A-2. Reference Window Statistic [37]

When the background noise is white Gaussian of unknown level, the probability density function of the output at each range cell is

$$P_{Q_i}(q_i) = \frac{1}{2\sigma^2} e^{-q_i/2\sigma^2}, \quad q_i \geq 0 \quad (A-3)$$

where σ^2 is the average noise power. In cell-averaging, the outputs of these range cells are assumed to be statistically independent. A reference window U of N range cells is the sum of all these cells, i.e.,

$$U = \sum_{i=1}^N q_i \quad (A-4)$$

where $P_{Q_i}(q_i)$, $i=1,2,\dots,N$, is as defined in equation (A-3).

To find $P_U(u)$ we use the following theorem from [37].

Theorem. If q_1, q_2, \dots, q_N are mutually independent random variables with the exponential distribution function as in equation (A-3), then the sum $U = q_1 + q_2 + \dots + q_N$ has a probability density function $P_U(u)$ and a distribution function $F_U(u)$ given by

$$P_U(u) = \frac{1}{2\sigma^2} \cdot \frac{1}{\Gamma(N)} \left(\frac{u}{2\sigma^2}\right)^{N-1} e^{-u/2\sigma^2}, \quad u \geq 0 \quad (\text{A-5})$$

$$F_U(u) = 1 - e^{-u/2\sigma^2} \left[1 + \frac{u}{2\sigma^2 \cdot 1!} + \left(\frac{u}{2\sigma^2}\right)^2 \cdot \frac{1}{2!} + \dots + \left(\frac{u}{2\sigma^2}\right)^{N-1} \frac{1}{(N-1)!} \right] \quad u > 0 \quad (\text{A-6})$$

Proof. We prove this theorem by induction. For $N=1$, the theorem holds because equation (A-5) simply reduces to equation (A-4). Now, assuming that the theorem is true for N , we will show that it is also true for $N+1$. The density $P_U(u)$ for U defined in equation (A-4) is given by the following convolution

$$P_{N+1}(t) = \int_0^t P_N(t-q) P_1(u) du \quad (\text{A-7})$$

which reduces to

$$\begin{aligned} P_{N+1}(t) &= \frac{(1/2\sigma^2)^{N+1}}{(N-1)!} e^{-t/2\sigma^2} \int_0^t u^{N-1} du \\ &= \frac{1}{2\sigma^2} \frac{(t/2\sigma^2)^N}{N!} e^{-t/2\sigma^2} \end{aligned} \quad (\text{A-8})$$

equation (A-8) is of the form of equation (A-5) which means that equation (A-5) holds by induction for all N . Taking

the derivative of equation (A-6), we obtain equation (A-5) which justifies that equation (A-6) holds.

A-3. Detection Probability Without Interference in the Range Cells

In the conventional CA-CFAR with N reference cells and reference windows U, V , the normalized probability density functions of U and V are

$$P_U(u) = \frac{1}{\Gamma(\frac{N}{2})} u^{\frac{N}{2}-1} e^{-u}, \quad u \geq 0 \quad (\text{A-9})$$

$$P_V(v) = \frac{1}{\Gamma(\frac{N}{2})} v^{\frac{N}{2}-1} e^{-v}, \quad v \geq 0 \quad (\text{A-10})$$

The threshold Q is the sum of U and V , and therefore, the probability density function of Q is given by the convolution

$$\begin{aligned} P_Q(q) &= \int_{-\infty}^{\infty} P_U(u) P_V(q-u) du \\ &= \frac{e^{-q}}{[\Gamma(\frac{N}{2})]^2} \int_0^q u^{\frac{N}{2}-1} (q-u)^{\frac{N}{2}-1} du \\ &= \frac{1}{[\Gamma(\frac{N}{2})]^2} e^{-q} q^{N-1} B(\frac{N}{2}, \frac{N}{2}) \\ &= \frac{1}{\Gamma(N)} e^{-q} q^{N-1} \end{aligned} \quad (\text{A-11})$$

The probability of detection for a target SNR S of Swerling Case 1 is

$$P_D = \int_0^{\infty} e^{-\frac{Tq}{1+S}} P_Q(q) dq \quad (\text{A-12})$$

From [38], we obtain

$$P_D = \left[\frac{1+S}{1+S+T} \right]^N \quad (\text{A-13})$$

A-4. A Reference Window Statistic With One Interfering Target [14]

If the reference window is U with one interfering target, having an SNR I , of Swerling type I and N range cells, U can be written as

$$U = \sum_{i=1}^{N-1} q_i + q_N \quad (\text{A-14})$$

where,

$$P_{Q_i}(q_i) = e^{-q_i}, \quad q_i \geq 0, \quad i=1,2,\dots,N-1 \quad (\text{A-14.a})$$

and

$$P_{Q_N}(q_N) = \frac{1}{1+I} e^{-\frac{q_N}{1+I}}, \quad q_N \geq 0 \quad (\text{A-14.b})$$

Note that we have assumed that the interference is in the N th cell, but it could be in anyone of the N range cells.

Let,

$$X = \sum_{i=1}^{N-1} q_i \quad (\text{A-15})$$

and

$$Y = q_N \quad (\text{A-16})$$

then, from equation (A-2)

$$P_X(x) = \frac{1}{(N-2)!} x^{N-2} e^{-x}, \quad x \geq 0 \quad (\text{A-17})$$

Since U is the sum of X and Y, the probability density function of U is

$$P_U(u) = \int_0^u P_X(x) P_Y(u-x) dx \quad (\text{A-18})$$

Substituting equations (A-14.b), (A-16) and (A-17) into equation (A-18), we obtain

$$\begin{aligned} P_U(u) &= \frac{1}{\Gamma(N-1)} \cdot \frac{1}{1+I} \int_0^u x^{N-2} e^{-x} e^{-(u-x)/1+I} dx \\ &= \frac{1}{\Gamma(N-1)} \cdot \frac{1}{1+I} e^{-u/1+I} \int_0^u x^{N-2} e^{-x \left(\frac{1}{1+I}\right)} dx \end{aligned} \quad (\text{A-19})$$

From [38], we have

$$\int_0^u x^n e^{-\mu x} dx = \frac{n!}{\mu^{n+1}} - e^{-\mu u} \sum_{k=0}^n \frac{n!}{k!} \frac{u^k}{\mu^{n-k+1}}$$

$$[u > 0, \quad \text{Re } \mu > 0] \quad (\text{A-20})$$

Thus, using equation (A-20) in equation (A-19) and re-arranging terms, the probability density function of U is

$$P_U(u) = \frac{1}{I} \left[\frac{1+I}{I}\right]^{N-2} e^{-\frac{u}{1+I}} - e^{-u} \sum_{j=0}^{N-2} \frac{1}{j!} \left[\frac{I}{1+I}\right]^j u^j, \quad u \geq 0 \quad (A-21)$$

A-5. Some Values of α and β

The values of α and β are obtained by solving the nonlinear equations (2-43), (2-44) and (2-46). The values of α and β for the cases considered are given below.

| $P_F = 10^{-4}$, $I = S \times 10, N=4$ | | |
|--|----------|---------|
| S | α | β |
| 5 | 1.4318 | 8.4275 |
| 10 | .2711 | 15.738 |
| 15 | .0680 | 19.412 |
| 20 | .0207 | 20.233 |
| 25 | .0065 | 20.451 |
| 30 | .0021 | 20.515 |

| $P_F = 10^{-4}$, $I = S \div 10, N=4$ | | |
|--|----------|---------|
| S | α | β |
| 10 | 6.4312 | 9.2558 |
| 15 | 4.0062 | 9.9211 |
| 20 | 1.8451 | 12.081 |
| 25 | .6714 | 15.332 |
| 30 | .2136 | 18.191 |
| 35 | .06612 | 19.692 |

| $P_F = 10^{-4}$, $I = S, N=4$ | | |
|--------------------------------|----------|---------|
| S | α | β |
| 5 | 4.5081 | 8.8527 |
| 10 | 2.2875 | 9.9921 |
| 15 | .7479 | 14.176 |
| 20 | .2179 | 17.975 |
| 25 | .0663 | 19.666 |
| 30 | .02068 | 20.26 |
| 35 | .0065 | 20.454 |

REFERENCES

- [1] H.M. Finn and R.S. Johnson, "Adaptive Detection Mode with Threshold Control as a Function of Spatially Sampled Clutter-Level Estimates," RCA Review, September 1968, Vol. 29, pp. 414-464.
- [2] H.M. Finn, "Adaptive Detection in Clutter," Proceeding National Electronics Conference, 1966, Vol. 22, pp. 562-567.
- [3] H.M. Finn, "Adaptive Detection with Regulated Error Probabilities," RCA Review, December 1967, Vol. 29, pp. 653-678.
- [4] R. Nitzberg, "Analysis of the Arithmetic Mean CFAR Normalizer for Fluctuating Targets," IEEE Transactions on Aerospace and Electronic Systems, January 1978, AES-14, pp. 44-47.
- [5] V.G. Hansen, "Constant False-Alarm Rate Processing in Search Radars," Proceeding of IEE International Radar Conference, London, 1973, pp. 325-332.
- [6] V.G. Hansen and J.H. Sawyers, "Detectability Loss due to Greatest of Selection in a Cell-Averaging CFAR," IEEE Transactions on Aerospace and Electronic Systems, January 1980, AES-16, pp. 115-118.
- [7] J.D. Moore and N.B. Lawrence, "Comparison of Two CFAR Methods Used with Square Law Detection of Swerling I Targets," IEEE International Radar Conference, 1980, pp. 403-409.
- [8] R. M. O'Donnell, C. E. Muehe, and M. Labbit, "Advanced Signal Processing for Airport Surveillance Radars," EASCON, October 1974, Washington, DC.
- [9] R. Nitzberg, "Clutter Map CFAR Analysis," IEEE Transactions on Aerospace and Electronic Systems, July 1986, AES-22, pp. 419-421.
- [10] G. V. Trunk, "Range Resolution of Targets Using Automatic Detectors," IEEE Transactions on Aerospace and Electronic Systems, September 1978, AES-14, pp. 750-755.
- [11] J.T. Rickard and G.M. Dillard, "Adaptive Detection Algorithms for Multiple Target Situations," IEEE Transactions on Aerospace and Electronic Systems, July 1977, AES-13, pp. 338-343.

- [12] P.J. McLane, P.H. Wittke and C.K-S Ip, "Threshold Control for Automatic Detection in Radar Systems," IEEE Transactions on Aerospace and Electronic Systems, March 1982, AES-18, pp. 242-248.
- [13] E.K. Al-Hussaini and B.M. Ibrahim, "Comparison of Adaptive Cell-Averaging Detectors for Multiple Target Situations," IEE Proceedings, June 1986, Vol. 133. Pt. F, No. 3, pp. 217-223.
- [14] M. Weiss, "Analysis of Some Modified Cell-Averaging CFAR Processing in Multiple Target Situations," IEEE Transactions on Aerospace and Electronic Systems, January 1980, AES-18, pp. 102-114.
- [15] H. Rohling, "Radar CFAR Thresholding in Clutter and Multiple Target Situations," IEEE Transactions on Aerospace and Electronic Systems, July 1983, AES-19, pp. 608-621.
- [16] J.A. Ritcey, "Performance Analysis of the Censored Mean-Level Detector," IEEE Transactions on Aerospace and Electronic Systems, July 1986, AES-22, pp. 443-453.
- [17] P. Swerling, "Probability of Detection for Fluctuating Targets," IRE Transactions on Information Theory, April 1960, IT-6, pp. 269-289.
- [18] R.R. Tenney and N.R. Sandell, "Detection with Distributed Sensors," IEEE Transactions on Aerospace and Electronic Systems, July 1981, AES-22, pp. 501-509.
- [19] F. Sadjadi, "Hypothesis Testing in a Distributed Environment," IEEE Transactions on Aerospace and Electronic Systems, March 1986, AES-22, pp. 134-137.
- [20] L.K. Ekchian and R.R. Tenney, "Detection Networks," Proceedings of the 21st IEEE Conference on Decision and Control, Florida, December 1982, pp. 686-691.
- [21] D. Teneketzis, "The Decentralized Wald Problem," presented at the IEEE International Large-Scale Systems Symposium, Virginia Beach, Virginia, October 1982.
- [22] D. Teneketzis, "The Decentralized Quickest Detection Problem," presented at the IEEE International Large-Scale Systems Symposium, Virginia Beach, Virginia, October 1982.
- [23] R. Srinivasan, "Distributed Radar Detection Theory," IEE Proceedings, February 1986, vol. 133, Pt.F, pp. 55-60.

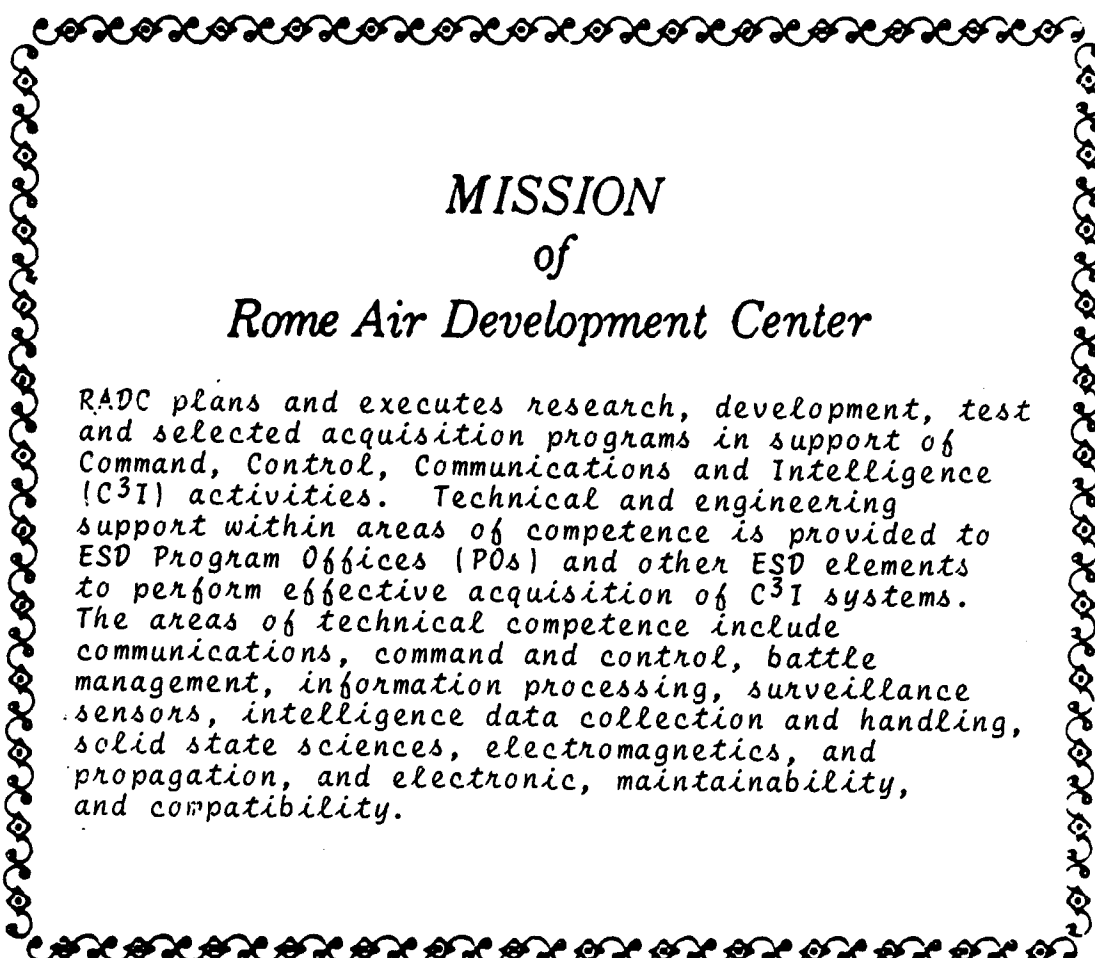
- [24] H.J. Kushner and A. Pacut, "A Simulation Study of a Decentralized Detection Problem," IEEE Transactions on Automatic Control, October 1982, Vol. 27, No. 5, pp. 1116-1119.
- [25] J.J. Chao and C.C. Lee, "A Distributed Detection Scheme Based on Soft Local Decisions," Presented at the 24th Annual Allerton Conference on Communication, Control, and Computing, Monticello, Illinois, October 1-3, 1986.
- [26] E. Conte, E. D'Addio, A. Farina and M. Longo, "Multi-static Radar Detection: Synthesis and Comparison of Optimum and Suboptimum Receivers," IEE Proceedings, October 1983, Vol. 130, Pt.F, No. 6.
- [27] Z. Chair and P.K. Varshney, "Optimum Data Fusion in Multiple Sensor Detection Systems," IEEE Transactions on Aerospace and Electronic Systems, January 1986, Vol. 1, AES-222, pp. 98-101.
- [28] I.Y. Hoballah and P.K. Varshney, "Neyman-Pearson Detection Using Multiple Radars," Proceedings of the 25th IEEE Control and Decision Conference, Athens, Greece, December 1986.
- [29] I.Y. Hoballah and P.K. Varshney, "An Information Theoretic Formulation of the Distributed Detection Problem," Presented at the 1986 IEEE International Symposium on Information Theory, October 1986.
- [30] Z. Chair and P.K. Varshney, "Distributed Detection of Signals Perturbed by Random Channels," Presented at the 1986 IEEE International Symposium on Information Theory, October 1986.
- [31] Z. Chair, I.Y. Hoballah and P.K. Varshney, "Distributed Sequential Probability Ratio Test," Presented at the Twentieth Asimolar Conference on Signals, Systems and Computers, November 1986.
- [32] B. Barbo, A. Lomes and E. Perkalski, "Cell-Averaging CFAR for Multiple Target Situations," IEE Proceedings, April 1986, Vol. 133, Pt.F, No. 2.
- [33] J.A. Ritcey, "Calculating Radar Detection Probabilities by Contour Integration," Ph.D. Dissertation, University of California, San Diego, 1985.
- [34] R. Nitzberg, "Application of Invariant Hypothesis Testing Techniques to Signal Processing," Ph.D. Dissertation, Syracuse University, NY, 1970.

- [35] I.Y. Hoballah, "On the Design and Optimization of Distributed Signal Detection and Parameter Estimation Systems," Ph.D. Dissertation, Syracuse University, NY, 1986.
- [36] M.I. Skolnik, Introduction to Radar Systems, New York: McGraw-Hill, 1980.
- [37] W. Feller, An Introduction to Probability Theory and Its Applications, Volume 1 and 2, New York: John Wiley and Sons, 1971.
- [38] I.S. Gradshteyn and I.M. Ryzhik, Table of Integrals, Series, and Products, Orlando, Florida: Academic Press, Inc., 1980.
- [39] N. Piskunov, Differential and Integral Calculus, Groningen, The Netherlands: P. Noordhoff LTD, 1965.
- [40] G.R. Walsh, Methods of Optimization, London: John Wiley and Sons, 1975.
- [41] A. Papoulis, Probability, Random Variables, and Stochastic Processes, New York: McGraw-Hill, 1965.
- [42] R.P. Wishner, "Distribution of the Normalized Periodogram Detector," IRE Transactions on Information Theory, March 1958, IT-4, pp. 53-57.
- [43] J.I. Marcum, "A Statistical Theory of Target Detection by Pulsed Radar: Mathematical Appendix," IRE Transactions on Information Theory, April 1960, IT-6, pp. 155-267.
- [44] R. Nitzberg, "Constant False-Alarm Rate Signal Processors for Several Types of Interference," IEEE Transactions on Aerospace and Electronic Systems, January 1972, AES-8, pp 207-34.
- [45] R. Nitzberg, "Low-Loss Almost Constant False-Alarm Rate Processors," IEEE Transactions on Aerospace and Electronic Systems, September 1979, AES-15, pp. 719-723.
- [46] H.I. Jacobson, "A Simple Formula for Radar Detection Probability on Swerling I Targets," IEEE Transactions on Aerospace and Electronic Systems, March 1981, AES-17, pp. 304.
- [47] J.V. DiFranco and W.L. Rubin, Radar Detection, Englewood Cliffs, NJ: Prentice-Hall Inc., 1968.

- [48] M.D. Srinath and P.K. Rajasekaran, An Introduction to Statistical Signal Processing with Applications, New York: John Wiley and Sons, 1979.
- [49] H.L. Van Trees, Detection, Estimation, and Modulation Theory, New York: John Wiley and Sons, 1968.
- [50] L.K. Ekchian, "Optimal Design of Distributed Detection Networks," Ph.D. Dissertation, M.I.T., 1980.
- [51] D.P. Meyer and H.A. Mayer, Radar Target Detection, Handbook of Theory and Practice, New York: Academic Press, Inc., 1973.
- [52] F.E. Nathanson, Radar Design Principles, New York: McGraw-Hill, 1969.
- [53] M.I. Skolnik, Radar Handbook, New York: McGraw-Hill, 1970.
- [54] R.S. Berkowitz, Modern Radar, Analysis, Evaluation, and System Design, New York: John Wiley and Sons, 1965.
- [55] A.V. Balakrishnan, Communication Theory, New York: McGraw-Hill, 1968.
- [56] W.B. Davenport, Jr. and W.L. Root, An Introduction to the Theory of Random Signals and Noise, New York: McGraw-Hill, 1958.
- [57] A.U. Rihaczek, Principles of High Resolution Radar, New York: McGraw-Hill, 1958.
- [58] W.S. Burdick, Radar Signal Analysis, Englewood Cliffs, N.J.: Prentice-Hall, Inc., 1968.
- [59] R. Benjamin, Modulation, Resolution and Signal Processing in Radar, Sonar and Related Systems, London: Pergamon Press, 1966.
- [60] J. Constant, Introduction to Defense Radar Systems Engineering, New York: The MacMillan Press, 1972.
- [61] M. Abramowitz and I.S. Stegun, Handbook of Mathematical Functions with Formulas, Graphs, and Mathematical Tables, Washington, D.C.: U.S. Department of Commerce, National Bureau of Standards Applied Mathematics Series, 55, 1972.
- [62] R.E. Schwartz, "Minimax CFAR Detection in Additive Gaussian Noise of Unknown Covariance," IEEE Transactions on Information Theory, November 1969, pp. 722-725.

- [63] J.M. Moser, "Detection Probabilities for a Rank Statistic," IEEE Transactions on Information Theory, May 1971, pp. 346-349.
- [64] E. Dalle Mese and D. Guili, "Detection Probability of a Partially Fluctuating Target," IEE Proceedings, April 1984, Vol. 131, Part F, No. 2, pp. 179-182.
- [65] J. F. Roulston and M. Jackson, "Optimization of a Digital Autodetector for Linear and Logarithmic Radar Video," IEE Proceedings, February 1980, Vol. 127, Pt. F, No. 1, pp. 22-29.
- [66] G.B. Goldstein, "False-Alarm Regulation in Log-Normal and Weibull Clutter," IEEE Transactions on Aerospace and Electronic Systems, January 1973, AES-9, pp. 85-92.
- [67] A. Farina, A. Russo and F.A. Studer, "Coherent Radar Detection in Log-Normal Clutter," IEE Proceedings, February 1986, Vol. 133, Pt. F, No. 1, pp. 39-54.
- [68] R.A. Dana and D. Moraitis, "Probability of Detecting a Swerling I Target on Two Correlated Observations," IEEE Transactions on Aerospace and Electronic Systems, AES-17, pp. 727-730.
- [69] E. Brookner, "False Alarm-Rate and False-Alarm Number for Discrete and Continuous Time Sampling," IEEE Transactions on Aerospace and Electronic Systems, November 1981, AES-17, pp. 809-814.
- [70] G.H. Robertson, "Computation of the Noncentral F Distribution (CFAR) Detection," IEEE Transactions on Aerospace and Electronic Systems, September 1976, AES-12, pp. 568-571.
- [71] D.W. Kelsey and A.H. Haddad, "Detection and Prediction of a Stochastic Process Having Multiple Hypothesis," Information Sciences 6, 1973, pp. 301-311.
- [72] V.K. Rohatgi, An Introduction to Probability Theory and Mathematical Statistics, New York: John Wiley and Sons, 1976.
- [73] H. Stark and J. W. Woods, Probability, Random Processes, and Estimation Theory for Engineers, Englewood Cliffs, N.J.: Prentice-Hall, 1986.
- [74] P.Z. Peebles, Jr., Probability, Random Variables, and Random Signal Principles, New York: McGraw-Hill, 1980.
- [75] E.J. Dudewicz, Introduction to Statistics and Probability, New York: Holt, Rinehart and Winston, 1976.

- [76] J.C. Hancock and P.A. Wintz, Signal Detection Theory, New York: McGraw-Hill, 1966.
- [77] A.P. Sage and J.L. Melse, Estimation Theory with Application to Communications and Control, New York: McGraw-Hill, 1971.
- [78] A.D. Whalen, Detection of Signals in Noise, New York: Academic Press, 1971.
- [79] D.A. Wismer, Optimization Methods for Large-Scale Systems with Applications, New York: McGraw-Hill, 1971.
- [80] D.J. Wilde, Optimum Seeking Methods, Englewood Cliffs, N.J.: Prentice-Hall, 1964.
- [81] Y. Sawaragi, H. Nakayama and T. Ranino, Theory of Multiobjective Optimization, Orlando, Florida: Academic Press, 1985.



*MISSION
of
Rome Air Development Center*

RADC plans and executes research, development, test and selected acquisition programs in support of Command, Control, Communications and Intelligence (C³I) activities. Technical and engineering support within areas of competence is provided to ESD Program Offices (POs) and other ESD elements to perform effective acquisition of C³I systems. The areas of technical competence include communications, command and control, battle management, information processing, surveillance sensors, intelligence data collection and handling, solid state sciences, electromagnetics, and propagation, and electronic, maintainability, and compatibility.

END

DATE

FILMED

9-88

DTIC